Guidelines on the geometry of groynes for river training

DJ Seed

Report SR 493
October 1997

HR Wallingford

Address and Registered Office: **HR Wallingford Ltd.** Howbery Park, Wallingford, OXON OX10 8BA
Tel: +44 (0) 1491 835381 Fax: +44 (0) 1491 832233

Registered in England No. 2562099. HR Wallingford is a wholly owned subsidiary of HR Wallingford Group Ltd.

Contract

This report describes work funded by the Department of the Environment under research Contract CI 39/5/89 for which the DoE nominated officer was P Woodhead and the HR nominated officer was WR White. The HR job number was RTS 50. It is published on behalf of the Department of the Environment, but any opinions expressed in this report are not necessarily those of the funding department. The work was carried out by David Seed and the project was managed by RWP May.

Prepared by David Seed (name) Senior Scientist (Title)

Approved by Richard May Principal Engineer

Date 22 January 1998

Summary

Guidelines on the geometry of groynes for river training

DJ Seed

SR 493
October 1997

This guide describes recommendations for positioning river groynes and a method for determining the flow velocity at key locations in the flow field. A three-dimensional numerical model was used to predict flows in a number of configurations of groynes.

This is the second of two reports investigating the use of a three-dimensional numerical model to model river groynes. The first report, (HR Report, SR 480) described the validation of the numerical model against laboratory experiments.

This present report uses the results of the validated model to predict flows in a straight channel with a number of configurations of river groynes. The geometric parameters that are considered include the length, spacing, angle and taper of the groynes. Tests include groynes placed on one side and on both sides of the river channel. Three key velocities are identified as being important when designing the geometry of the river groynes. These are the maximum velocity in the main channel, the maximum near-bed velocity close to the groyne tip and the maximum near-bed velocity at the toe of the bank. Using the results of the simulations, a design procedure has been developed which allows engineers to predict the values of the key velocities from the groyne geometry. General guidance is given regarding the length, spacing and taper of the groynes.

Notation

A^*	Area ratio: Blockage area of groynes divided by flow area of the main channel $= sA_g / (A - sA_g)$
A	Total cross sectional area of flow in river (m^2)
A_g	Groyne blockage area: cross-sectional area of groyne below waterline viewed from the direction of flow
A_r	Relative groyne area: blockage area of a single groyne divided by river area = (A_g/A)
B_a	Area ratio term for estimating near-bank velocity (V_{bank})
B_n	Roughness correction term for estimating near-bank velocity (V_{bank})
B_s	Groyne spacing term for estimating near-bank velocity (V_{bank})
B_t	Taper ratio term for estimating near-bank velocity (V_{bank})
C_a	Area ratio term for estimating main channel velocity (U_{ch})
C_z	Chezy coefficient ($\approx 1.81\ H^{1/6}/n$, where H is in metres) ($ft^{1/2}/s$)
D	Mean depth of river =(A/W) (m)
F_n	Roughness correction term for fully developed rough turbulent flow
G_a	Area ratio term for estimating depth-averaged velocity near the groyne tip (U_{tip})
G_s	Groyne spacing term for depth-averaged velocity near the groyne tip (U_{tip})
G_t	Taper ratio term for depth-averaged velocity near the groyne tip (U_{tip})
H	Maximum depth in main channel of river (m)
k	Turbulent kinetic energy (Joules/kilogram).
k_s	Bed roughness of river bed (m)
L	Exposed groyne length (viewed from direction of flow) (m)
L^*	Normalised groyne length: length of groyne divided by width of river = (L / W)
n	Manning's roughness coefficient
P	Wetted perimeter of river cross section (m)
Q	River discharge (m^3/s)
R	Hydraulic radius = (A/P) (m)
s	Index: (s=1: groynes on one side of channel, s=2: groynes on both sides)
S_b	Lateral bank slope
S_f	Longitudinal energy slope
S_g	Slope of tapered groyne
S	Longitudinal spacing of groynes (m)
S_L	Recirculation length behind a groyne or groynes (m)
S^*	Spacing ratio: Longitudinal spacing of groynes divided by groyne length = (S / L)
S^+	Normalised groyne spacing = S / (L-b)
T_a	Area ratio term for estimating tip velocity (V_{tip})
T_n	Roughness term for estimating tip velocity (V_{tip})
T_s	Groyne spacing term for estimating tip velocity (V_{tip})
T_t	Taper ratio term for estimating tip velocity (V_{tip})
t	Taper length: Horizontal distance from groyne tip to water surface (m)
t^*	Taper ratio: Taper length divided by groyne length = (t / L)
u	Depth-averaged velocity (m/s)
u_{ch}	Depth-averaged velocity in the main channel (m/s)
u_{mean}	Section-averaged velocity = (Q / A) (used for normalisation)
U	Normalised depth-averaged velocity (u_{ch}/u_{mean})
U_{bank}	Normalised depth-averaged velocity at the toe of the river bank
U_{ch}	Normalised depth-averaged velocity in the main channel
U_{tip}	Normalised depth-averaged velocity at the groyne tip
v	Near-bed velocity (velocity at a depth of 10% of the local water depth) (m/s)
V	Normalised near-bed velocity = (v/u_{mean})
V_{bank}	Bank velocity (Maximum normalised near-bed velocity between groynes, at the toe of the river bank)
V_{max}	Bank velocity (Maximum normalised near-bed velocity behind a single groyne)
V_{tip}	Tip velocity (Maximum normalised near-bed velocity along a line 5%W from groyne tip
V_r	Bed ratio (near-bed velocity divided by depth-averaged velocity = v/u)
W	Width of river at water surface

Notation *continued*

θ Angle between groyne and upstream bank

ϕ Angle from groyne tip to toe of bank at next groyne. (For straight channels $\phi = \tan(1/S^+)$

Subscripts

$_T$ Total flow including shallows next to bank

$_{surf}$ surface flow at 85% of depth

$_A$ factor dependent on relative groyne area (A_r)

Superscript

$'$ Alternative analysis used for estimating (V_{bank}/C_a)

Note: On some graphs, where it is not practicable to use subscripts, normal text may be used, and an underline may be added for clarity. Thus V_{bank} may appear as V_bank or Vbank.

Contents

Contents continued

Contents continued

1 Introduction

1.1 The use of river groynes

The behaviour of rivers is determined by the interaction of the transport of water and the transport of sediment. At low or declining flows sediment is deposited and at higher flows sediment may be eroded. The accretion or erosion of sediment can alter the conveyance of a river and increase the risk of flooding, cause bank erosion or alter the river plan form. This natural development of a river may not suit the needs of its users or of those living or working close to its banks and thus river training may be required. River training is a method of stabilising or modifying the geometry of a natural river either by protecting the river bank or by the introduction of structures in the flow. There are several reasons why river training may be required:

- To make the river sufficiently deep to allow navigation;
- To increase hydraulic conveyance and so reduce the risk of flooding;
- To increase velocities so that sediment will be prevented from accreting;
- To guide the flow of the river particularly in the region of structures such as bridges;
- To prevent the erosion of the river bank;
- To maintain or modify the plan form of the river.

River groynes are most likely to be used in one of two situations. One of these is in large meandering or braided rivers, where the river flows through fine-grained, non-cohesive sediment. Here the main application is likely to be the maintenance or adjustment of plan form so that the river does not threaten the stability of man-made structures. Such rivers are typically found on the Indian subcontinent.

The other situation is in smaller but still substantial rivers, typically found in Europe. These types of rivers often have cohesive banks and non-cohesive sediments in the bed. Here the main application is likely to be the maintenance of a navigable channel in the waterway. In addition, river groynes may be used for environmental purposes, such as the creation of fish holes (Tamai et al, 1996).

There are many previous recommendations on the design and layout of river groynes, which have largely been based on local conditions and preferences. For example, HR Wallingford (1990) quotes twelve different recommendations for river groyne spacing (see Table 1) and Przedwojski at al.(1995) quote a further fifteen. Physical models of river groynes have been used in the past but these can be expensive to set up and changes in river geometry and other factors can be difficult to simulate. Computer models have the advantage that such changes can be made more easily and thus allow a wider range of conditions to be tested. For flow around river groynes, a three-dimensional model is required but until recently the use of such models has not been practicable for this application. However, recent developments in computer software and hardware have now made possible a systematic study of the performance of river groynes. In this project a three-dimensional, steady-state, open channel, flow model has been used to simulate the flow around river groynes. The software used was SSIIM written by Dr Olsen of the University of Trondheim (Olsen 1996). SSIIM takes its name from the title "Simulation of Sediment movements In water Intakes with Multiblock option". The main advantages of the software for this project were its particular suitability for open channel flow problems and its general availability on the Internet. The latter was important to ensure that the experience gained from the project would be valuable to others wishing to model river groynes.

This guidance report is the second of two documents produced as a result of a research contract part funded by the Construction Directorate of the Department of the Environment, Transport and the Regions. The first document (HR report SR 480) described the validation of the numerical model (SSIIM) against a number of experimental tests.

These tests included the following conditions:

- straight, curved and meandering channels;
- rectangular and trapezoidal channel cross-sections;
- groynes with crests that are horizontal and those that are tapered in elevation;
- impermeable and permeable groynes;
- groynes at different angles to the river bank;
- submerged and full depth groynes;
- groynes singly or in groups of two or more.

The main conclusion from these tests was that SSIIM could be used to predict the flow conditions around impermeable groynes but that the simulation of permeable groynes requires further research. Consequently, permeable groynes are not included in this present report.

1.2 Scope of the document

The main purpose of this guidance report is to provide experienced hydraulic engineers with quantitative data on flow conditions around impermeable groynes that will assist them in designing effective and economic river training works.

Due to the large number of factors that need to be considered in the design of river training works, the scope of this report is restricted to consideration of a straight river whose shape is typical of those likely to require river groynes. Tests showed that the absolute size and discharge in the river did not alter the pattern of flow. Thus, both the design and the performance of the groynes are presented in a dimensionless form, which can be scaled to suit different applications.

In considering the design of a groyne field, the significant factors to be considered are:

- The groyne length,
- The spacing between groynes,
- The angle of the groynes to the river bank,
- The degree of taper towards the groyne tip,
- Whether the groynes are placed on one side or on both sides of the river bank,
- The slope of the river bank and
- The roughness of the river bed.

The performance of a field of groynes can be described in terms of the modifications made to the flow in the river. An example of the flow pattern in a groyne field is shown in Figure 1. It can be seen that the flows are increased in the main channel, particularly near the groyne tips and that a slow recirculating pattern of flow is generated in the spaces between each pair of groynes. The overall performance of the groyne field is described in this report by three parameters that were identified as important to engineers designing river training works. These are

- The maximum depth-averaged velocity in the main channel in the groyne field,
- The maximum near-bed velocities close to the tips of the groynes and
- The maximum near-bed velocity at the toe of the protected bank.

The relevance of these velocities and the main effects of river groynes are described in the next chapter. Chapter 3 summarises the results from the numerical tests, which are fully described in Appendix 1. Chapter 4 gives general recommendations and Chapter 5 describes the method for predicting flow velocities in a groyne field. Chapter 6 contains conclusions and recommendations.

2 The effects of groynes

2.1 Velocities used to describe the performance of groynes

In Chapter 1 several possible reasons for using river groynes were identified. However, when designing a series, or 'field' of groynes, it is usually necessary to consider all the effects of the groynes to ensure that the design is completely acceptable.

The main effect of river groynes is to reduce flow velocities near the river bank and to increase them in the main channel. Between the groynes, the flow circulates and the strength of the recirculating flow depends on the geometry of the groynes. In the main channel, the flow increases and particularly high velocities can be seen in the proximity of the groyne tip. Thus, the river bed may need protection close to the groynes.

In quantifying the effects of the groynes, three key velocities were identified. Figure 2 shows the location of these key velocities, which are as follows:

a) The maximum depth-averaged velocity in the main channel. This may be used to determine the increases in flow velocity that affect navigation and the change in sediment-transporting capacity. Also important is the longitudinal variation in main channel velocity that occurs when groynes are relatively long and widely spaced.

b) The maximum near-bed velocity, close to the groyne tip. Following the work of Escarameia and May (1992, 1995), the near-bed velocity is defined as the horizontal velocity at a height above the bed equal to 10% of the local water depth. In this region of highly changing velocity, the value taken was the maximum velocity on a line parallel to the bank and a distance of 5% of the free surface width from the groyne tip. This value may be used to estimate the armouring required at the groyne tip

c) The maximum near-bed velocity at the toe of the river bank. This value may be used to estimate the shear velocity that can be used to estimate potential erosion of the river bank.

The near-bed velocity is used in the last two cases because in these regions the velocity profile does not usually follow the standard logarithmic distribution for fully developed open channel flow. Thus, conditions at the bed, which may cause scour or deposition, cannot be reliably estimated from the depth-averaged velocity. This has been found to be particularly true for tapered groynes.

2.2 Navigational effects

As groynes reduce the velocities near the bank of the river, the velocities in the main channel increase. This effect can be used for navigational purposes since the increased velocities may cause sufficient erosion to maintain navigable depths in the main channel. To be effective the groynes must create sufficiently high velocities to reduce bed levels, but it is also important to avoid unacceptably high velocities under flood conditions. This is usually achieved by building the groynes to the level of the mean annual flood so that at very high flows the groynes become submerged - thus limiting main channel velocities. However, in these cases the velocities close to the groyne are increased and additional protection may be required. A comparison of the simulated flows for submerged and unsubmerged conditions at a single model groyne is shown in Figure 3.

Where groynes are long and widely separated, the main channel flow spreads out between the groynes. This causes the velocities to fall at sections between the groynes and to rise again close to the groynes. This can be seen in Figures 4 and 5. The variation in velocity may also cause variations in depth in a mobile river. Both variations may be undesirable in a navigable river.

2.3 Local scour effects

As the flow is diverted around a groyne, the flow accelerates and is deflected downwards, increasing the potential for scour. To protect the groyne, stone or other protection is often placed along the shanks of the groyne and at the groyne tip. The near-bed velocity in the region of the groyne tip can be significantly greater than upstream values. Turbulence can also be high in this region, further increasing the likelihood of scour.

2.4 Bank protection

The main reason for installing river groynes is often a need to prevent bank erosion and the migration of bends and meanders, but several factors need to be borne in mind. Longer groynes provide more bank protection up to a point but for relatively large groynes, the increase in main channel velocities outweighs the additional protection provided by the increased groyne length. Furthermore, if the groynes are widely separated, the main channel flow 'spreads' into the space between the groynes, which may cause large recirculating currents that can undercut the groyne root.

2.5 Flood protection

The use of river groynes normally increases the hydraulic resistance of a river and this can have two main effects on the water levels.

- The increased resistance tends to reduce the conveyance of the river and this can increase upstream levels.
- For unsteady flood conditions, the extra resistance can increase the attenuation of the flood wave thereby improving protection against flooding at downstream locations by reducing peak discharges.

However, these effects may be reversed in rivers with highly mobile beds because as the groynes obstruct the flow near the sides of the channel, so the velocities and sediment transport in the main channel are increased. The increased sediment transport can cause scour in the main channel, thus increasing the overall conveyance of the channel.

3 Results from numerical model tests

3.1 Method

This chapter summarises the methods used to determine the recommendations and formulae that are presented in this report. The numerical model used for this study is a three-dimensional steady-state model designed to predict flows in an open channel. The model, named SSIIM, uses a rigid lid approximation to the water surface and incorporates a k-epsilon model of turbulence. The software was validated for modelling river groynes by comparing the results of a large number of numerical tests with measurements in laboratory models. The validation of the software is described in HR report SR480 (Seed, 1997). The validation study showed that the velocities from an individual simulation could be relied upon within about ±20%, except in the case of porous groynes and close to the shear layers where velocity gradients are high. The study indicated the most suitable choice of numerical scheme and other parameters used in the numerical modelling. Porous groynes were not studied further for this present report.

The tests used to produce the results described in this present report were conducted in two phases. In the first phase, tests were carried out to determine the most suitable grid for the numerical tests and to investigate the influence of the dimensions and roughness of the river on the flow patterns. These tests were based on a single groyne similar to that used in the validation study. In the second phase, tests were made to determine the influence of groyne geometry on the performance of a field of six groynes. The shapes of the groynes used in these tests are shown in Figures 6 and 7.

3.2 Results

The single groyne tests were conducted to find a suitable mesh and to determine the influence of variations in river geometry. These tests showed that a linear scaling of all dimensions made no significant difference to the pattern of flow. However, changes in proportion (e.g. the depth/width ratio of the river) can significantly change the strength of flow between the groynes. A reduction in the relative depth of the river increases the frictional resistance of the banks and this reduces both the velocities downstream of the groyne and the size of the recirculation zone. Further tests showed that an increase in Manning's n has a similar effect. These effects are difficult to quantify thus the overall result should be treated with some care.

The groyne field tests were made to determine the influences of the geometry, orientation and spacing of the groynes and to further investigate the effect of different values of Manning's n. Tests were conducted for a number of shapes, sizes and configurations of groynes in a river with a representative cross-sectional shape derived from regime theory. From these tests, analytic equations have been derived which provide quantitative guidance on the performance of a field of groynes. The performance is expressed in terms of relative velocities at key locations in the river.

It has obviously not been possible to validate the method against all the combinations of river geometry, river roughness, groyne geometry and groyne positioning. Thus, the results presented should be understood to be only indicative of the dependency of each value of velocity on the various parameters that define the river and groynes. Nonetheless, the results lead to useful conclusions and may be used to predict the comparative effect of various designs. A full description of the numerical tests is presented in Appendix 1.

4 Predictions and recommendations

4.1 Introduction

In this chapter, we summarise the findings of the numerical tests to provide guidance in the dimensions and positioning of river groynes. This guidance is limited to the scope of the test work and thus is limited to a uniform field of groynes in a straight river of uniform cross-section. The results also apply only to unsubmerged groynes. The river conditions that were investigated were the absolute size of the river, the bank slope and the bed roughness. The influence of the dimension of the first groyne in a groyne field has also been studied.

The significant factors that were found to influence the flow around a field of groynes are as follows:

- The groyne blockage area (i.e. the area of the groyne below the waterline measured perpendicular to the flow, A_g).
- The Spacing of the groynes along the river (S)
- The angle between the river groyne and the downstream bank (θ)
- The degree of taper for the groyne (defined as the fraction of the groyne length below the water, t*).

A groyne with a crest height that falls for at least half of the crest length is termed tapered and a groyne with a horizontal crest is referred to as rectangular. Tapered groynes with more than half the crest length horizontal are outside the scope of this report.

The dimensions and dimensionless terms used to describe the groyne and the river channel are defined in Figure 2.

The performance of river groynes is presented with reference to the three key velocities that were introduced in section 2.1. These are:

- The maximum depth-averaged velocity in the main channel (u_{ch}),
- The near-bed velocity close to the groyne tip (v_{tip}) and
- The near-bed velocity at the toe of the river bank (v_{bank}).

It has been found that for geometrically similar rivers, the flow patterns do not vary with the scale of the river. Thus it is possible to describe the performance of a field of groynes in terms of the relative or *normalised* velocities. The normalised velocity at any point in the flow is the local velocity divided by the mean or section-averaged velocity (u_{mean}). The latter is obtained by dividing the river discharge (Q) by the flow area of the river channel (A), i.e.

$$u_{mean} = Q/A \quad (1)$$

In this report, lower-case letters (u, v) are used, to indicate actual velocities (in metres per second), while capital letters (U, V) are used to indicate normalised velocities. Thus, for example, u_{ch} is the maximum depth-averaged velocity in the main channel between the groynes, whilst the normalised main channel velocity is written as U_{ch}.

As discussed in section 2.1, some velocities are given as depth-averaged values and these are shown as U or u. Velocities at 10% of the local water depth (i.e. the near-bed velocities) are indicated by V or v. Near-bed velocities are used in many formulae for calculating the stability of riprap and other protection. Thus near-bed velocities are used in this report in locations where stability is important i.e. at the groyne tip (V_{tip}) and at the toe of the river bank (V_{bank}).

The terms used for calculating the normalised velocities are dependent on the geometry of the groynes and on the geometry and bed roughness of the river channel. Terms such as B_a are used to indicate an influence on the bank velocity (V_{bank}). Similarly, the terms T_a, and C_a are used in the equations for tip velocity and main channel velocity respectively.

The subscripts to these terms indicate the influencing factor, for example:

T_a The effect of groyne area on the tip velocity.
T_n: The effect of channel roughness (Manning's n) on the tip velocity.
T_s : The effect of groyne spacing on the tip velocity.
T_t: The effect of groyne taper on the tip velocity.

All such terms are dimensionless and are used in the following formulae for the normalised velocities.

The normalised main channel velocity is given by the equation

$$U_{ch} = C_a \quad (2)$$

The normalised tip velocity is given by the equation

$$V_{tip} = T_n (T_a + T_s + T_t) \quad (3)$$

and the normalised bank velocity is given by the equation

$$V_{bank} = B_n (B_a + B_s + B_t) \quad (4)$$

4.2 Upstream conditions

It is generally recommended that at the start of a groyne field, the groyne length should be increased gradually from the upstream end. This advice is designed to ensure that the velocities at the groyne tips are not excessive. The numerical tests indicated a further reason for avoiding this configuration. It was found that where a groyne field started abruptly, the flow tended to form a *vena contracta* such that downstream of the first groyne, the flow was well separated from the line of the groynes. This caused an uneven pattern of flow behind successive groynes, which could lead to excessive accretion between the first and second groynes. Similarly, if the initial groyne is too short, insufficient protection is provided to the second groyne and a vena contracta forms downstream of the second groyne. The occurrence of a vena contracta can be seen from the contours of U=0.2 in Figure 8.

The numerical tests were limited to finding a configuration that would ensure that a consistent pattern of flow developed between successive pairs of groynes. In Figure 9 the tip velocities at the first and second groynes are compared with the average downstream value. These tests showed that the use of a single short groyne with a length of approximately 75% of the remaining groynes ensured the development of this consistent pattern of flow. However, in practical applications, a gradual increase in groyne length is recommended to minimise tip scour and to provide a satisfactory transition to the groyne field under a range of flow conditions.

4.3 Groyne angle

Where a single groyne is placed in the river flow, the angle between the groyne and the flow can be significant. A groyne facing upstream is referred to as an attracting groyne. Facing the groyne upstream increases the energy loss at the groyne tip and reduces the length of the recirculation zone. This pattern of flow for single groynes at different angles can be seen in Figure 10 ; the turbulent kinetic energy (k) can be seen in Figure 11. The turbulent kinetic energy shown is the kinetic energy of the rapidly varying flow, which is typically too small and rapid to be directly modelled in a numerical model. SSIIM uses the k-epsilon method of determining turbulence. This is described in HR report SR 480.

Where a groyne is facing downstream, the flow makes a more gradual transition to the groyne tip, and the length of the recirculation zone is increased. A groyne in this configuration is called a repelling groyne.

When groynes are placed in a series or field, the influence of groyne angle is far less significant than when a groyne is used in isolation, because the size of the recirculation zone is constrained by the groyne spacing. Figure 12 shows the variation in the bank velocities with groyne angle. For both upstream and downstream facing groynes, velocities in the protection of the groynes are slightly increased, compared to the case where the groynes are at right angles to the flow. The tip velocity and main channel velocity are largely independent of groyne angle. It follows from this result that the most economic orientation for groynes in a groyne field is at 90° to the flow. The predicted turbulence is also much less sensitive to groyne angle than in the case of single groynes. All the formulae used for predicting velocities in a groyne field are based on this condition. However, groynes facing at other orientations may be preferred for other reasons. For example, groynes facing downstream encourage accretion between groynes.

4.4 Groyne length

The length of river groynes has two counteracting influences on the velocities in a river channel. The first is that the groynes reduce the effective area through which the water can flow. This blockage effect increases flow velocity in the main channel. In a field of groynes, it is the main channel velocity that induces the circulating currents between the groynes. Thus, an increase in groyne blockage area will tend to increase the velocities in the groyne field.

The second influence on the velocities between the groynes is that longer groynes increase the distance from the bank to the high velocities in the main channel. Thus, for the same main channel velocity, an increase in groyne length tends to reduce the velocity at the toe of the river bank (V_{bank}).

The overall effect of increasing groyne length is dependent on the circumstances. For relatively short groynes, an increase in groyne length provides better protection and hence lower velocities on the river bank. For groynes which obstruct a significant fraction of the river flow area, an increase in groyne length increases velocities at the toe of the bank.

The blockage effect of the groynes may be predicted using the area ratio (A*). The area ratio is defined as the total blockage area of the groynes (sA_g) divided by the main channel flow area ($A-sA_g$). Thus

$$A^* = sA_g / (A - sA_g) \qquad (5)$$

where A_g is the area of a single groyne
s is the number of sides of the river on which groynes have been installed, and
A is the total flow area of the channel

4.4.1 Main channel velocity

Clearly, an increase in groyne area ratio (A*) will cause an increase in main channel velocity (u_{ch}). If we were to assume a uniform flow across the main channel and zero net flow behind the groynes, the main channel velocity would be increased by the factor (1+A*) compared to the section-averaged velocity. However due to the non-uniformity of the flow, particularly in the main channel, the ratio is higher.

In the tests on groyne blockage area, it was found that effect of groyne blockage on normalised main channel velocity (C_a) is given by the expression

$$C_a = 1.34\, A^* + 1 \tag{6}$$

This relation is shown in Figure 13 together with the data from the simulations.

From further analysis of the data it was found that none of the other parameters of groyne geometry had a significant effect on the value U_{ch}. Thus, the complete formula for the normalised main channel velocity is

$$U_{ch} = 1.34\, A^* + 1, \text{ for } 0.13 \le A^* \le 1.3 \tag{7}$$

4.4.2 Tip velocity

The influence of groyne blockage on tip velocity (V_{tip}) has a similar form as can be seen from the following equation.

$$T_a = 0.87A^* + 0.61, \text{ for } 0.13 \le A^* \le 1.3 \tag{8}$$

This relationship is shown in Figure 14 together with results from the simulations.

The application of this term in determining the tip velocity will be described later.

4.4.3 Bank velocity

For similar velocities in the main channel, an increase in groyne length tends to reduce the velocities near the bank. However, for the tests conducted for this report, the dominant effect of increased groyne length is to increase main channel velocities and thus increase the speed of the recirculating currents between the groynes. The overall effect is that near bank velocities are increased with increasing groyne length The equation derived from the numerical results is

$$B_a = 0.13\, A^* + 0.05, \text{ for } 0.13 \le A^* \le 1.3 \tag{9}$$

This relation is shown in Figure 15 and indicates a continuing reduction in bank velocity for shorter groynes. It is clear that this equation is not applicable for lower groyne lengths since, as the groyne length tends to zero, the bank will be unprotected and the velocities will be higher ($V_{bank} \approx 0.5$ under the condition of the numerical tests). Another factor that is significant in the determination of bank velocity is the length of the groyne compared to the transverse width of the sloping river bank (b). This is considered in the next section.

4.5 Groyne spacing

4.5.1 Expansion of flow

The recommended separation between groynes is often specified by reference to the relative groyne spacing. The relative spacing S* is defined here as the distance (S) between successive groynes divided by the groyne length (L). The relative groyne spacing is a key factor in determining the cost of the groyne system, since the inverse of the groyne spacing is the total length of installed groynes per unit length of river bank. For economic reasons, therefore, a large relative groyne spacing is desirable. Where the groyne spacing is too large however, the groynes are ineffective since the groynes do not act as a continuous protection but tend to act as single groynes. The quantity that seems best to describe the effectiveness of the groynes is the location of the '20%' contour, that is the location where the local depth-averaged velocity at 20% of the average upstream velocity (i.e. U=0.2).

Between each pair of groynes within a groyne field, the position of the 20% contour moves towards the bank at an approximately constant angle of 7 degrees. The expansion of the flow between groynes of various designs is shown in Figure 16. It can be seen that at a relative groyne spacing of S* = 6 (Figure 16d), the 20% contour reaches the toe of the bank and the near-bank velocity is significantly higher than the corresponding value when S* = 4 (Figure 16e). This comparison is shown clearly in the lower graph of Figure 17.

The angle of expansion may be used to calculate the optimum groyne spacing. Used in this way, the angle of expansible is related to the other geometric parameters by expression

$$\tan\phi = \frac{1}{S^*}\left(1-\frac{b}{L}\right) = \frac{L-b}{S} \qquad (10)$$

In the numerical tests in which the effect of groyne spacing was investigated, the groyne length was 20% of the channel width and the toe of the river bank was at 10% of the channel width. Thus, the angle between the flow direction and a line from the tip of one groyne to the root of the next groyne is approximately twice the angle of expansion (i.e. 14 degrees). This result can be compared to the method of Maza Alvarez (1989) who suggests an angle of between 9 and 14 degrees for calculating groyne separation. The use of the expansion angle of 7 degrees as a design method may be preferable since it is not specific to a particular ratio of groyne length and bank width. However, further tests would be required to confirm the general applicability of this method.

4.5.2 Main channel velocity

It has been noted above that the most significant factor determining the velocity in the main channel is the obstruction area of the groyne. However, groyne spacing does have a significant effect on the longitudinal variation of main channel velocity. This can be seen in Figure 17 for groynes with an area ratio of about 20% spaced at intervals of four and six groyne lengths (i.e. S* = 4 and 6).

4.5.3 Tip velocity

The effect of groyne spacing on tip velocity is simpler. As the relative spacing between the groynes increases so too does the velocity at the tip of the groyne. The term T_s accounts for the effect of the groyne spacing on tip velocity. This is shown in Figure 18 and in the equation below.

$$T_s = 0.077\,(S^* - 4) \quad \text{for } 1.6 \le S^* \le 6 \qquad (11)$$

4.5.4 Bank velocity

The numerical tests showed that for a groyne spacing of less than four groyne lengths, the velocity at the toe of the bank increases as can be seen in Figure 19. The increase in velocity for more closely spaced groynes is somewhat unexpected, particularly as some authorities recommend values of S* less than 4 (see Table 1). It appears that, if the groynes are placed too close together, the retarding effect of the bank on the recirculating flow is relatively reduced and high velocities are more easily established. This will be particularly true where the groynes extend into the full depth of the river. Tests on single groynes showed that if banks are shallow or the bed roughness is high, the strength of the recirculating currents will be significantly reduced. These results indicate that the optimum groyne spacing may also be dependent on these factors.

In the tests conducted, the overall effect of groyne spacing on the bank velocity is given by the following equation:

$$B_s = -0.02\ (S^* - 4);\ \text{for } 1.6 \le S^* \le 5 \qquad (12)$$

For S* > 5, B_s increases, but this effect has not been quantified and groynes with this layout are not recommended.

4.6 Groyne taper

In navigation channels, rectangular groynes may be preferred to tapered groynes, since users of river craft can more easily see the extent of each groyne. Unsubmerged rectangular groynes also provide better protection than tapered groynes of the same length. Tapered groynes, however, have the advantage of being less liable to scour in mobile rivers.

The taper ratio (t*) is a parameter which describes the cross sectional shape of a groyne. It is defined as the fraction of the groyne length that is below the waterline. (i.e. t/L, where t is the horizontal distance from the groyne tip to the water line and L is the horizontal distance from the top of the groyne tip to the intersection of the bank and the waterline). For a full depth rectangular groyne, t*=0. These values can be seen in the definition sketch (Figure 2). The shapes of various tapered groynes used in the numerical tests are shown in Figure 6.

4.6.1 Tip velocity

Numerical tests indicate that tapered groynes are less liable to scour than rectangular groynes of the same obstruction area. Figure 20 and the following equation shows the reduction in near-bed tip velocity for groynes with increasing taper ratio.

$$T_t = -0.04t^*,\ \text{for } t^* > 0.5 \qquad (13)$$

By contrast, it is shown in Appendix 1 that the depth-averaged velocities at the tips of tapered groynes are greater than the corresponding velocities at the tips of rectangular groynes.

4.6.2 Bank velocity

The effect of groyne taper on bank velocity is shown in Figure 21. Compared with rectangular groynes of the same obstruction area, the near-bed velocities at the toe of the bank (V_{bank}) are increased for tapered groynes; thus the likelihood of erosion is also increased. Depth-averaged velocities at the toe of the bank (U_{bank}), which are affected by the flow of water over the tapered groyne, are much higher. However the use of near-bed velocities is more appropriate for predicting sediment transport and bank erosion. The effect of groyne taper on the near-bed velocity at the toe of the bank is given by the following equation:

$$B_t = 0.8\ (t^* - 0.6),\ \text{for } 0.6 \le t^* \le 1.0$$
$$B_t = 0,\ \text{for } 0.5 \le t^* < 0.6 \qquad (14)$$

4.7 Bank slope

In the numerical tests conducted in the preparation of this guide, the bank width was a fixed proportion of the river width. Thus, reductions in bank slope are associated with a reduction in depth in the main channel. However, it was found that the main consequence of reducing bank slope is a reduction in bank velocity. Figure 22 shows the reduction in relative bank velocity with bank slope. It can also be seen that a reduction in bank slope also reduces the size of the recirculation zone behind a single groyne. For the groyne field tests, the bank slope was 0.4. Most rivers in alluvial material have an overall bank slope less than this figure. Thus, for many for practical applications, the velocities predicted by the numerical modelling tests will be a conservative upper limit. (Appendix 1 describes some investigations into the effects of bank slope behind a single groyne).

4.8 Channel bed roughness

The main effect of channel bed roughness, on the performance of river groynes, is due to the changes in vertical velocity profile. The effect of roughness on velocity profile is complex. Where the normalised bed roughness (k_s/R) is high i.e. where the Chezy number is low, the vertical velocity profile upstream of the groyne field is less uniform, with reduced velocities near the bed. The presence of the groynes changes the vertical distribution of flow and this alters the near-bed velocities between the groynes. The influence of a river groyne on the velocity distribution is also dependent on the shape of the groyne. These matters are discussed further in Appendix 1. In summary it has been found that a theoretical correction factor (F_n) can be derived which accounts for the influence of bed roughness on near-bed velocities. The value of F_n depends on the Chezy number, which in turn depends on the water depth and the Manning's roughness coefficient (n). The value F_n may be found from Figure 23 or the following formula

$$F_n = 2.12\left\{1 - \frac{1.303}{6\ln(C_z/26.72) - 1}\right\} \qquad (15)$$

where C_z is the Chezy coefficient ($\approx 1.81\ H^{1/6}/n$, where H is the depth in metres)

A roughness correction term should be applied for velocities at the groyne tip and at the bank behind rectangular groynes. However, for tapered groynes, it appears that the vertical velocity distribution at the bank is mostly determined by the groyne geometry and thus the roughness correction term should not be applied.

<u>Summary</u>

The roughness correction coefficient for tip velocities is given the term T_n , where

$$T_n = \frac{1}{3}(2F_n + 1) \text{ for rectangular groynes} \qquad (16)$$

and $T_n = F_n$ for tapered groynes

The roughness correction coefficient for bank velocities is as follows:

$B_n = F_n$ (for rectangular groynes) (17)

or

$B_n = 1$ (for tapered groynes, where the taper ratio t* is greater than 0.5)

For groynes with a shorter taper (t* < 0.5) it is expected that the value for B_n takes an intermediate value between F_n and unity but the tests conducted do not cover these conditions.

5 Design calculations

5.1 Method

5.1.1 Guidance notes

This chapter describes a procedure for calculating the performance of a river groyne installation in a single straight channel. Before performing the calculations the following points should be considered.

Note 1: Application
The formulae used to predict the key velocities in a groyne field have been derived from an idealised channel with a width of 120m and a depth of 5.3m. The general shape of the channel and the definitions of all geometric parameters are shown in Figure 2. For a natural channel, shallow water near the bank is excluded from consideration and thus **all dimensions must be adjusted accordingly**. The next section describes a method for this adjustment.

The method is applicable to the following conditions:

- A single straight channel
- Impermeable groynes constructed on one or both banks
- At least 50% of the length of each groyne obstructs the full depth of flow
- The blockage area of each groyne is between 15% and 30% of the river flow area. For large rivers where the groyne obstruction area is relatively small, the general guidance given in this section may be used with care.

Note 2: Blockage effects
In the situations considered in this report, the area of each groyne is a significant fraction of the flow area of the channel (15%-30%). In such cases the installation of the groynes causes an acceleration of the flow in the nest of the flow cross-section. If the bed is mobile, this can cause an advantageous increase in the sediment transport capacity of the channel, but may also lead to erosion at the tips of the groynes. If groynes are placed on one side of the river only, then care should be taken to ensure that velocities at the far bank are not excessive and may result in erosion. As a rough guide, the near bed velocities at the toe of the far bank may be calculated from

$$v_{far\_bank} = 0.4\, F_n\, u_{ch} \qquad (18)$$

where F_n is given in Equation 14 , (see Figure 23) and u_{ch} may be found from step 16 of the procedure in the next section

Note 3: Toe of the Bank
The position of the toe of the bank cannot be defined precisely and requires engineering judgement. The toe of the bank is a limiting position for the stability of the bank. The position of the toe of the bank should be chosen such that erosion of the river bed beyond the toe is not likely to lead to bank erosion. Bank stability is outside the scope of this report (see, for example, Hemphill and Bramley, 1989).

Note 4: Groyne angle
The numerical results indicate that the groyne angle has little effect on the key velocities in the flow field and thus groynes at right angles to the flow are preferred for the sake of economy. However, other work indicates that upstream facing groynes are more efficient at trapping sediment and that downstream facing groynes are less prone to scour at the groyne tips. Although the predictive formulae are based on groynes placed at right angles to the flow, the numerical results indicate that similar flow velocities can be expected at other groyne angles.

Note 5: Groyne spacing
Groynes should be placed sufficiently close together such that the main flow does not expand excessively into the spaces between the groynes. The numerical tests indicate that the main

flow expands at an angle of 7 degrees. Thus the line from the tip of one groyne to the toe of the bank at the next groyne should be at an angle of not less than 7 degrees from the flow direction.

Note 6: Groyne length
From consideration of the flow expansion angle it is recommended that the groyne should extend to 50 to 100% of the bank width beyond the toe of the bank. i.e.

$$0.5 < \frac{L-b}{b} < 1 \quad \text{or} \quad 1.5b < L < 2b$$

Note 7: Tapered groynes
Tapered groynes may be considered suitable in cases where bank protection is required but flood flows would cause unacceptable scour at the tips of rectangular groynes. Tapered groynes generally give less bank protection than rectangular groynes of the same obstruction area. However, partly tapered groynes, which extend full height to the toe of the bank but are tapered beyond that point, were found to give the best bank protection in the numerical tests (i.e. at $t^* = 0.5$ in Figure 21).

Note 8: Cost
For rectangular groynes, an approximate estimate of cost may be obtained by using the relative groyne spacing (S^*), which is equal to the total length of groynes constructed per unit length of river bank. For tapered and angled groynes, an effective total groyne length may be determined from the function $S^*(1-0.5t^*)/\sin(\theta)$.

5.1.2 Calculation method

The three normalised velocities that are used to describe the hydraulic effect of the groyne field are:

U_{ch} : average velocity at mid-channel
V_{tip} : near-bed velocity (at 10% depth) at 6 m away from the tip.
V_{bank} : near-bed velocity (at 10% depth) at 12 m away from the near bank.

The normalised values should be multiplied by the section-averaged velocity (u_{mean}) to obtain the true velocities. Thus

$$u_{ch} = U_{ch}\ u_{mean} \qquad (19)$$
$$v_{tip} = V_{tip}\ u_{mean} \qquad (20)$$
$$v_{bank} = V_{bank}\ u_{mean} \qquad (21)$$

where $u_{mean} = Q/A$ (see steps 7 and 8 below) (1)

The steps to be followed in calculating these velocities are:

1) Under representative conditions calculate the total channel discharge (Q_T).

2) From bed surveys and water levels at representative sections, determine the flow area (A_T), the mean velocity (Q_T/A_T) and the hydraulic radius (A_T/P_T).

3) Determine the energy slope (S_f) from the mean velocities and water levels at two sections.

4) Use Manning's equation to estimate a value for Manning's roughness coefficient (n). $\{n=A_T R_T^{2/3} S_f^{1/2}/Q_T\}$

5) Under a variety of flow conditions, use the value of Manning's n to calculate the flow area and depth of flow.

6) If a significant part of the flow area is relatively shallow and does not contribute significantly to the conveyance of the main channel (such as would exist in just out of bank conditions) then that part of the flow should be disregarded in the following calculations. For the purposes of this procedure, shallow flow can be considered to be

flow at depths of less than 10% of the flow depth at the tips of the groynes. Various methods exist to calculate the discharge in such cases. For example, Chow (1959) describes methods for calculating the discharge in channels with a compound section, in which Manning's equation is solved separately for the main channel and the shallow flow. **All the following calculations are based on dimensions with this shallow water excluded.**

7) Recalculate the flow area (A) and main channel discharge (Q).

8) Calculate the mean velocity ($u_{mean} = Q/A$)

9) Select the position of the toe of the bank to be protected by the groynes. Calculate the bank width (b). The bank width in the distance from the limit of the shallow water determined in Step 6 to the toe of the bank (see note 3).

10) Select the length (L) and the blockage area (A_g) of the groynes (see note 6). The groyne should extend about 50% to 100% of the bank width beyond the toe of the bank. I.e. $1.5b \leq L \leq 2b$.

11) If the groynes are to be placed on both sides of the channel, set s=2 and use the average values of A_g and L. Otherwise set s=1 and calculate the velocity on the far bank (see note 2). Calculate the relative groyne area ($A_r = A_g/A$) and the groyne area ratio (A^*)

$$A^* = sA_g/(A - sA_g) = sA_r/(1 - sA_r)$$

For the application of the method, check that the groyne area ratio (A^*) lies in the range: $0.15 \leq A^* \leq 1.3$

12) Choose the spacing for the groynes (S). Ensure that the groynes are spaced sufficiently closely so that the toe of the bank is protected by the groyne tip, using an expansion angle of 7 degrees. (See note 5 and section 4.5.1).
Calculate $S^* = S/L$.
For the application of the method, check that groyne spacing ratio (S^*) lies in the range $1.6 \leq S^* \leq 5$

13) Choose the shape of the groyne.
EITHER
For rectangular groynes (i.e. full height groynes with a level crest),
   a) The taper ratio is zero. $t^* = 0$
   b) Calculate the roughness correction term (F_n) using the depth of water at the toe of the bank (see Figure 23). Set $B_n = F_n$.
   c) Recalculate the roughness correction term (F_n) using the depth of water at the tips of the groynes. Calculate $T_n = {}^1/_3(2F_n + 1)$

OR
For tapered groynes,
   a) Calculate the fraction of the length of the groyne that is below the water line (t^*) (see note 7). For the application of the method ensure that the taper ratio(t^*) lies in the range: $0.5 \leq t^* \leq 1$
   b) The bank roughness correction term is unity. Set $B_n = 1$.
   d) Calculate the roughness correction term (F_n) using the depth of water at the tips of the groynes(see Figure 23). Calculate $T_n = F_n$.

14) Calculate the mean velocity in the groyne field

$u_{ch} = u_{mean}(1.34A^* + 1)$ (from Equation 7, Figure 13)

15) Calculate the near-bed velocity at the tip of the groyne (v_{tip}) using:

$v_{tip} = u_{mean} T_n (T_a + T_s + T_t)$ (from Equation 3)
where T_n and u_{mean} are taken from steps 15 and 16 and

$T_a = 0.87A^* + 0.61$ (Equation 8, Figure 14)

$T_s = 0.077(S^* - 4)$ (Equation 11, Figure 18)
$T_t = -0.04t^*$ (Equation 13, Figure 20)

If the velocity is at the tip of the groyne excessively high, consider using tapered groynes.

16) Calculate the near bed velocity at the toe of the bank (v_{bank}) using :

$v_{bank} = u_{mean} B_n (B_a + B_s + B_t)$ (from Equation 4)
where B_n and u_{mean} are taken from steps 15 and 16 and

$B_a = 0.13A^* + 0.05$ (Equation 8, Figure 14)
$B_s = -0.02(S^* - 4)$ (Equation 11, Figure 18)
$B_t = -0.8(t^* - 0.6)$ for $t^*>0.6$ (Equation 13, Figure 20)
$B_t = 0$ otherwise

5.2 Worked example

5.2.1 Description of problem

A navigation channel is to be stabilised in the centre of a straight channel, by introducing full height groynes on both sides of the channel. The channel is 120 m wide and has a maximum depth of 6 m. The discharge is 650 cumecs. Using a groyne length of 24 m and groyne spacing of 100 m, determine the key velocities. An approximation of the cross-section of the river is shown in Figure 24. The width of both the left and right bank is 12m and the depth at the toe of each bank is 4 m. Beyond the toe of each bank, the bed slopes gently for a further 24 m towards the centre of the channel. The central 48 m of the channel width is level with a depth of 6 m. The flow area is 576 square metres.

5.2.2 Example 1: rectangular groynes

Steps 1 to 7. From measurements of water surface slope — n=0.03

Step 8) Calculate the mean upstream velocity
$u_{mean} = Q/A$ — $u_{mean} = 650/576$
u_{mean} ≈**1.13 m/s**

Step 9) Estimate the position of the toe of the bank (note 3).
The toe of the bank is at 12m from the bank — b=12 m

Step 10) Determine L and A_g — L=24 m
L/b = 2 — $A_g = 78\ m^2$

Step 11) Calculate A*
Groynes are placed on both sides of the channel — s=2
$A_r = A_g / A$ — $A_r = 78/576$
$A_r = 0.135$
$sA_r = 2 \times 0.135$
$sA_r = 0.271$
$A^* = sA_r/(1-sA_r)$ — $A^* = \frac{0.271}{1 - 0.271}$
$A^* = 0.197$

A* is in the acceptable range ($0.15 \leq A^* \leq 1.3$)

Step 12) Choose the spacing for the groynes (S) — S = 100m
Calculate $S^* = S/L$. — $S^* = 4.16$
The groyne spacing ratio (S*) lies in the range
$1.6 \leq S^* \leq 5$ required for this method
The angle from tip to bank (ϕ) is given by
$\phi = \arctan(1/S^+)$ where $S^+ = S/(L-b)$ — $S^+ = 100/(24-12)$

$S^{+} = 8.33$
$\phi = 6.8$ degrees

$\phi \approx 7$ degrees
Thus the groyne spacing is at the limit of the maximum recommended.

Step 13) For rectangular groynes

a) Calculate the roughness correction term (F_n) using the depth of water at the toe of the bank — h= 4 , n=.03; $C_z = 76$

Using Equation 14 or Figure 23 — $F_n = 1.57$; $B_n = 1.57$

b) Recalculate the roughness correction term (F_n) using the depth of water at the tips of the groynes. — H=5 , n=0.03; $C_z = 78.9$; $F_n = 1.6$

Calculate $T_n = {}^{1}/_{3}(2F_n + 1)$ — $T_n = 1.4$

Step 14) Calculate the mean velocity in the groyne field
$u_{ch} = u_{mean}\,(1.34A^{*} + 1)$ — $u_{ch} =$ **1.43 (m/s)**

Step 15) Calculate the near-bed velocity at the tip of the groyne (v_{tip}) using:

$T_a = 0.87A^{*} + 0.61$	(blockage term, Figure 14)	$T_a = 0.782$
$T_s = 0.077(S^{*} - 4)$	(spacing term, Figure 18)	$T_s = -0.013$
$T_t = -0.04t^{*}$	(taper term, Figure 20)	$T_t = 0$
From Step 13		$T_n = 1.4$

Thus
$V_{tip} = T_n\,(T_a + T_s + T_t)$ — $V_{tip} = 1.11$
$v_{tip} = u_{mean}\,.\,V_{tip}$ — $v_{tip} =$ **1.25 (m/s)**

If the tip velocity is excessively high, consider using tapered groynes.

Step 16) Calculate the near bed velocity at the toe of the bank (v_{bank})

$B_a = 0.13A^{*} + 0.05$	(Blockage term, Figure 14)	$B_a = 0.076$
$B_s = -0.02(S^{*} - 4)$	(Spacing term, Figure 18)	$B_s = 0.003$
$B_t = -0.8(t^{*} - 0.6)$ for $t^{*}>0.6$	(Taper term, Figure 20)	
$B_t = 0$ otherwise		$B_t = 0$

Normalised near bed velocity at the toe of the bank
$V_{bank} = B_n\,(B_a + B_s + B_t)$ — $V_{bank} = 0.114$
$v_{bank} = u_{mean}\,.\,V_{bank}$ — $v_{bank} =$ **0.128 (m/s)**

Summary:
$U_{ch} = 1.43$, $v_{tip} = 1.5$, (m/s) $v_{bank} = 0.128$ (m/s)

5.2.3 Example 2: tapered groynes

If the above design is modified, by using tapered groynes of the same obstruction area L=36m , t=22m. Steps 1 to 12 are the same as for the previous example.

Step 13) For tapered groynes,

a) Calculate the fraction of the length of the groyne that is below the water line(t^{*}) (see note 7).
the taper ratio(t^{*}) lies in the range: $0.5 \le t^{*} \le 1$ — $t^{*}=22/36 = 0.611$

b) The bank roughness correction term is unity. Set $B_n = 1$.

c) Calculate the roughness correction term (F_n)
The depth of water at the tips of the groynes = 6m
(see Figure 23). Calculate $T_n = F_n$. $T_n = 1.61$

Step 14) Calculate the mean velocity in the groyne field
$u_{ch} = u_{mean}\,(1.34A^* + 1)$ **u_{ch} = 1.43 (m/s)**

Step 15) Calculate the near-bed velocity at the tip of the groyne (v_{tip}) using:

$T_a = 0.87A^* + 0.61$ (blockage term) $T_a = 0.782$
$T_s = 0.077(S^* - 4)$ (spacing term) $T_s = -0.094$
$T_t = -0.04t^*$ (taper term) $T_t = -0.024$
normalised near bed velocity at the tip
$V_{tip} = T_n\,(T_a + T_s + T_t)$ $V_{tip} = 1.068$
$v_{tip} = u_{mean} \cdot V_{tip}$ **v_{tip} = 1.2 (m/s)**

Step 16) Calculate the near bed velocity at the toe of the bank (v_{bank})

$B_a = 0.13A^* + 0.05$ (Figure 14) $B_a = 0.076$
$B_s = -0.02(S^* - 4)$ (Figure 18) $B_s = 0.024$
$B_t = -0.8(t^* - 0.6)$ for $t^* > 0.6$ (Figure 20)
$B_t = 0$ otherwise $B_t = 0.009$
Normalised near bed velocity at the toe of the bank
$V_{bank} = B_n\,(B_a + B_s + B_t)$ $V_{bank} = 0.109$
$v_{bank} = u_{mean} \cdot V_{bank}$ $v_{bank} =$ 0.123 (m/s)

Summary :
u_{ch} = 1.43 (m/s) , v_{tip} = 1.2 (m/s), v_{bank} = 0.123 (m/s)

5.2.4 Summary of results

The following table compares the velocities calculated from rectangular and tapered groynes of the same obstruction area and spacing. The effect of the longer tapered groynes is to provide slightly greater protection. For groynes of the same length the tip velocity is less for tapered groynes than rectangular groynes. In this case, the tips of the tapered groynes are in deeper, faster water and the overall effect is that the tip velocity is only slightly reduced.

Velocity	'Rectangular' groynes	Tapered groynes
Depth averaged velocity in main channel u_{ch} (m/s)	1.43	1.43
Near bed velocity near groyne tip v_{tip} (m/s)	1.2	1.2
Near bed velocity at toe of bank v_{bank} (m/s)	0.128	0.123

6 Conclusions

6.1 Summary of work

1) The numerical model (SSIIM) has been used to predict flows in a straight channel with river groynes.

2) Flow patterns are largely independent of river discharge and the absolute size of the river channel and thus the groyne design can be based on velocities normalised by the average upstream velocity.

3) The performance of groyne fields has been described in terms of the normalised velocities at three key locations: in the main channel, near the groyne tip and at the river bank.

4) Equations have been derived for these velocities in terms of geometric parameters describing: the groyne shape; the groyne area ratio; the groyne taper; and the groyne spacing.

5) The influence of channel roughness on the performance of river groynes has been studied and a theoretically derived equation has been found which approximately predicts this influence.

6) The importance of the distinction between depth averaged and near bed velocities has been established. This also demonstrates the value of a 3D numerical model.

6.2 The layout and design of groynes

1) The aspect ratio of the river section has a significant effect on the flow patterns in a groyne field. Shallower rivers and shallower banks reduce velocities in the lee of the groynes, reducing both the size and strength of the recirculation.

2) Increased roughness in the river bed has a similar effect to that of shallow rivers, with reduced flows in the lee of the groynes.

3) Rectangular groynes tend to significantly increase the flow velocity near the bed. This is particularly the case where the upstream channel has a high roughness producing relatively low near-bed velocities. Thus, to avoid scour at the groyne tip tapered groynes are particularly useful in rivers with a high value of Manning's coefficient.

4) The blockage area of groynes is a key factor in determining all velocities in the groyne field.

5) The numerical results indicate that groynes placed at right angles to the flow give the optimum performance.

6) The flow at a groyne tends to expand towards the bank at an angle of about seven degrees to the main flow. This makes it possible to determine the point at which high velocity flow will reach the toe of the bank and potentially cause extra erosion.

6.3 The use of 3D computational models in predicting flows around groynes

1) The numerical grid must be refined in the region of the groyne tips and in shear layers between the main channel and the recirculating flow between the groynes.

2) The number of layers in the vertical grid may be as low as four for adequate resolution of the vertical distribution of flow. However, in particular circumstances the sensitivity of the results to the vertical grid spacing should be checked.

3) Although 3D numerical models are more flexible than physical models, they have their own limitations. These include:

- The time taken to design and construct a suitable numerical grid, which is sufficiently accurate without being too large to be run in an acceptable time.
- The need to select internal parameters, such as relaxation factors, that affect the behaviour of the numerical model with the possibility that the model will converge slowly (or not at all) if these parameters, or the grid, are not chosen correctly.
- The time required to extract and present suitable numerical and visual summaries of the large amount of data produced.
- The approximations within the numerical model, particularly the turbulence model and thus the need to validate the model's ability to solve a particular class of problem.

4) Despite the above limitations, with the rapid development of computer hardware and software, it is likely that 3D numerical models will find an increasing role in practical applications in river engineering.

6.4 Recommendations for further work

The scope of this guide has been limited by the number of computer simulations that could be made. Thus, many conditions, which may be important in practical applications, are not covered by the present report. Future work should include the following items:

1) Further investigation of the influence on bank velocities of the slope and relative width of the river bank; and the roughness of the river bed. It would then be possible to determine a recommended groyne length and groyne spacing that specifically includes the above factors and accounts for the separate effects of blockage and bank protection.

2) Calibration of the numerical model for predicting turbulence, so that the effect of groyne angle on sediment transport and armour stability can be quantified.

3) Comparison of design manual predictions with experimental or prototype measurements for a natural river geometry.

4) Calibration of the numerical model for simulating permeable groynes.

5) Extension of the guidelines to include sinuous and meandering channels.

7 References

Chow VT (1959). Open-Channel Hydraulics, McGraw Hill, Tokyo.

Escarameia M and May RWP (1995). Stability of riprap and concrete blocks in highly turbulent flows. Proc. Inst. Civil Engrs., Wat. Marit. & Energy, 1995,**112**, Sept, pp227-237

Escarameia M and May RWP (1992). Channel protection: Turbulence downstream of structures", HR Wallingford, Report SR313.

Hemphill RW and Bramley ME "Protection of River and Canal Banks guide to selection and design". CIRIA water engineering report, Butterworths 1989.

Henderson FM (1996). Open Channel flow, Macmillan, New York.

HR Wallingford (1990). Groynes and Training works affecting River Planform - A literature review. HR Wallingford, Report SR229, August.

Izbash, S.V. and Khaldre, K.Y. (1970). Hydraulics of River Channel closure, Butterworths, London.

Maza Alvarez J.A. (1989). Design of groins and bridge piers . Hydraulic Engineering. Proc. of 1989 Nat. Conf. on Hydr. Eng., New Orleans. ASCE Louisiana, Aug., 14-18; 296-301.

Przedwojski B, Blazejewski R and Pilarczyk (1995). "River Training Techniques – Fundamentals, Design and Applications". AA Bakerna, Rotterdam, ISBN 90 5410 196 2.

Seed DJ (1997). River Training and Channel Protection - Validation of a 3D numerical model. HR Wallingford, Report SR480, March.

Simons DB and Albertson ML (1960), Uniform Water Conveyance Channels in Alluvial material. Proc. Am. Soc. Civil Engrs, vol. 86, HY5, May, p33

Olsen NR (1996) " A Three-dimensional numerical model for the Simulation of Sediment Movements in Water Intakes with Multiblock option (Version 1.4 beta). Univ. Trondheim, March 1996

Tamai N, Kawahara Y, Aoki M, Matumoto A, Ishikawa Y and Yasuda M (1996), Ecohydraulics of Spur dikes in Ushizu River, Kyushu Region, Japan. Proc. 2nd International Symposium on Habitat Hydraulics, Ecohydraulics 2000, Quebec, June 1996, ppB631-B642.

Table

Table 1 Recommended groyne spacing for bank protection (from HR report, SR229)

Reference	Bank	Spacing	Comment
Grant, 1948	Concave	$3L_t$	
UNCAFE, 1953 UNCAFE, 1953	Concave Convex	$1L_t$ 2 to $2.5L_t$	General practice General practice
Richardson & Simons, 1973	Concave	4 to $6L_t$	Bank may need riprap
Neill, 1973	Either	2 to $4L_t$	Four or more
Jansen et al, 1979	Either	$<0.6d^{4/3}/2gn^2$	Model tests at DHL
Los Angeles District, 1980 Los Angeles District, 1980 Los Angeles District, 1980	Straight Concave Convex	$2L_t$ $1.5L_t$ $2.5L_t$	Embankment should be protected with riprap
Garg et al, 1980	Either	3 to $4L_t$	Upstream orientation
Maccaferri, 1980 Maccaferri, 1980	Concave Convex	$4L_t$ $6L_t$	Gabions Gabions
Copeland, 1983	Concave	Up to $3L_t$	Bank may need riprap
Bognar & Hanko, 1987	Either	$1.2L_t$	Maximum siltation
Alvarez, 1989 Alvarez, 1989	Straight Concave	4 to $6L_t$ 2.5 to $4L_t$	For irregular curves spacing found graphically
Salikov, 1987	Concave	7 to $10L_t$	

Figures

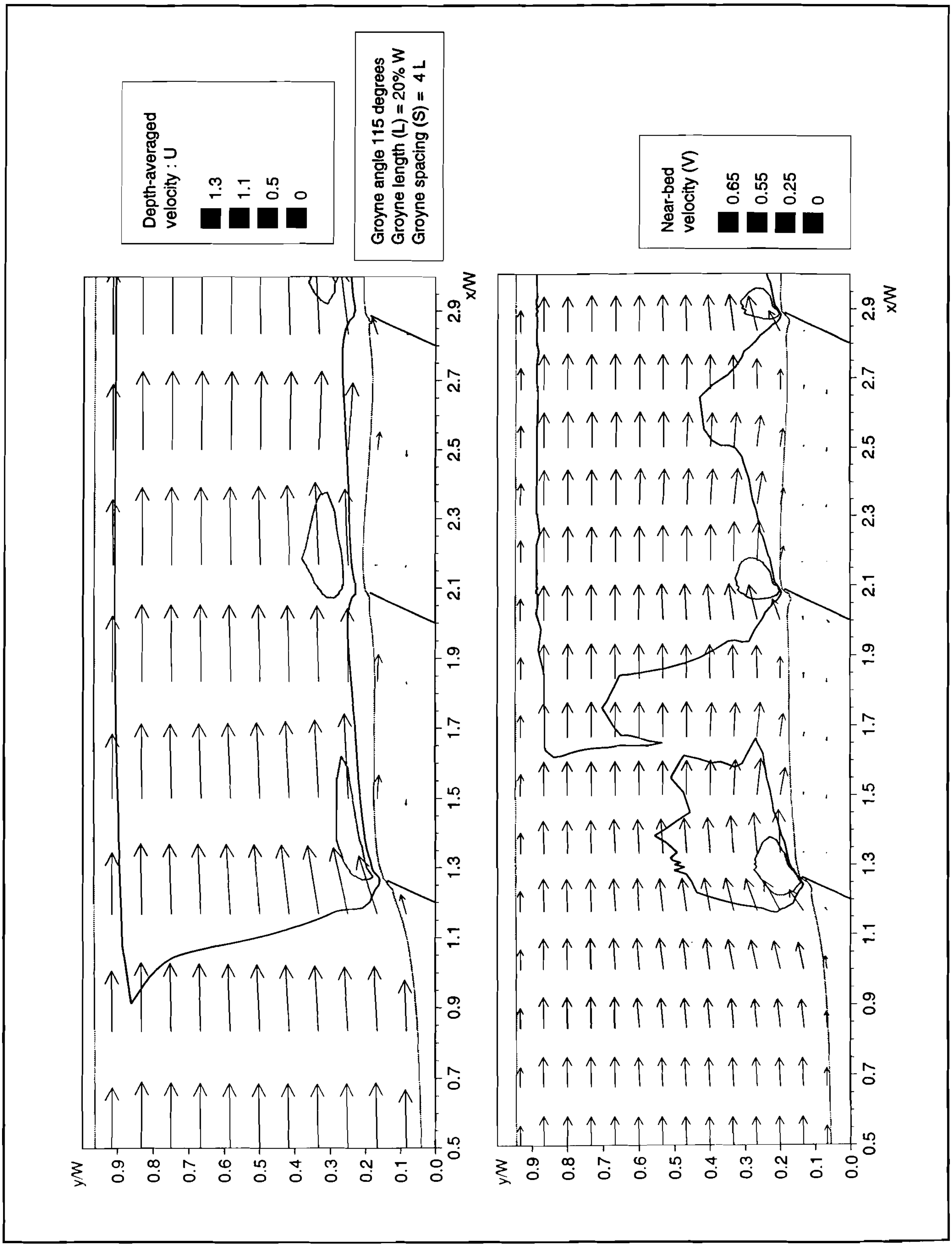

Figure 1 Flow patterns in a field of groynes

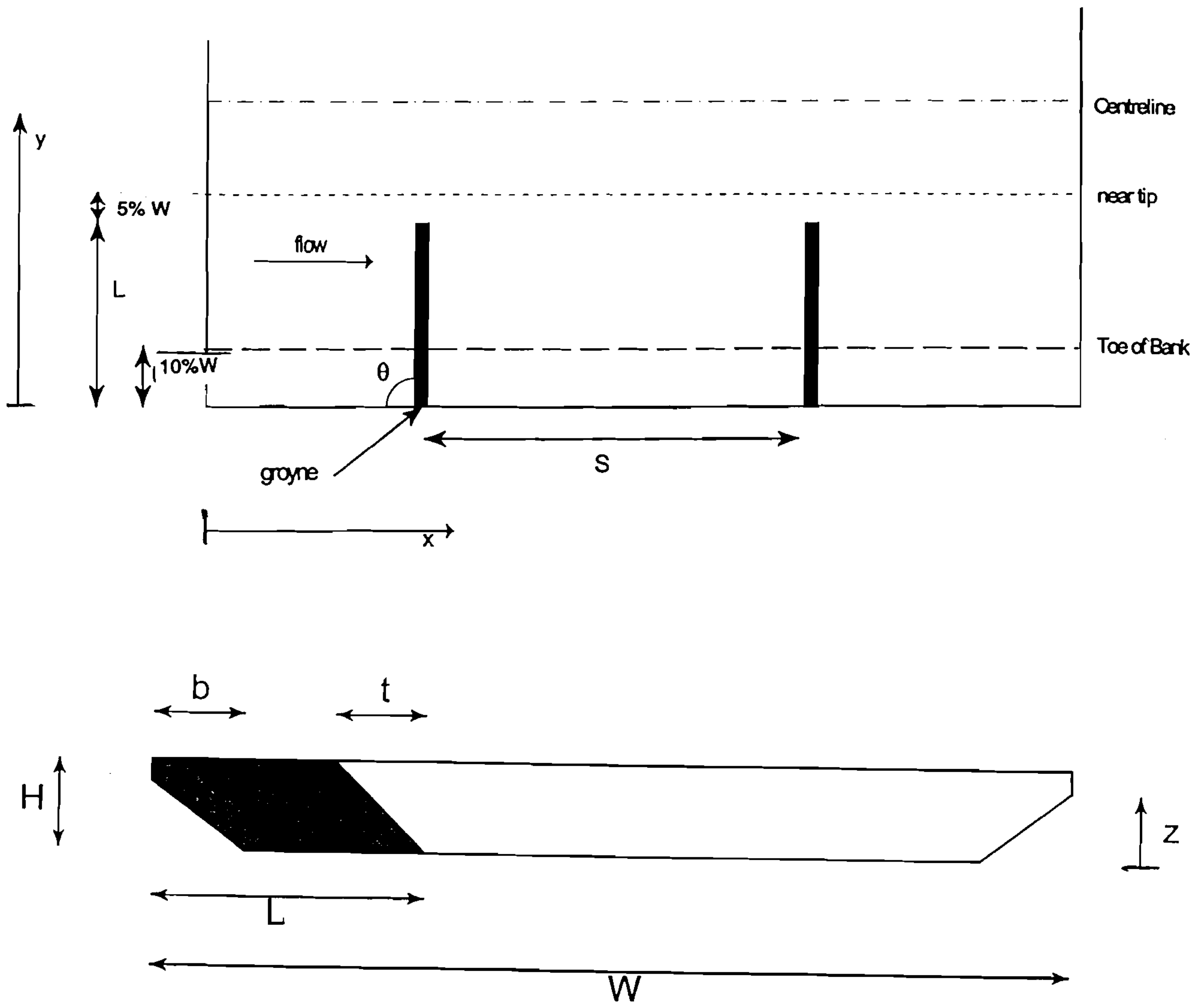

W - River width
b - Bank width $b^* = b / W$
L - Groyne length $L^* = L / W$
S - Groyne spacing $S^* = S / W$
A_g - Groyne blockage area A - River flow area
A_r - (A_g /A) Relative groyne area (blockage area)
θ - Groyne angle measured from upstream bank
H - Maximum depth $D = A / W$ Mean depth
x - Downstream
y - Cross stream
z - Vertical

Figure 2 Definition sketch for geometric parameters

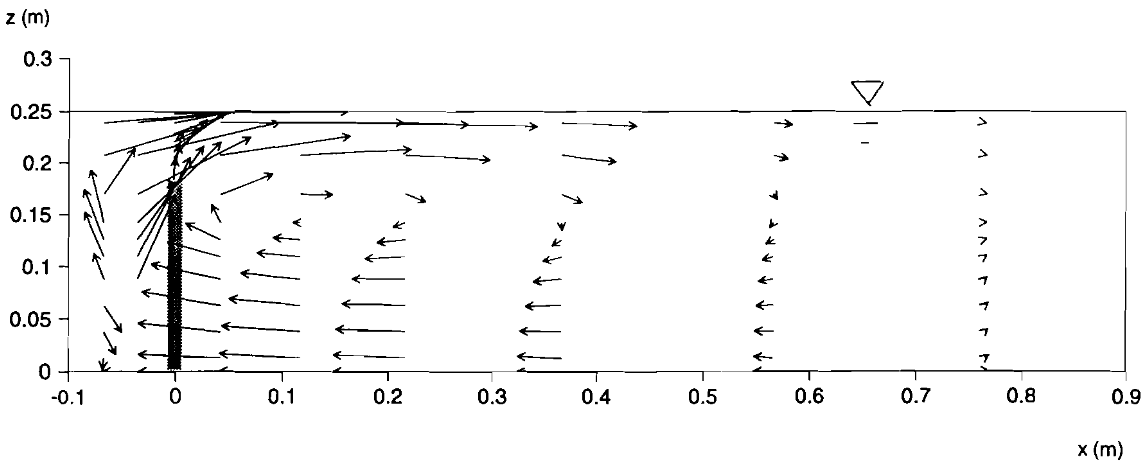

Long section of flows at toe of bank for a submerged groyne
Free surface width of test channel =2.3m (Test TB)

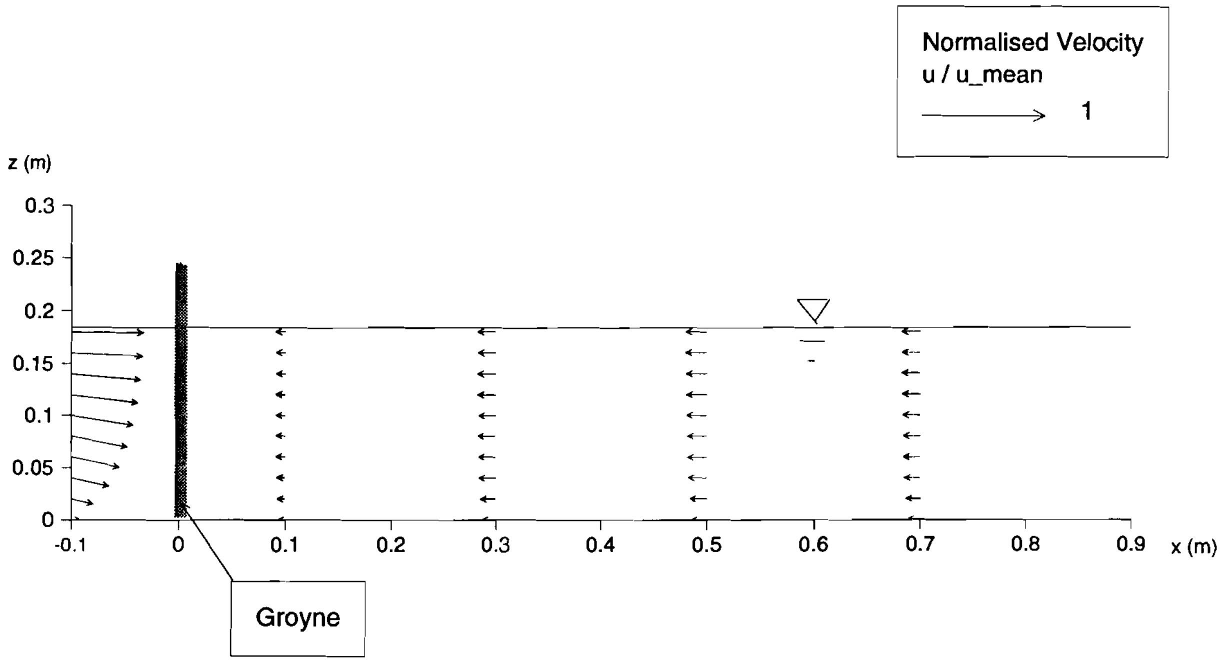

Long section of flows at toe of bank for an unsubmerged groyne
Free surface width of test channel =2.0m (Test TA)

fig3h

Figure 3 Comparison of submerged and unsubmerged groynes

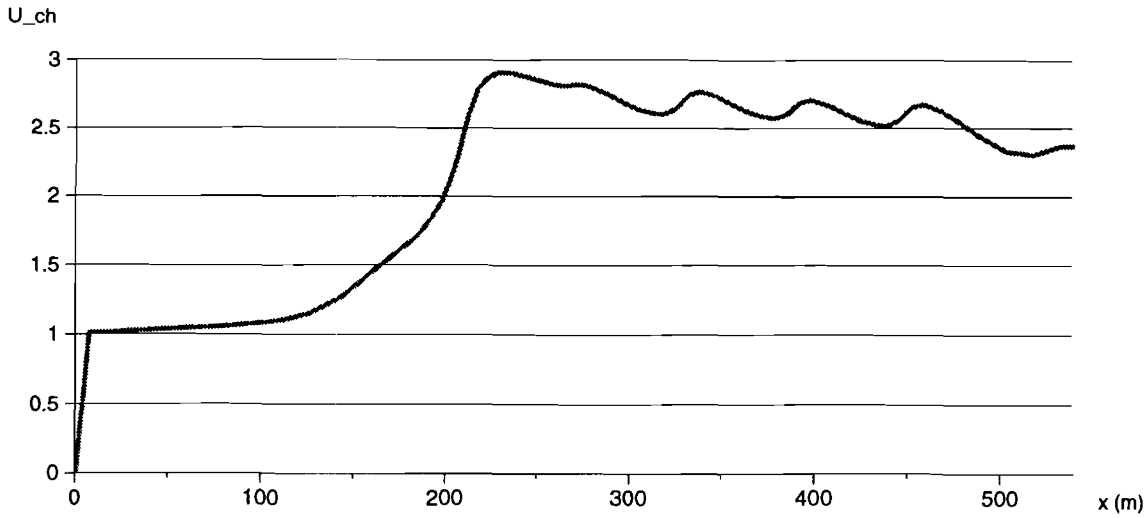

Longitudinal variation of normalised main channel velocity
(U_ch = u_ch/u_mean)

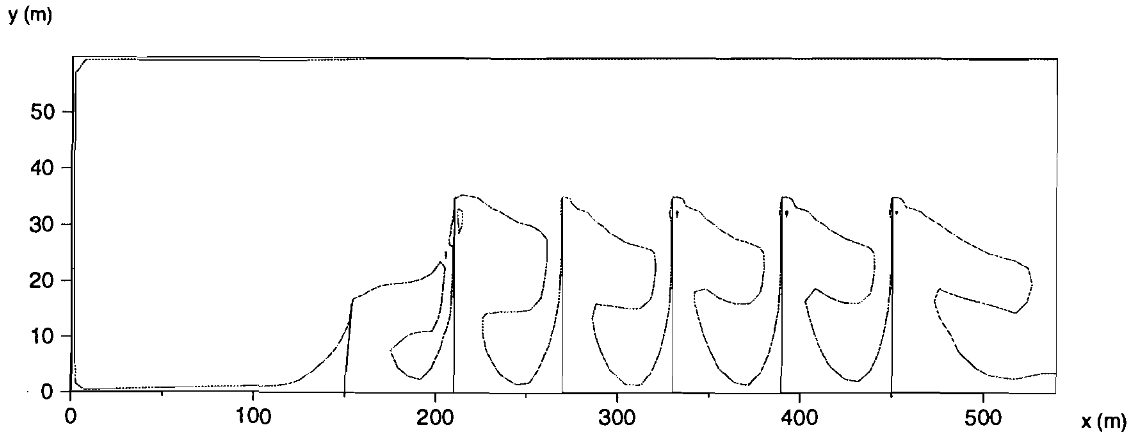

Contour of depth averaged velocity = 20% of mean upstream velocity
(U=u/u_mean =0.2)

Test WFb
Groyne spacing = 1.67 * groyne length
Groyne length = 30% river width
Groynes on both sides of the river
Half river modelled

Figure 4 Longitudinal variation in velocity with long groynes

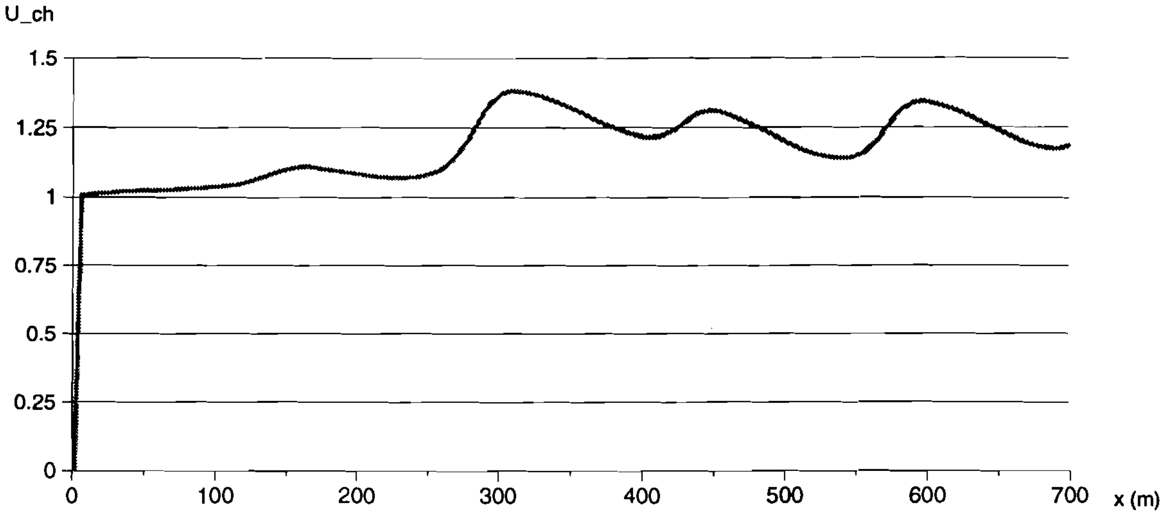

Longitudinal variation of normalised main channel velocity (U_ch = u_ch/u_mean)

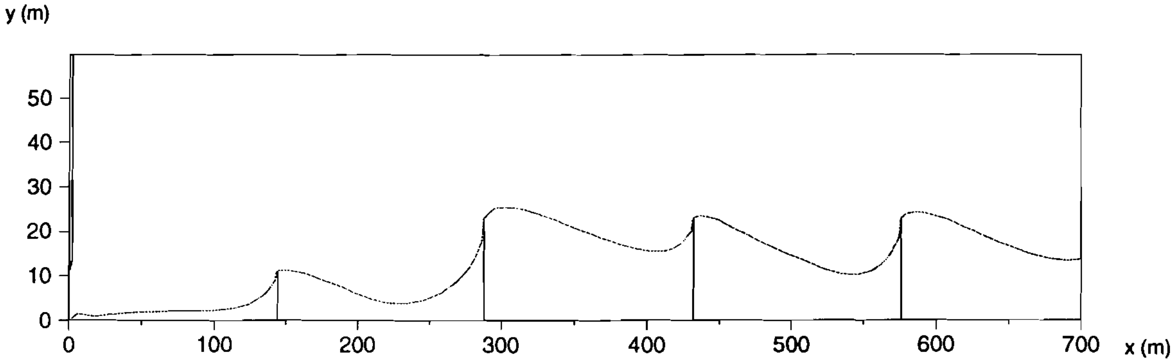

Contour of depth averaged velocity = 20% of mean upstream velocity (U=u/u_mean =0.2)

Test vjk-21
Groyne spacing = 6 * Groyne length
Groyne length = 20% river width
Groynes on one side of the river
Whole river modelled

Figure 5 Longitudinal variation in velocity with widely spaced groynes

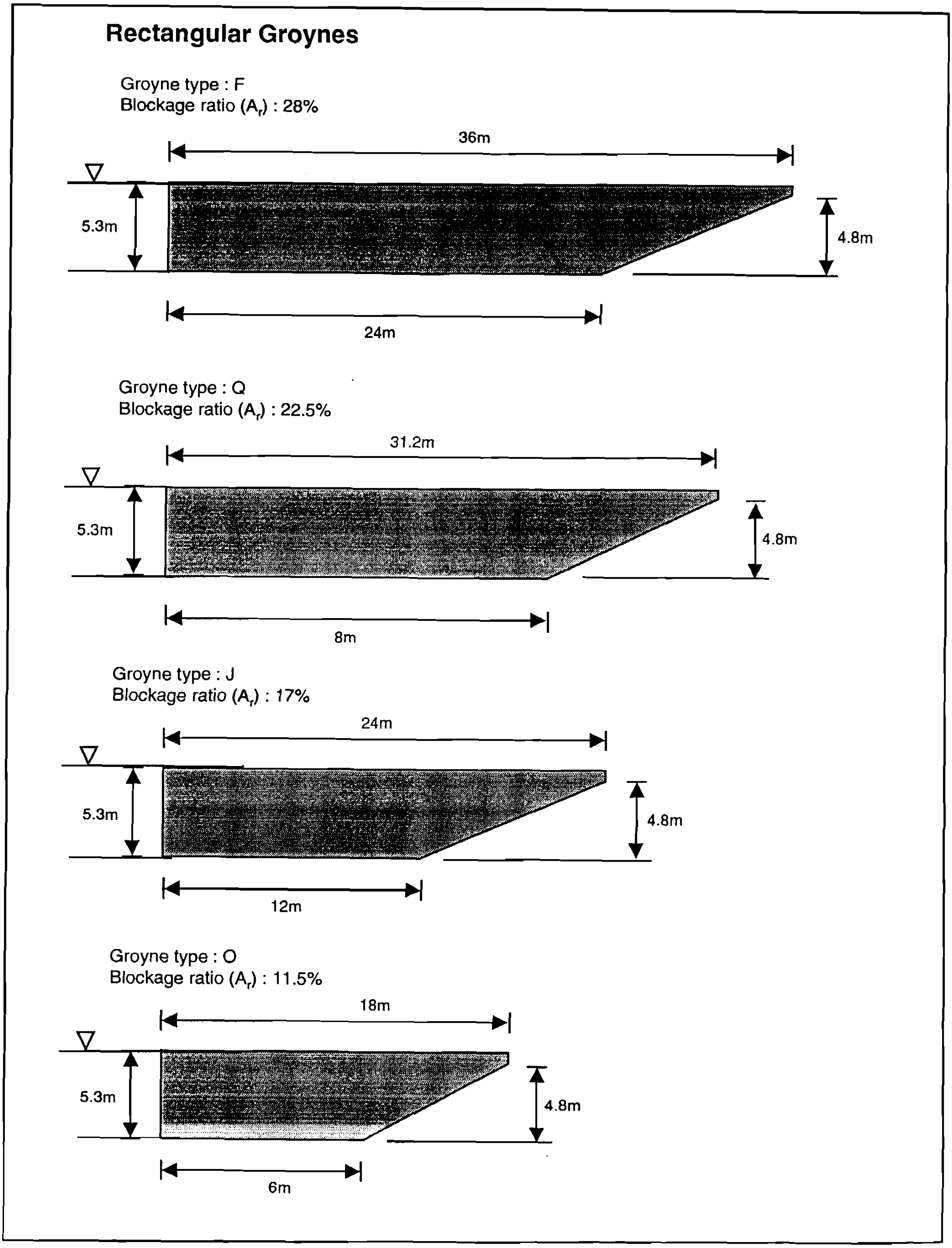

Figure 6 Cross-sections of rectangular groynes used in numerical model tests

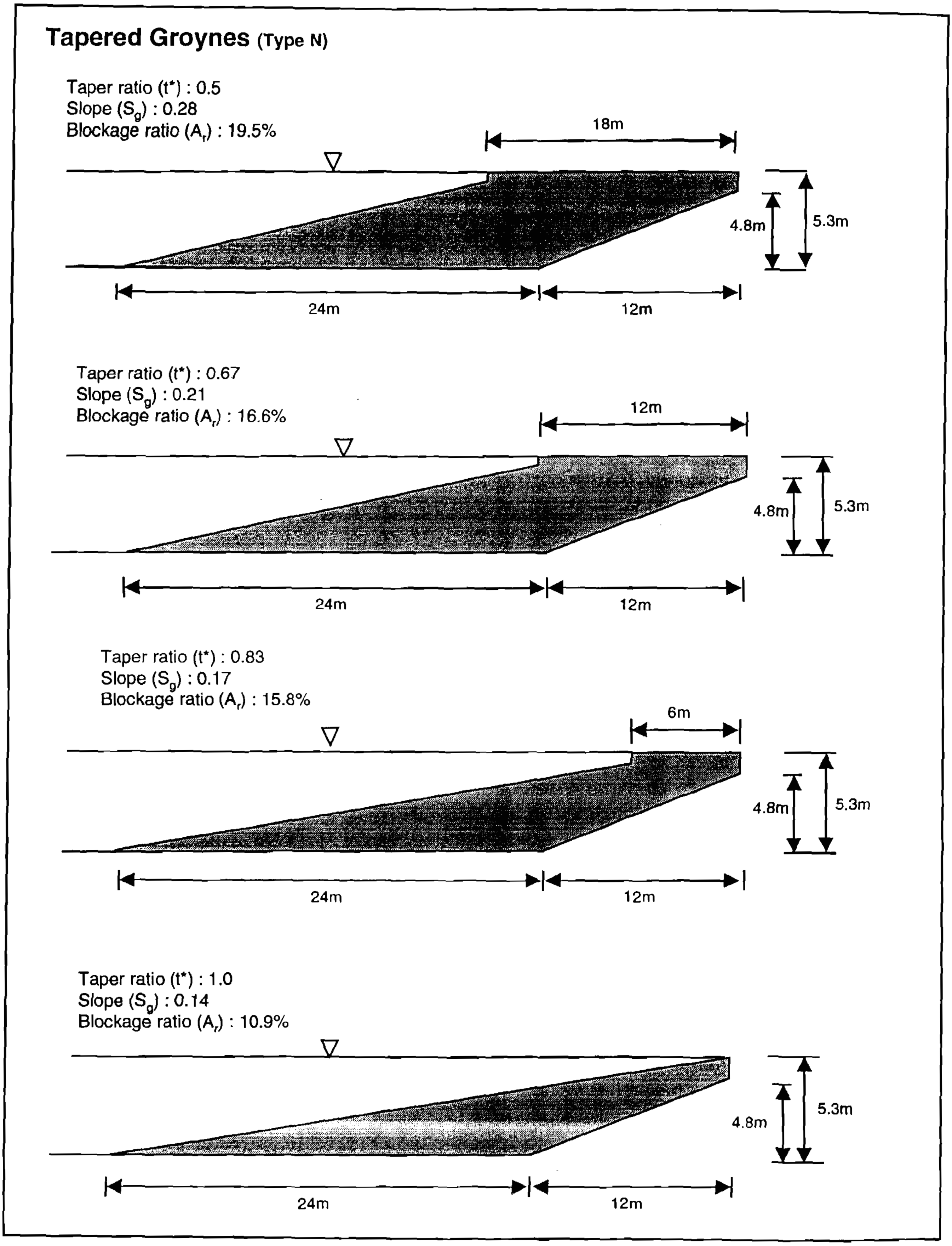

Figure 7 **Cross-sections of tapered groynes used in numerical model tests**

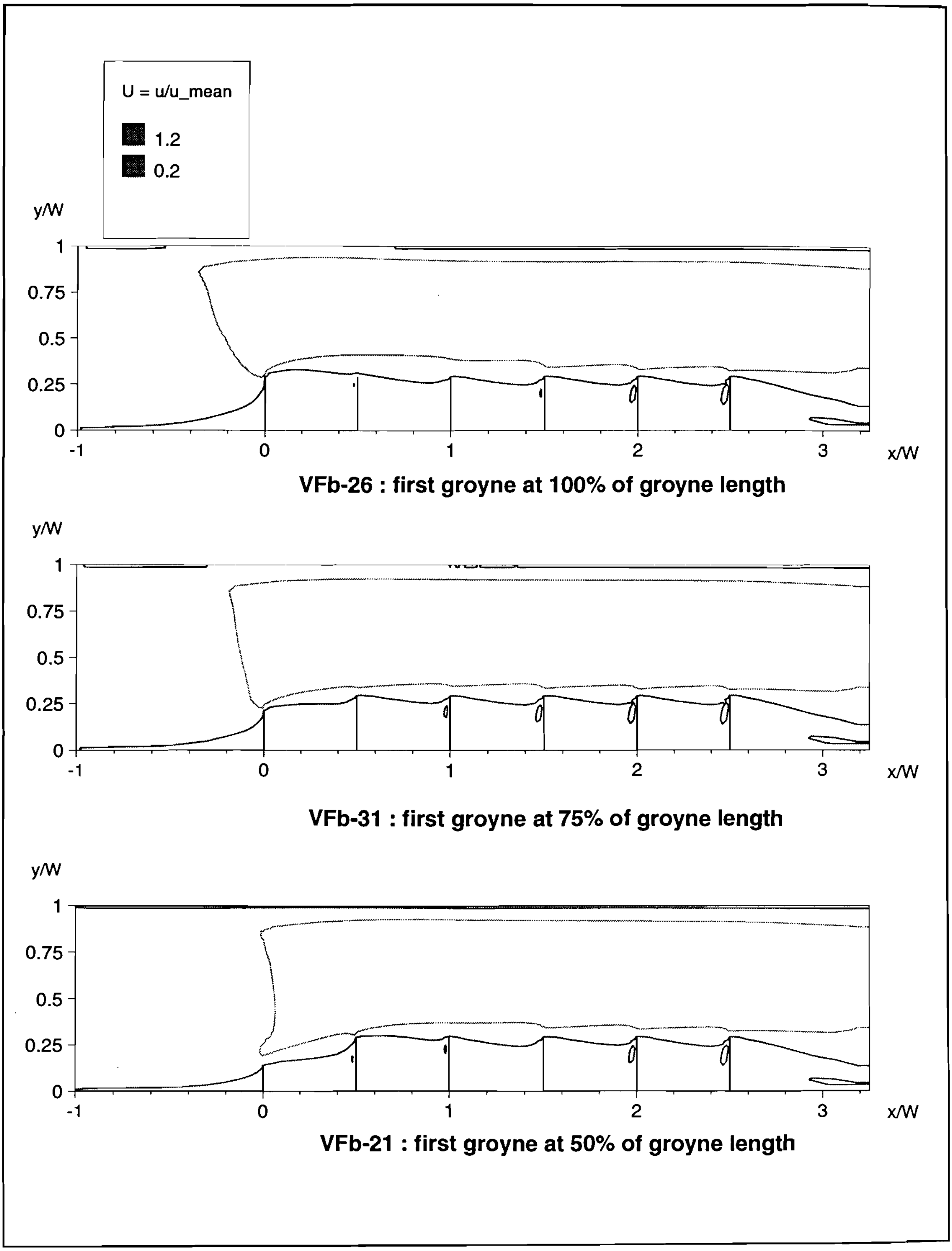

Figure 8 Effect of upstream groyne length on depth-averaged velocity

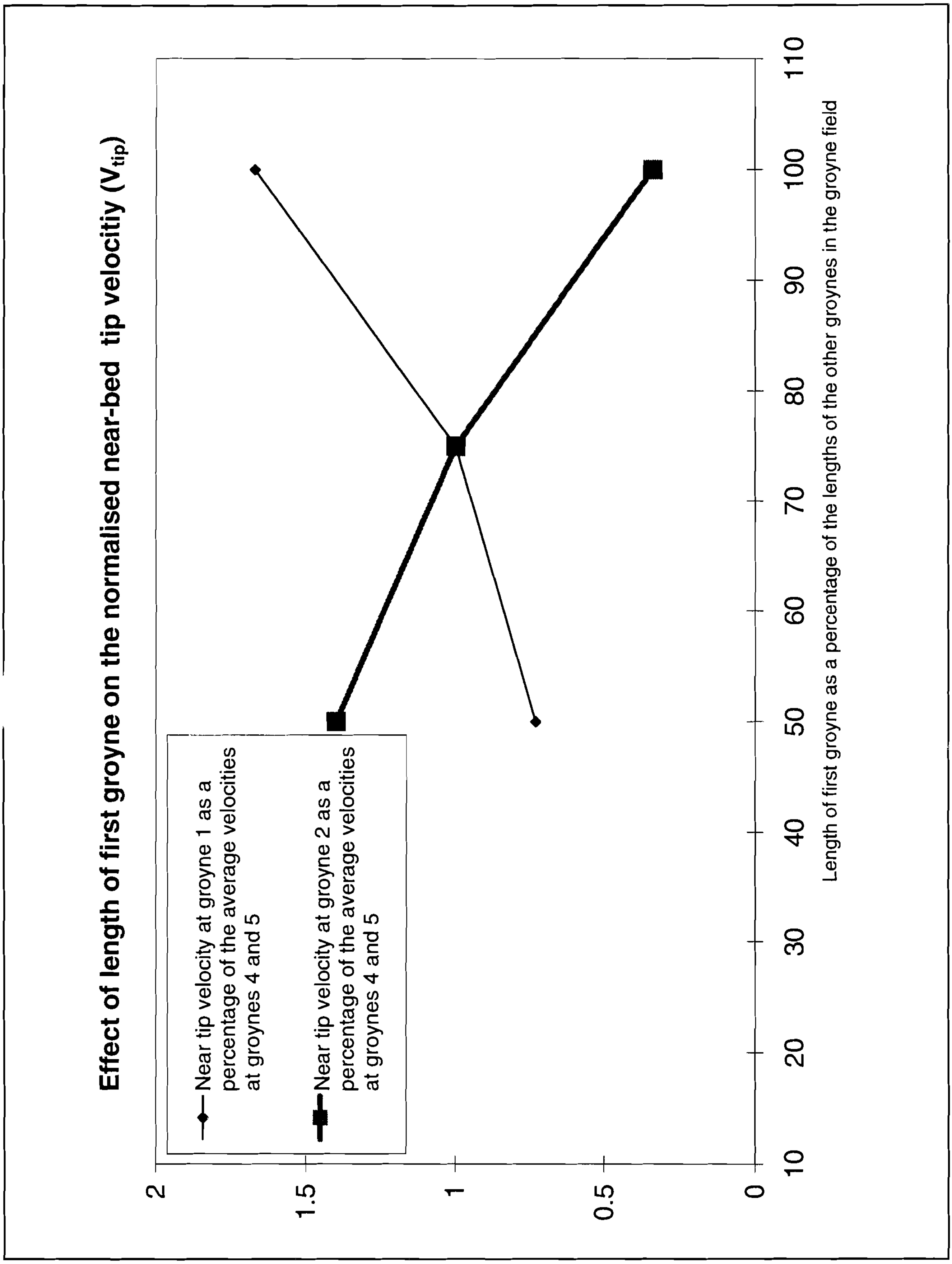

Figure 9 **Effect of upstream groyne length on tip velocity**

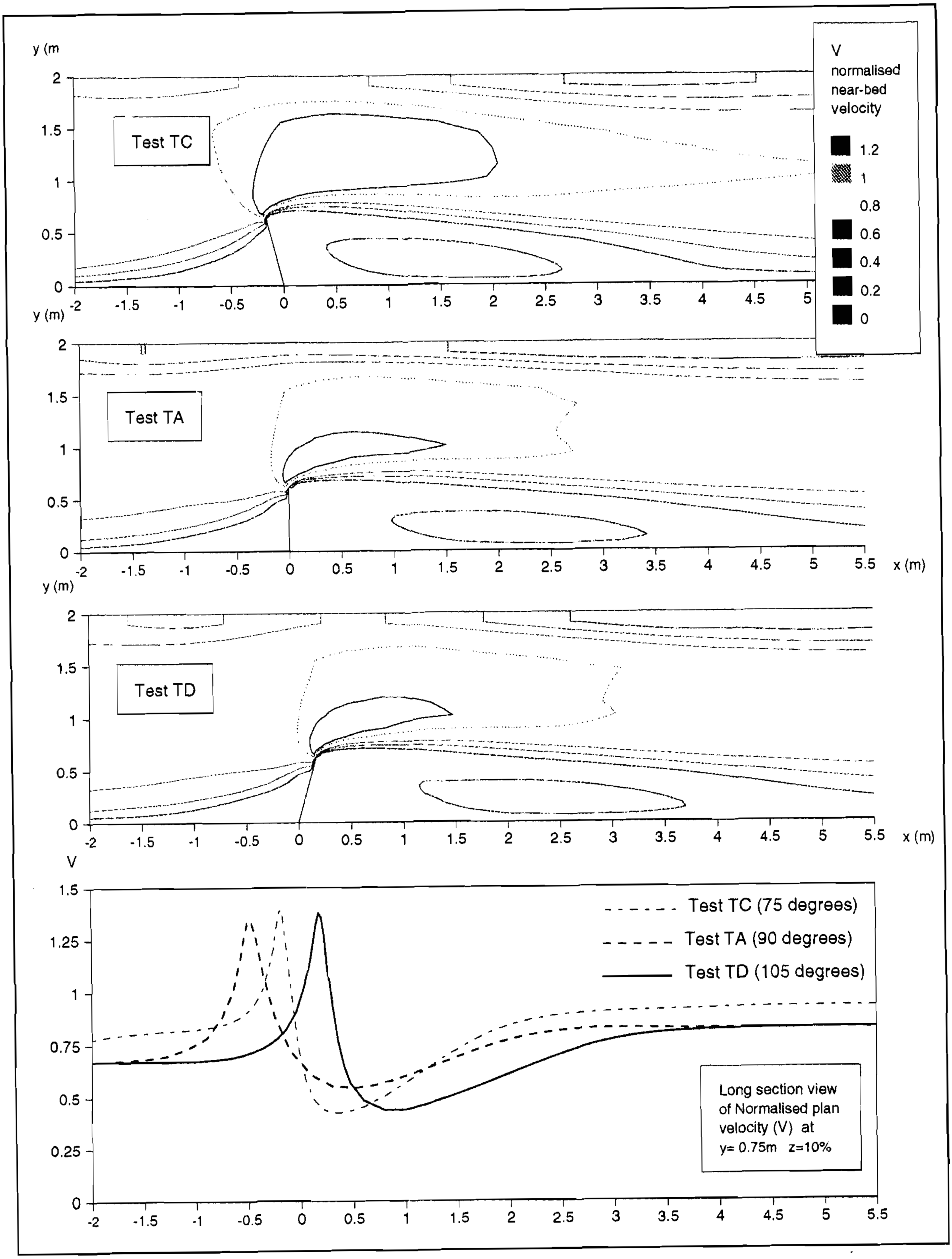

Figure 10 **Effect of groyne angle on normalised near-bed velocity in a 2m trapezoidal channel**

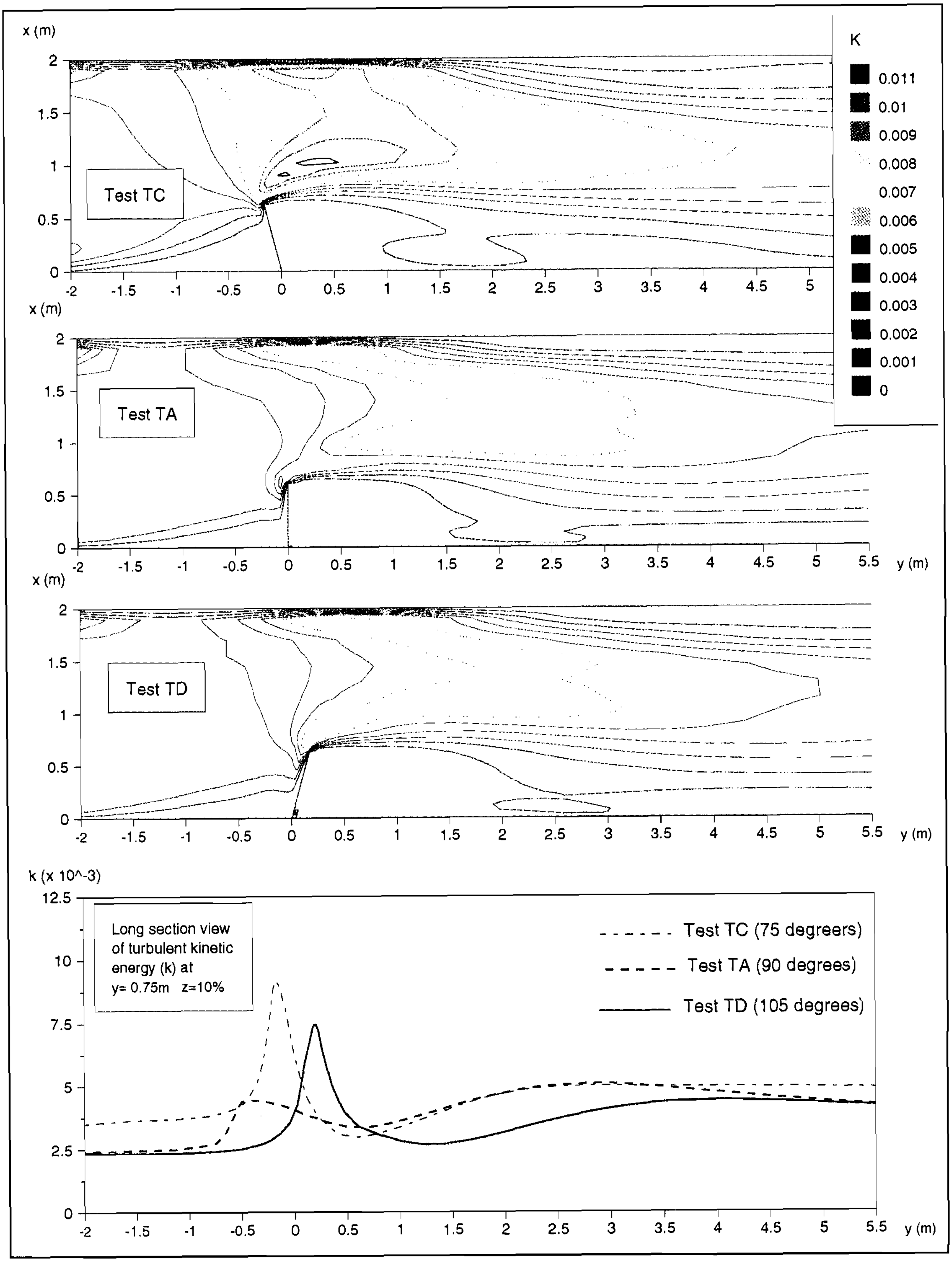

Figure 11 **Effect of groyne angle on near-bed turbulent kinetic energy in a 2m trapezoidal channel**

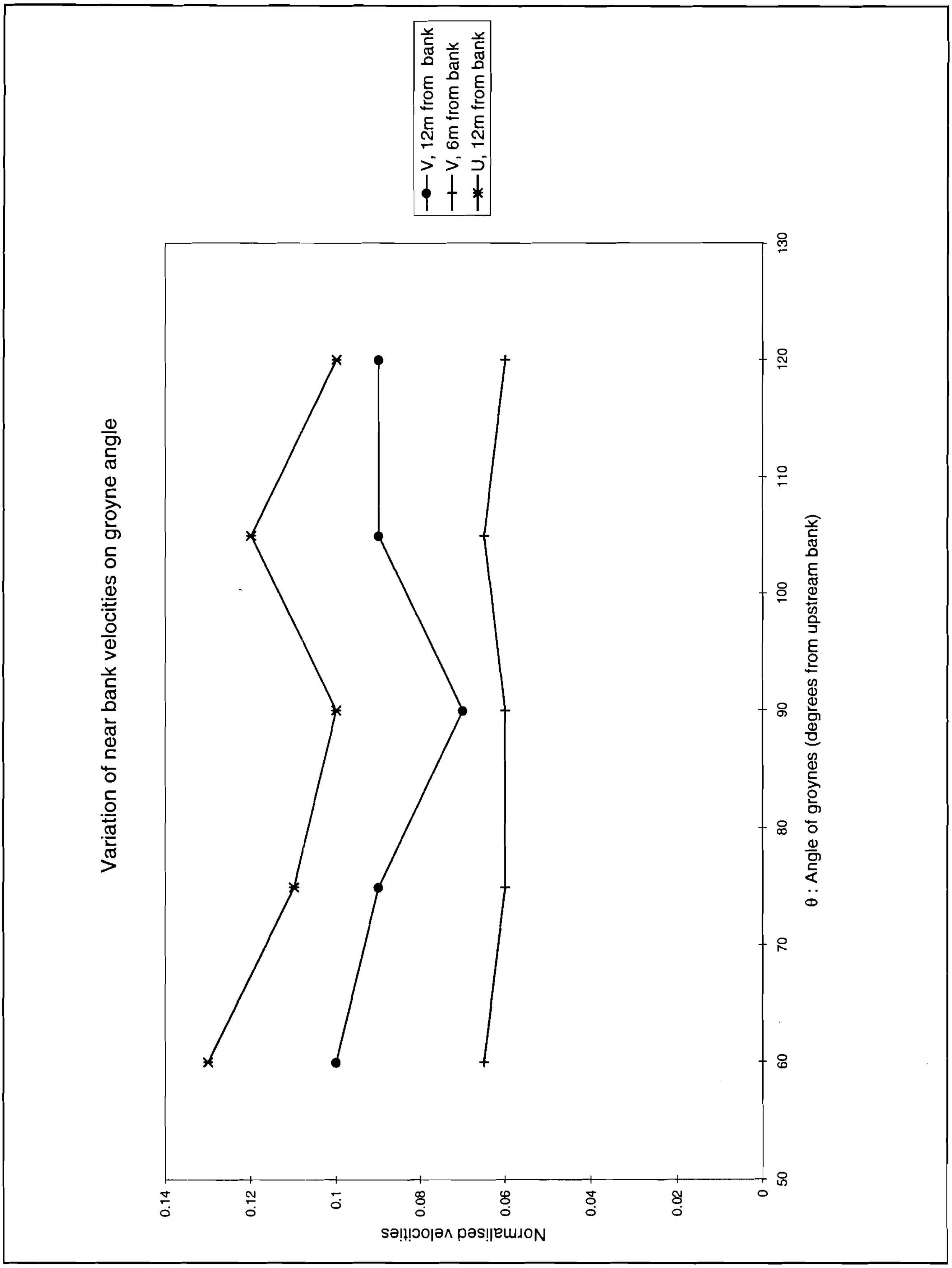

Figure 12 Effect of groyne angle bank velocity

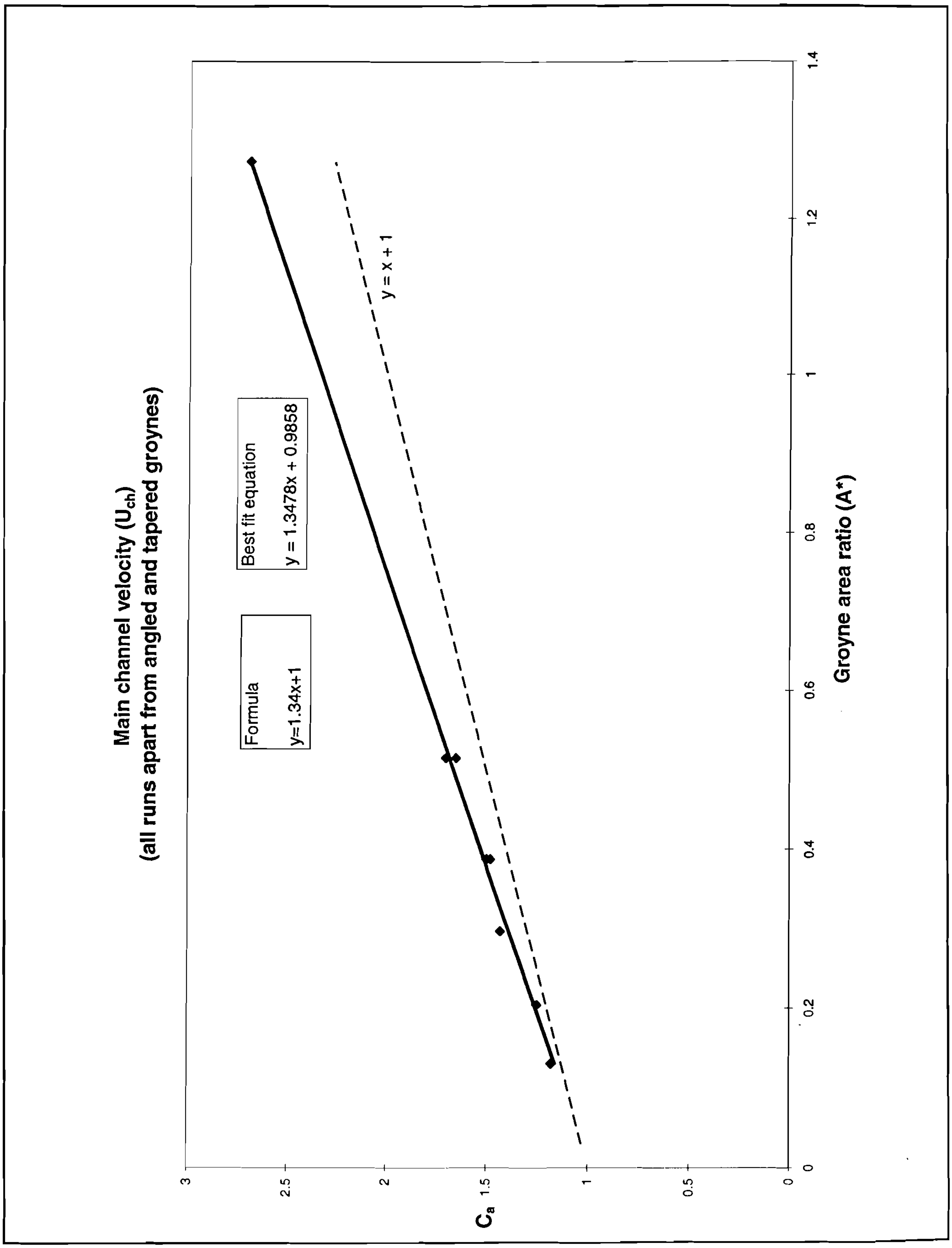

Figure 13 C_a : Effect of groyne angle on main channel velocity

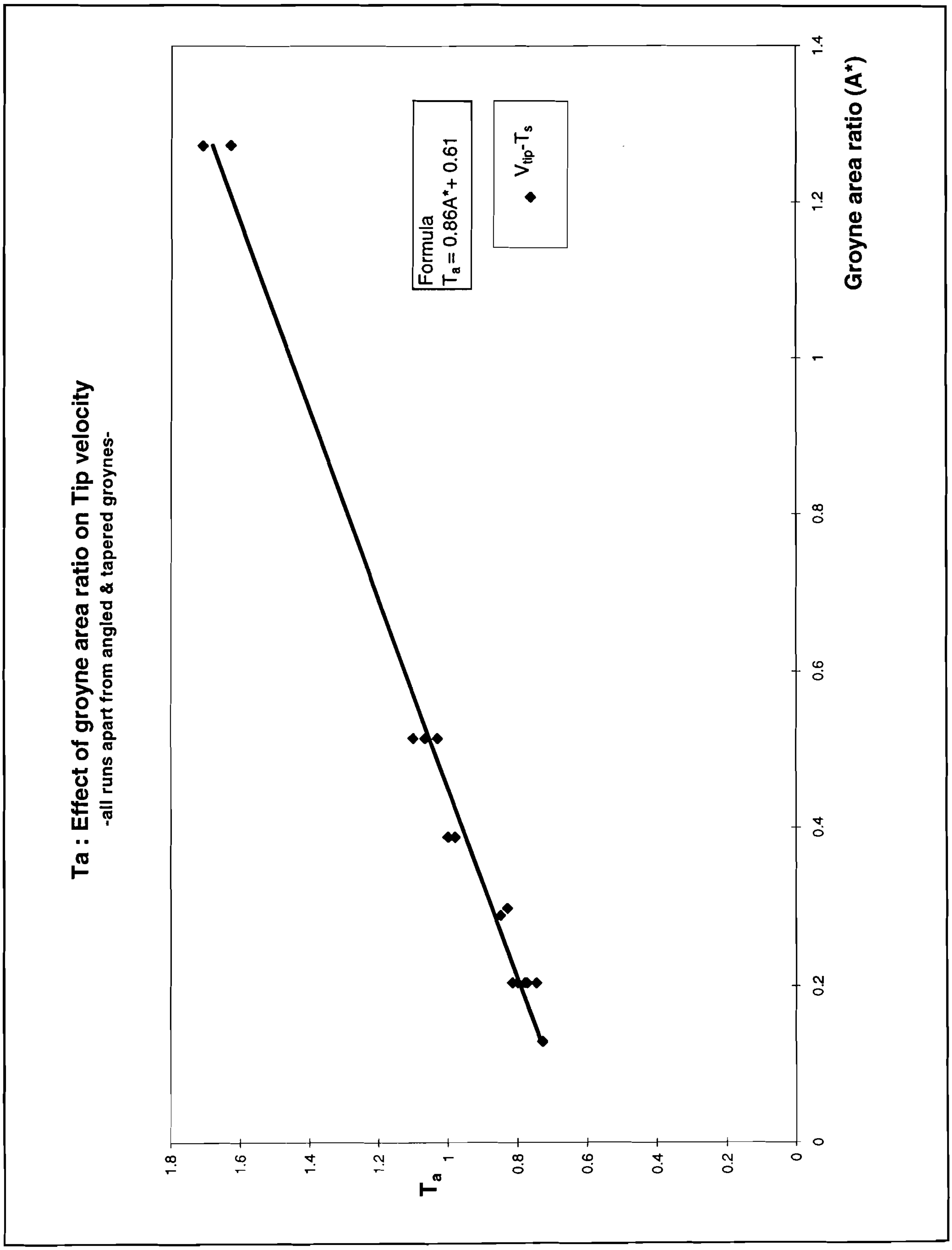

Figure 14 T_a: Effect of groyne area on tip velocity

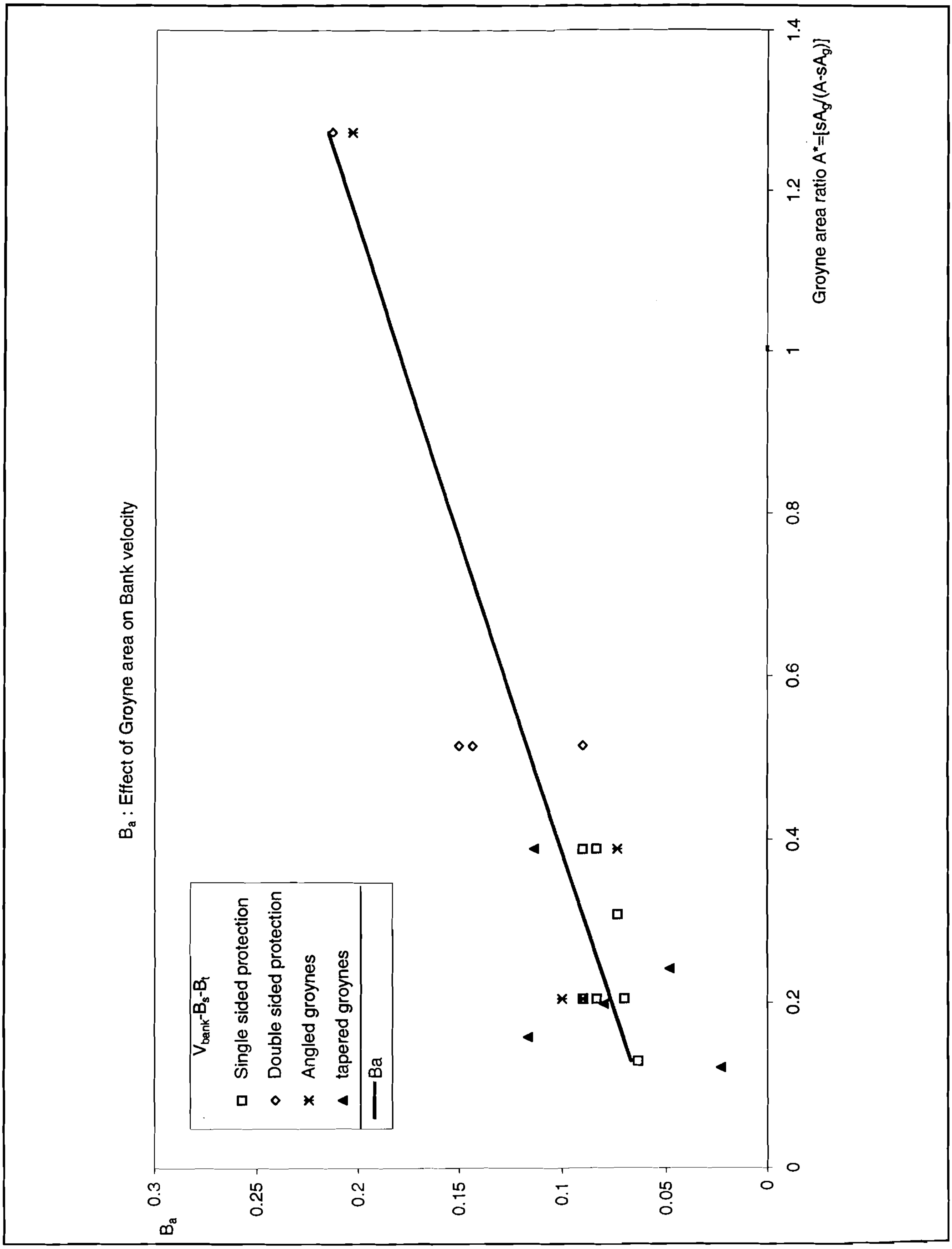

Figure 15 B_a : Effect of groyne area on Bank velocity

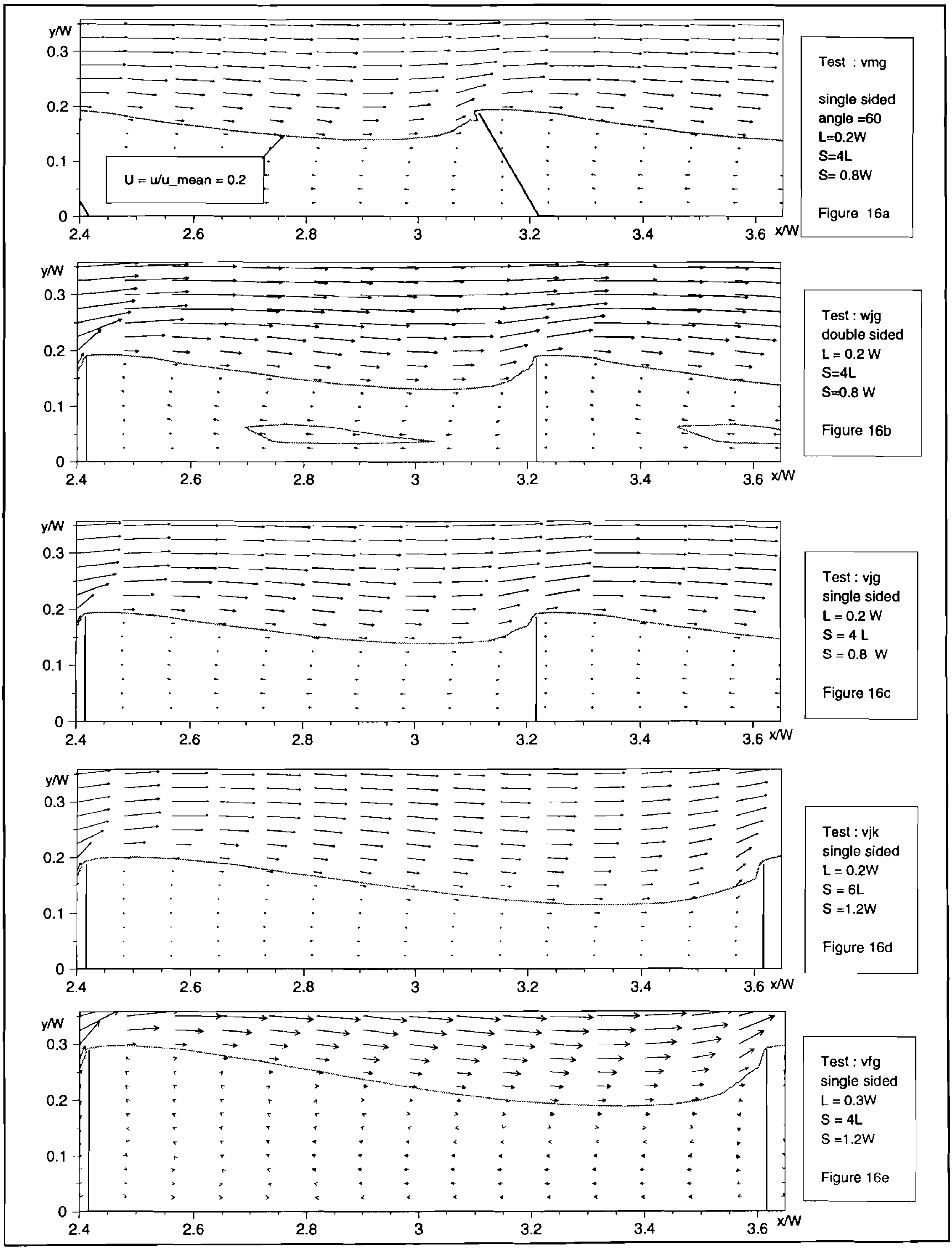

Figure 16 Flow patterns between groynes

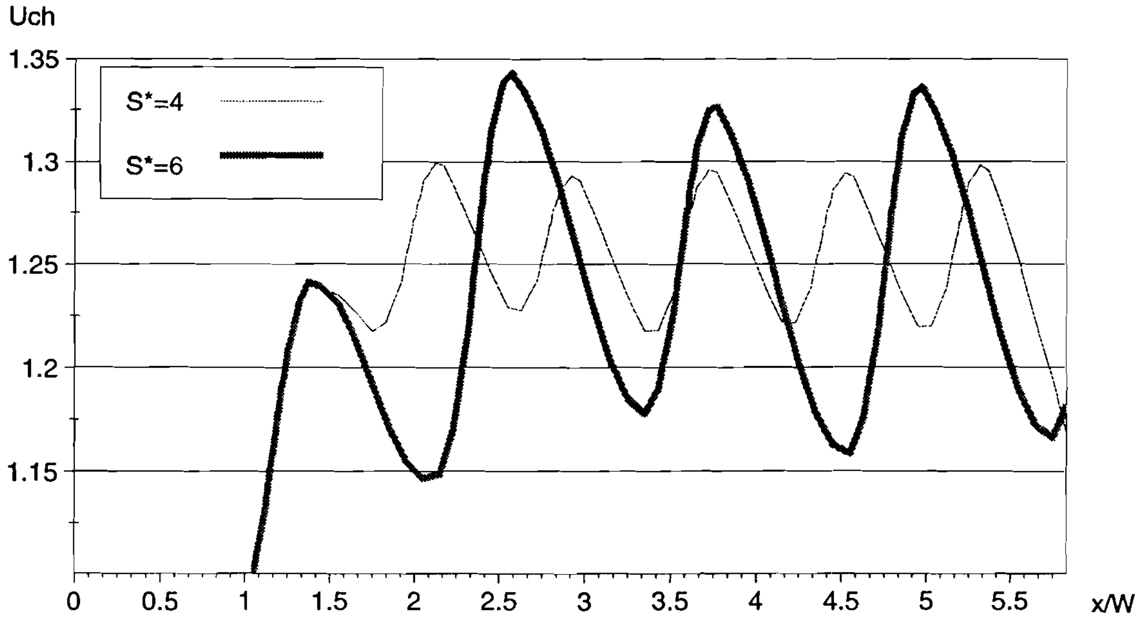

Longitudinal variation of normalised main channel velocity (Uch)

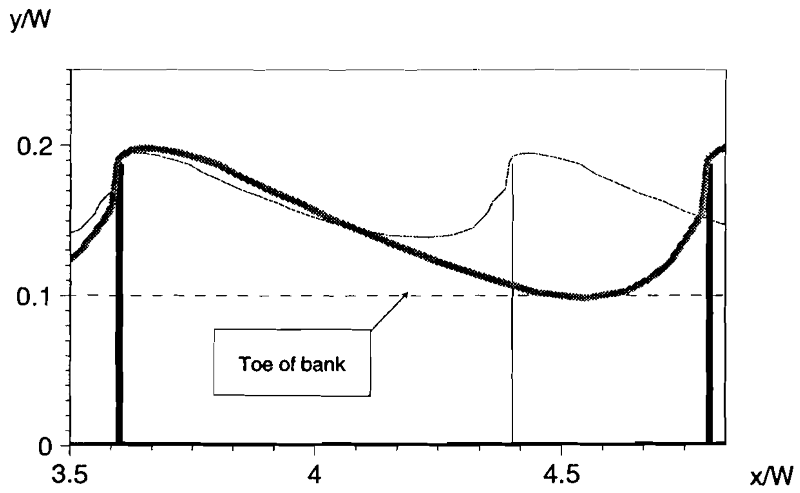

Contours of depth-averaged velocity = 20% of section-averaged velocity (U=0.2) at S*=4 and S*=6

Test vjg (S*=4)
Groyne spacing = 4 * Groyne length
Groyne length = 20% river width
groynes on one side of the river

Test vjk (S*=6)
Groyne spacing = 6 * Groyne length
Groyne length = 20% river width
groynes on one side of the river

Figure 17 Effect of groyne spacing – expansion of flow

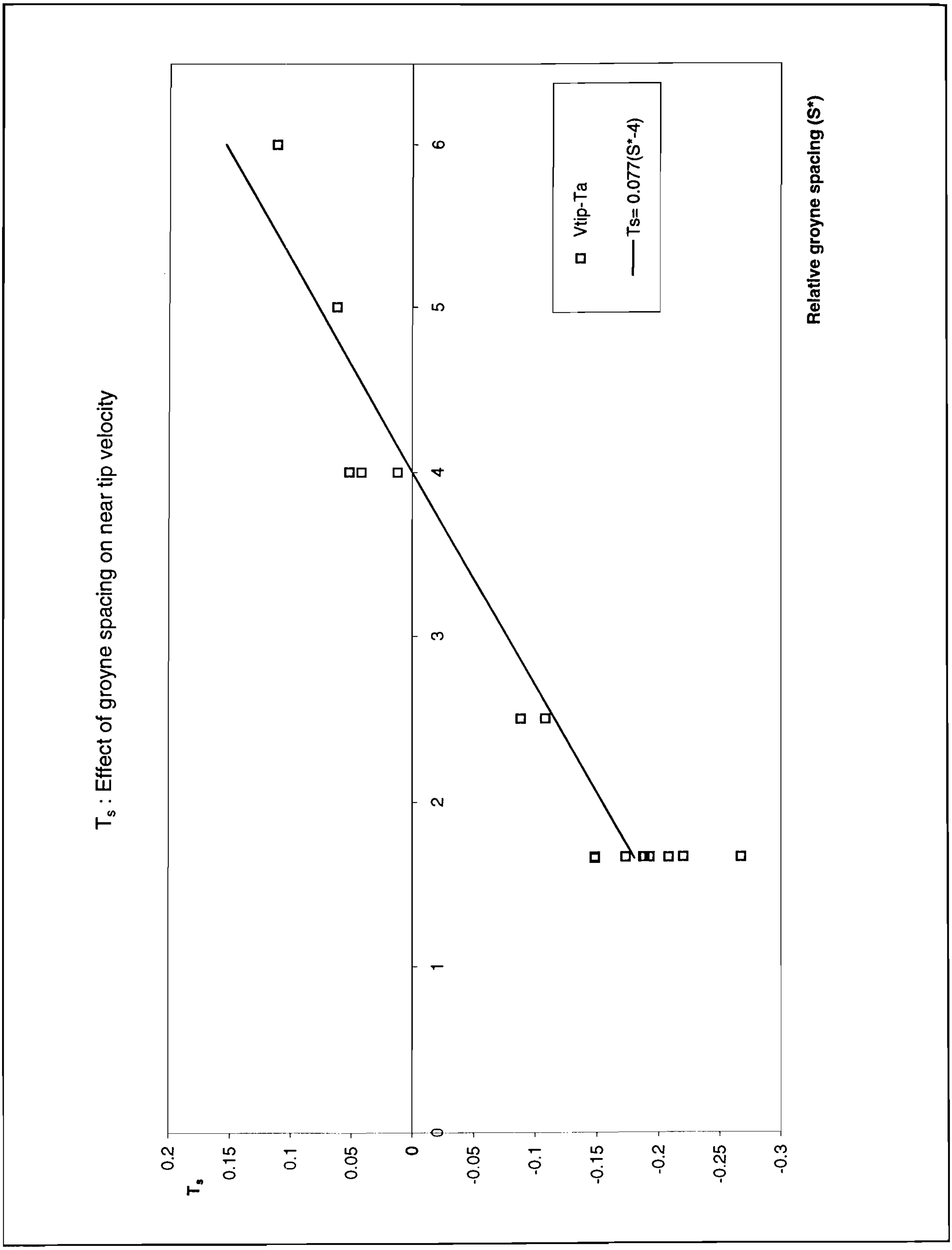

Figure 18 T_s : **Effect of groyne spacing on tip velocity**

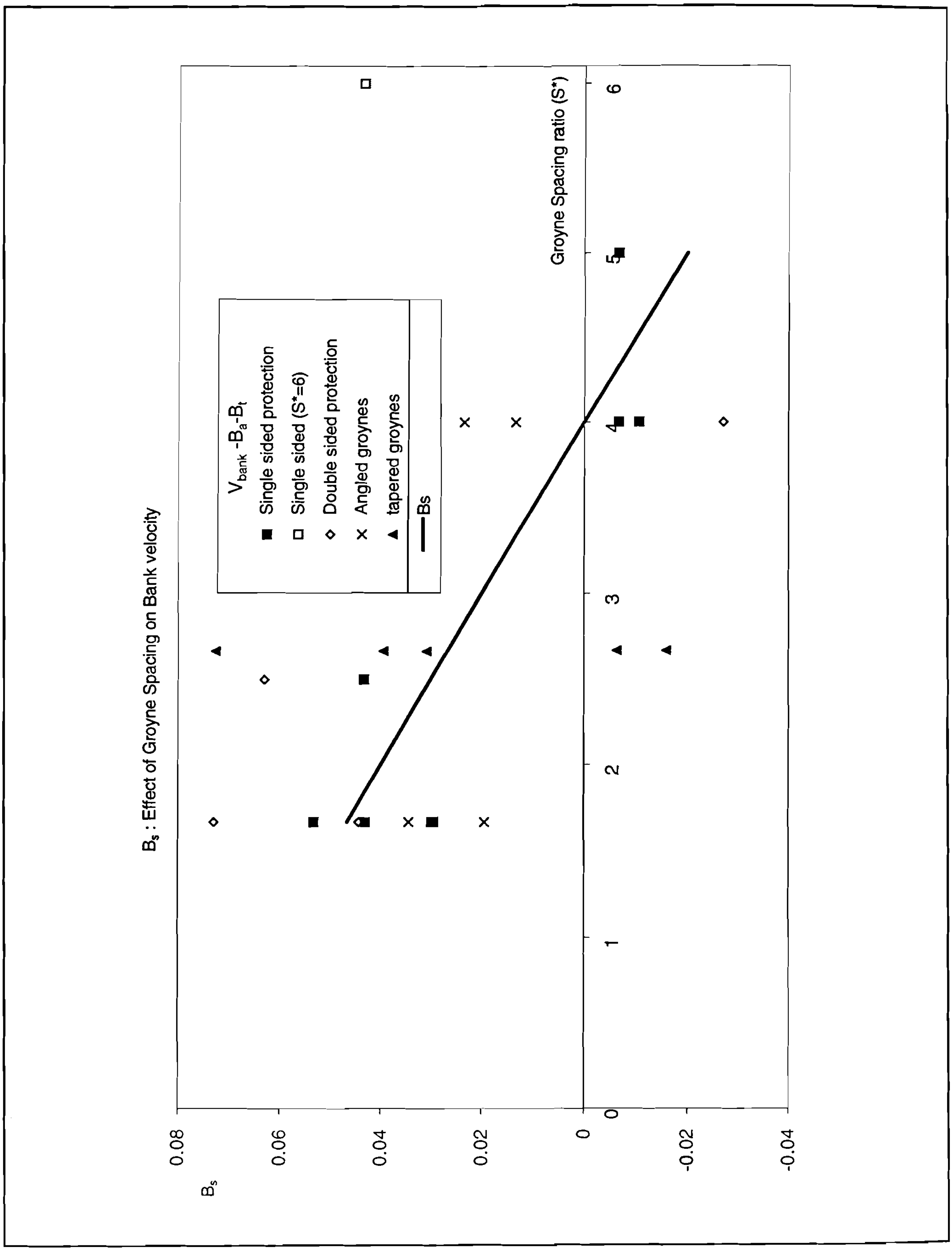

Figure 19 **B_s : Effect of groyne spacing on Bank velocity**

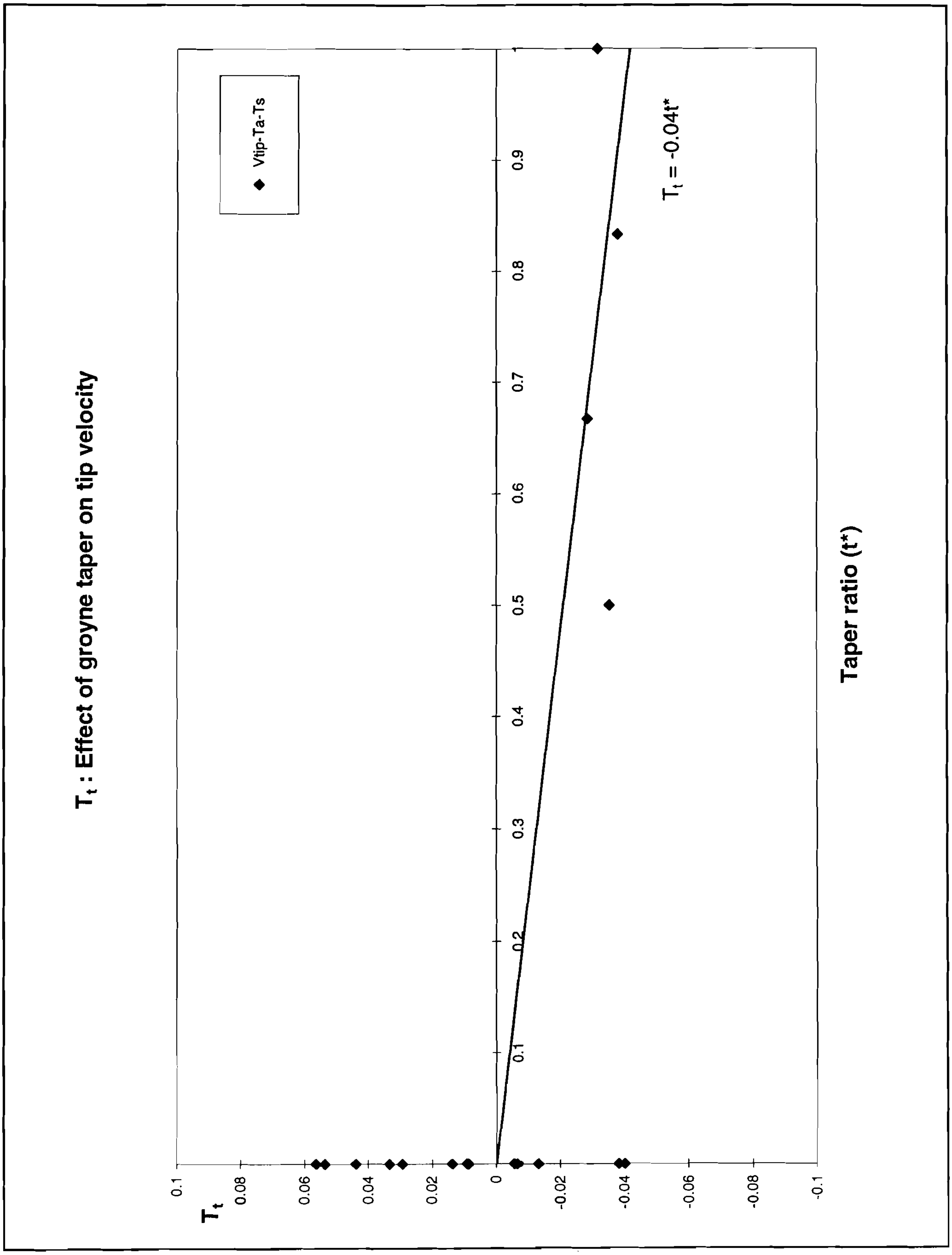

Figure 20 T_t : Effect of groyne taper on tip velocity

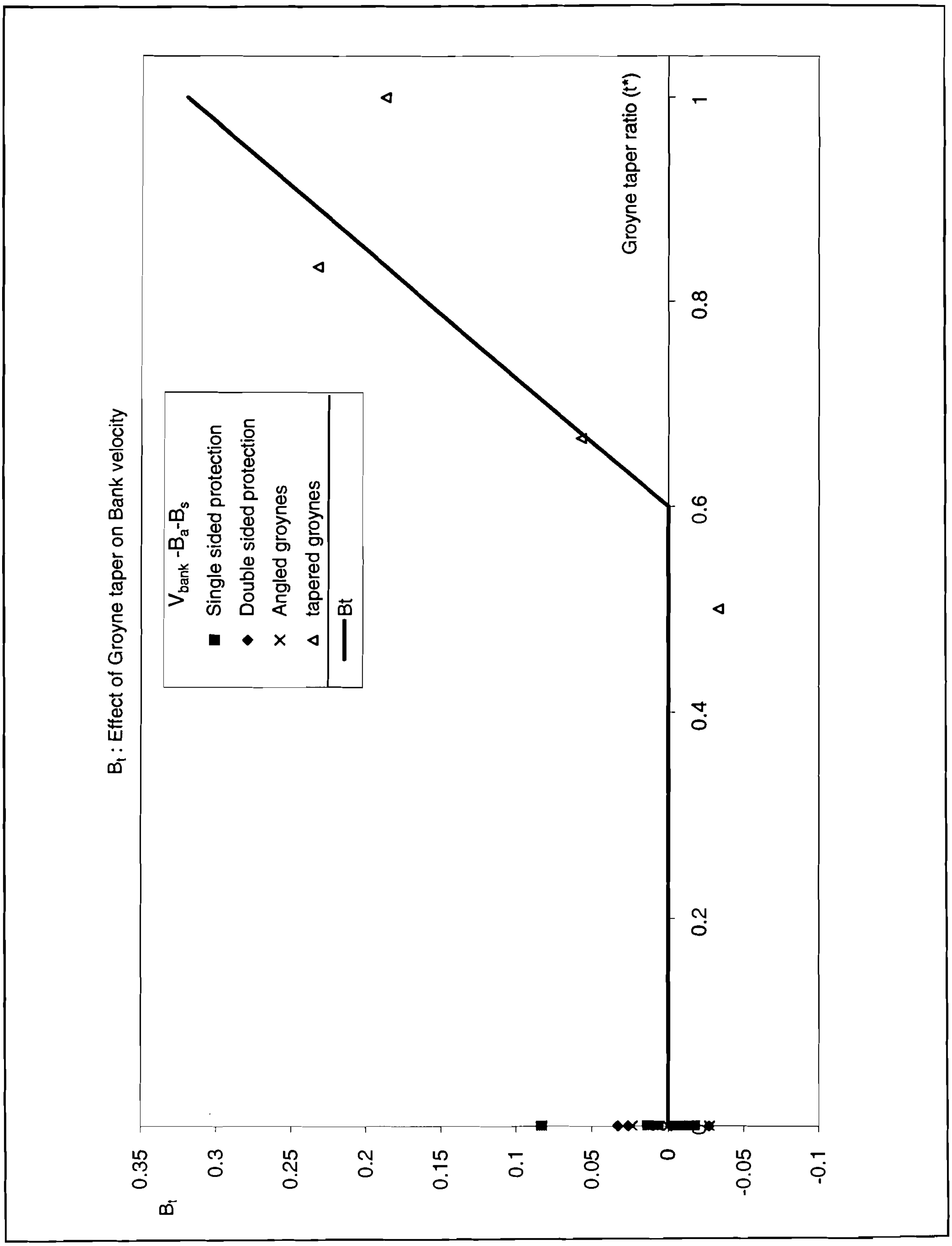

Figure 21 B_t **: Effect of groyne taper on Bank velocity**

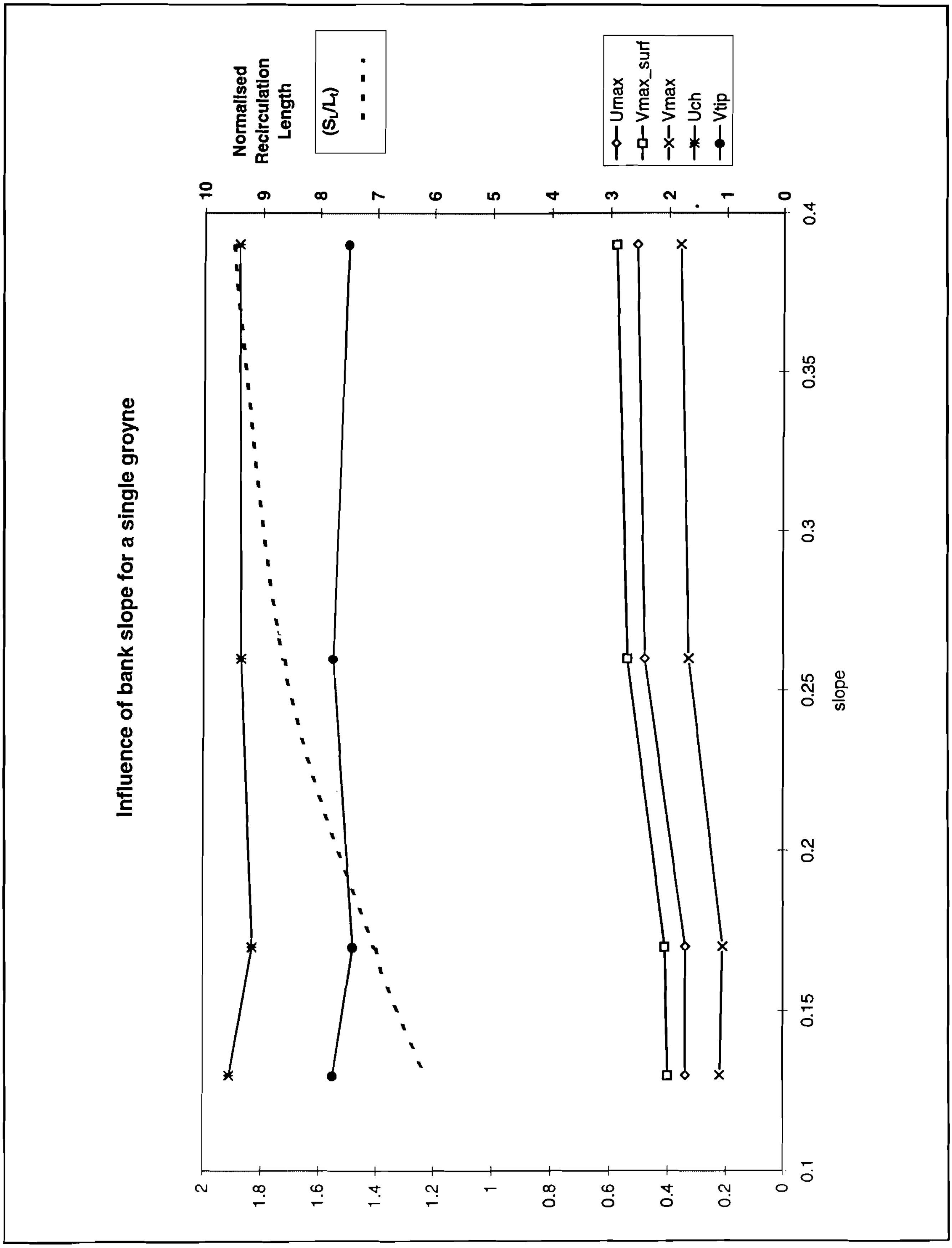

Figure 22 Influence of bank slope for a single groyne

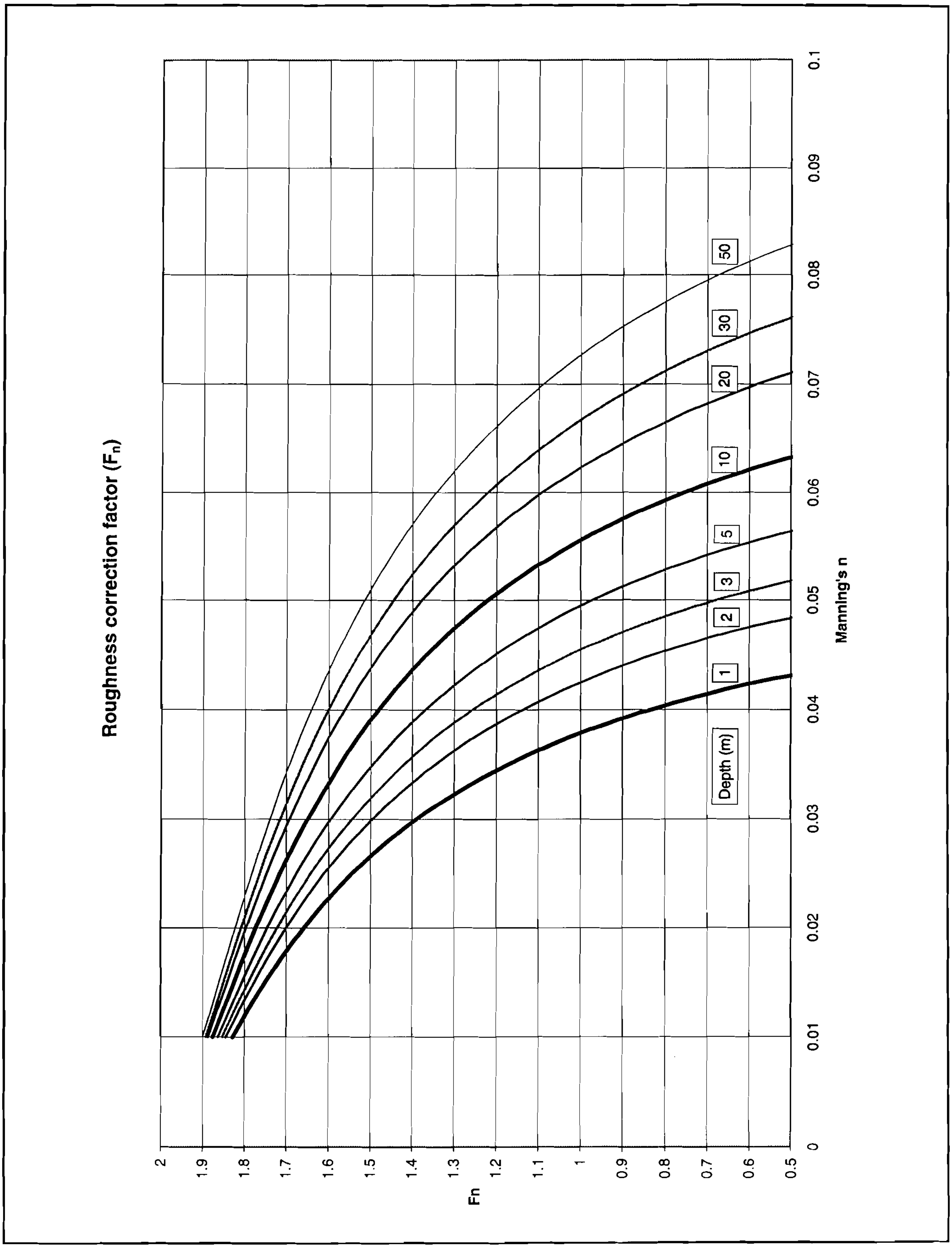

Figure 23 Roughness correction factor (F_n)

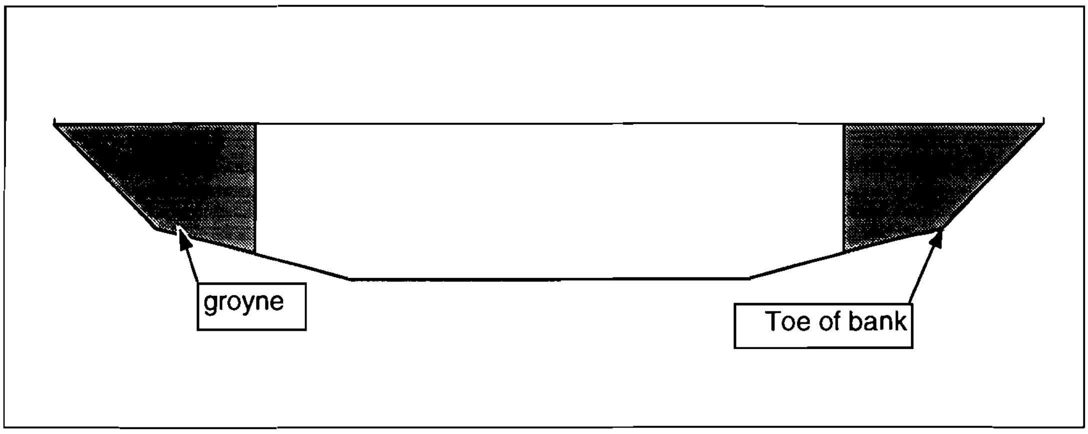

'Rectangular' groynes

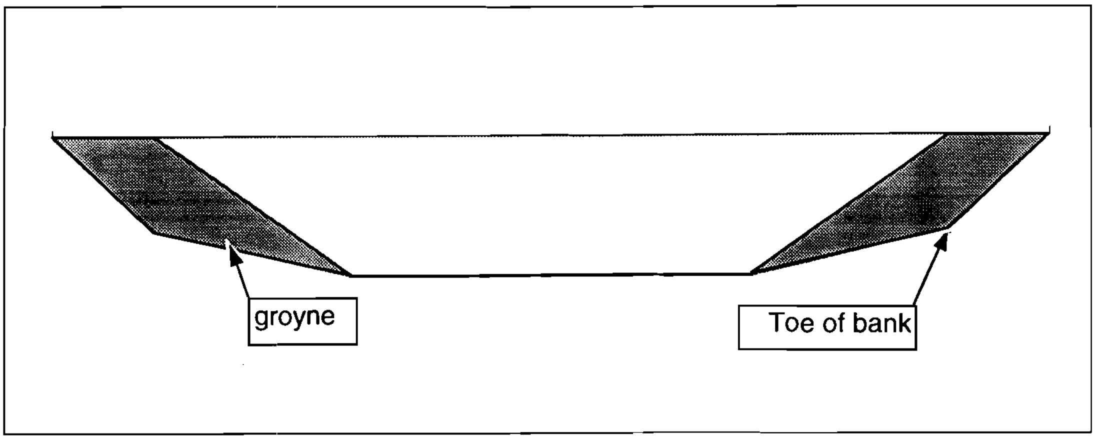

Tapered groynes

Figure 24 Example : River section with groynes

Appendices

Appendix 1

Description of tests

Appendix 1 Description of tests

A1.1 Method

This Appendix describes the tests undertaken to produce the guidelines described in Chapters 4 to 6 of this report. The tests were conducted using the three-dimensional numerical model SSIIM, which had been previously validated against the results from laboratory models of river groynes (see HR report SR480). The present tests were conducted in two phases: single groyne tests and groyne field tests. The tests, which are briefly described in Chapter 3, are described here in detail.

A1.2 Single groyne tests

The first purpose of these tests was to determine a suitable arrangement of grid for the numerical simulations of groyne fields. Factors that needed to be established included the optimum number of vertical layers and the horizontal mesh size that was required close to the groynes. The second purpose of the tests was to investigate the way in which the flow patterns and proportionate changes in velocity were dependent on the dimensions and bed roughness of the channel.

These tests were based on a single groyne similar to that used in the validation study. Thus, the coding system used to identify these numerical tests follows the convention of the validation report (HR report SR480). The tests are identified by a code of two letters followed by up to two digits. The first letter indicates the geometry of the river. The letter 'T' is used to indicate a laboratory-scale trapezoidal channel as used in the validation study. Other initial letters refer to river sections that are horizontally and vertically scaled from the dimensions of the 'T' channel. The second letter (A) indicates that a single rectangular groyne was used in all these tests. The two digits (if present) are used to distinguish different tests with the same geometry, but with changes in the mesh arrangement or modelling parameters. The conditions of the single groyne tests are summarised in Table A1. In making comparisons between the results of the single groyne tests, the key parameters recorded from the numerical tests were:

- The length of the recirculation zone behind the groyne expressed as a multiple of the groyne length. (S_L/L)
- The maximum near-bed velocity divided by the mean velocity (V_{max})
- The maximum near-surface velocity divided by the mean velocity ($V_{max, surf}$)

The "near-surface" velocity is the velocity in the top layer of the 4-layer numerical model at 85% of the local depth. The "near-bed" velocity is the value in the lowest layer at 10% of the local depth.

The results from the single groyne tests are shown in Table A2.

A1.2.1 Numerical grid

Tests (TA-11 to TA-14) were carried out determine a suitable numerical grid. It was found that substantially the same results were obtained using four layers as with 12 layers. It was therefore decided to use a grid with four layers in the later simulations, so as to minimise the storage requirements. Building on the work in the validation study, the longitudinal grid spacing was refined close to the groynes and the lateral grid spacing was refined in the region between the river banks and a line a short distance beyond the tips of the groynes. The numerical grid, viewed in vertical section, is constructed from quadrilaterals with finite vertical sides, thus at the edge of the river the bank must be vertical. To ensure that the numerical model worked satisfactorily, a small vertical wall is used at the river bank.

For situations where the geometry of the river channel and the groynes was symmetric about the channel centreline, it was established that a solution of half of the domain was acceptable by using a frictionless barrier on the line of symmetry. This method resulted in a slight approximation since the software is limited to specifying the same boundary condition on all vertical walls. Thus, the use of a frictionless boundary along the channel centreline required the use of a frictionless boundary at the top of the river bank. However, for these tests, the influence of the small vertical bank was found to be negligible compared with other influences such as the frictional effects of the sloping bank and the turbulent losses due to the flow separation behind the groyne. Thus, in the groyne field tests, a solution of only half the domain was used when simulating groynes on both sides of the river.

A1.2.2 Scaling

Four tests were conducted to check whether the flow behaviour was affected by the absolute size of the river channel. The first test, TA-20, simulated the channel used in the earlier laboratory experiments. This had a surface width of 2.0 metres and a downstream depth of 0.18m. The channel side slope was 1H:2.5V. In the tests HA, OA and NA, all the physical dimensions of the channel were scaled up by factors of 33, 50 and 75 respectively. Thus, the downstream depths were 5.94 m, 9 m and 13.5 m.

The cross-sections of the channel and grid used for test NA-22 is shown as the deepest channel in Figure A1. The cross sections for the other tests mentioned above (TA, HA, OA) were geometrically similar.

In order to maintain complete geometric similarity of the tests, the value of Manning's coefficient used in each test was chosen so that the scale of the bed roughness $k_s = (26\ n)^6$, remained approximately proportional to the water depth. This ensured that the Chezy coefficient (which is proportional to $H^{1/6}/n$) had an approximately constant value. It is shown in Appendix 2 that for fully turbulent flow, the Chezy coefficient determines the vertical velocity distribution in fully developed flow, as might be found upstream of a groyne field. Thus, the above approach ensured that the upstream flow conditions were similar in the tests conducted. The results presented in Table A3 show that the recorded velocities in these tests were proportional to the upstream velocities and that the recirculation lengths were proportional to the dimensions of the channel. These tests show that the flow patterns around a groyne are not affected by the absolute scale of the river or by the upstream velocities, provided that the Chezy number is constant. The importance of the Chezy coefficient is discussed later.

A1.2.3 Bank slope tests

Four tests (NA-22, FA-24, MA-22 and GA-22) were used to compare the effects of changing the aspect ratio of the river while maintaining a constant river surface width and bank width. The changes in aspect ratio had the effect of reducing the bank slope since the bank width was kept constant. The cross-sections of the river channels used in these tests are shown in Figure A1. During these tests the values of Manning's n were adjusted to ensure that the Chezy number remained approximately constant

The recirculation length and the various normalised velocities are plotted against bank slope in Figure 22. It can be seen that, as the bank slope increased, the bank velocity and the recirculation length also increased. The bank slopes found in natural rivers are not likely to exceed 0.4 (i.e. 1H:2.5V). Thus, using a bank slope of this value as a basis for the predictive equations will provide an upper bound on the velocities likely to be found in engineering situations.

A1.2.4 Roughness

In the previous section, tests were described in which the bank slope was varied while the Chezy coefficient was kept constant. Additional tests were conducted in which the bank slope and roughness were varied. It was found that for all these tests, the recirculation length was well correlated with maximum velocity in the recirculation zone (see Figure A2). Larger velocities and longer recirculation zones are associated with steep bank slope and low bed roughness. In Figure A3, it can be seen that, at a constant Manning's n, the maximum velocity in the recirculation zone increased rapidly with increasing bank slope. The effect of roughness on the upstream velocity distribution was included by the use of the roughness correction term (F_n) which is derived in Appendix 2. It can be seen that the correction term does not fully account for the difference in behaviour between tests with a constant Chezy co-efficient and tests with a constant Manning's n. By contrast, the following section shows that the effect of roughness on the near-bed velocities between successive groynes in a groyne field can be predicted by the roughness correction term.

A1.3 Groyne field tests

In the second phase of the present study, tests were carried out to determine the influence of groyne geometry on the performance of a field of six groynes. The dimensions of the river chosen for this study were based on a river 120 m wide; the depth and discharge for this river were determined using the regime formula of Simons and Albertson (1960) taken from Henderson (1996). The chosen channel type for use in this was method was a sand bed and cohesive banks. The calculated channel depth was 5.3m with a discharge of 675 cumecs. The numerical model grid was constructed to represent a channel with a maximum depth of 5.3m and a surface width of 120m. The shape of the modelled channel was approximately trapezoidal. At the edges of the channel, a vertical bank was introduced with a height of approximately 10% of the maximum river depth. From the base of each vertical bank, a sloping bank extended to 10% of the channel width. The central 80% of the channel bed was level. The dimensions and numerical grid for the test channel are shown in Figure A4. Although the simulated channel is somewhat idealised in shape, its overall proportions are typical of those rivers for which groynes are likely to be required.

The test conditions that were varied included that shape size and positioning of the groynes. For most tests, the initial groyne was shorter than the remainder in order that the flow pattern stabilised within a distance of four or five groynes. The test conditions, which are indicated by the run codes for the tests, are described below and summarised in Table A4.

1. The groynes under test were placed on one side or both sides of the river channel. Tests using a 'single sided' groyne field are indicated by a test code with an initial letter V. Tests using a 'double sided' groyne field are indicated by the letter W. The condition of single sided or double sided is indicated by the value s =1 or 2.

2. The second letter of the test code indicates the size, shape and orientation of the groynes. Rectangular groynes of various sizes, which are indicated by letters F, Q, J and O, are shown in Figure 6. The size of the groyne varied from 30% of the channel width (letter F) down to 15% of the channel width (letter O). The length of the groyne (L) divided by the width of the channel (W) is used to give the normalised groyne length ($L^* = L/W$)

3. The tapered groynes that were modelled extended to 30% of the river width at the channel bed. The slope of the taper was between 1:3 and 1:6 and the fraction of the groyne length below the waterline (t^*) varied from 0.5 to 1.0. Tapered groynes, which are indicated by the letter N, are shown in Figure 7

4. A number of tests were conducted to determine the influence of groyne angle. Angled rectangular groynes with an obstruction length measured normal to the river bank of 20% (or 30%) of the channel width were indicated by letters L (or M). The angle between the groyne and the upstream bank (θ) was varied from 60 to 120 degrees.

5. The spacing between the groynes was varied for a number of groyne designs. The groyne spacing ratio (S^*) is defined as the spacing between the groynes (S) divided by the length of the groyne into the river (L). The third letter in the run code indicates the spacing ratio. The spacing ratio varied from 1.66 times the groyne length (letter 'b') to six times the groyne length (letter 'k')

A summary of the conditions and results from the groyne field tests is given in Table A5.

A1.4 Normalisation

A1.4.1 River model

The overall channel shape that was modelled approximated to a trapezoidal section as shown in Figure A3. For simplicity in generating the grid, the centreline bed level was kept horizontal over the whole length of the channel. Thus, the water depth varied due to the backwater effect. To account for this effect, the velocities presented were normalised with respect to the local section-averaged velocity (u_{mean} = Q/A), with the flow area (A) being determined from the local water depth at that section. This method was required to avoid errors in calculating the normalised flow conditions. However, it is unlikely that this approach would be necessary when using the predictive equations. Since the longitudinal variation in u_{mean} will usually be small compared to other uncertainties in the calculations. The depth at the downstream end of the numerical model (H) was used to determine the Chezy coefficient ($\approx 1.811H^{1/6}/n$).

In the majority of the tests, the value of Manning's n used was 0.05. This value is rather high for a river of these dimensions. However, it did provide a significant vertical variation of velocity, which allowed the influence of the depth-averaged and near-bed velocities to be investigated.

A1.4.2 Groyne dimensions

The groyne types chosen for analysis were straight, impermeable groynes; both rectangular (i.e. full height) and tapered groynes were considered. The symbols and terms used to describe the geometry of the groyne and channel are shown in Figure 3. The exposed length of the groynes (L) is normalised with respect to the free surface width of the river. The groyne taper is represented as a percentage of the length of the groyne that is submerged (i.e. t/L). The groyne angle (θ) is defined in this guide as the angle between the upstream bank and the groyne.

In predicting normalised flow velocities, the most critical quantity was found to be the blockage area of the groyne (A_g) measured normal to the channel centreline. This is the submerged, cross-sectional area of the groyne when viewed from the direction of flow. Thus, compared with groynes set at right angles to the flow, angled groynes with the same value of A_g are longer by a factor of (1/sin θ). It was found convenient to normalise the total groyne blockage area (sA_g) in terms of the main channel flow area ($A - sA_g$). The resulting groyne area ratio (A^*) is defined below.

$$A^* = sA_g / (A - sA_g) = sA_r / (1 - sA_r) \qquad (5)$$

where s is the number of sides of the channel on which groynes are installed, and A_r is the relative groyne area (A_g / A)

The spacing between adjacent groynes (S) was normalised with respect to the groyne length (L). When studying tapered groynes, an effective groyne length was initially considered, defined as the groyne area divided by the mean water depth along the length of the groyne. Such a value is identical to L for rectangular groynes but less for tapered groynes. However, using this value did not improve the correlation of the data and thus the spacing ratio ($S^* = S/L$) is used for all groynes.

A1.5 Results from the groyne field tests

A1.5.1 Introduction

The predictive equations and the recommendations presented in chapters 4 and 5 of this report were derived by analysing the results of the groyne field tests which are summarised in Table A6. As stated in section 2.1, three key velocities were identified for measuring the performance of river groynes: the maximum main channel velocity (u_{ch}), the velocity at the groyne tip (v_{tip}) and the maximum near-bed velocity on the river bank (v_{bank}). The velocities were normalised by dividing by the local section averaged flow velocity (u_{mean}). The normalised velocities in the flow simulations were monitored along lines parallel to the banks, and the maximum value in the region of the fourth and fifth groynes was recorded. Best-fit linear equations were used to represent the effect of the various geometric factors on the normalised velocities.

These linear equations are described in terms of factors such as T_a, T_t and T_s that, respectively, define the influence of groyne area, taper ratio and groyne spacing. The effect of channel roughness is included in the terms T_n and B_n which are derived from the logarithmic expression (F_n) which is given in Equation 14. The formulae used to determine the three key velocities are:

$U_{ch} = C_a$ for Main channel velocity, (2)
$V_{tip} = T_n (T_a + T_s + T_t)$ for tip velocity and (3)
$V_{bank} = B_n (B_a + T_s + B_t)$ for bank velocity. (4)

A1.5.2 Upstream conditions

Three tests were conducted to study the influence of the length of the first (i.e. upstream) groyne on the pattern of flow in the groyne field. Figure 8 shows the flow patterns for a particular groyne field with different upstream conditions. The magnitude of the maximum velocity near each groyne tip can be seen to vary depending on the length of the first groyne and on the distance from the start of the groyne field. The limits of the main channel flow are indicated by the 20% velocity contour (i.e. where $u/u_{mean} = 0.2$).

It can be seen that where the first groyne in the field is of equal length to the others then the 20% contour moves away from the groyne tip and towards the centre of the channel. The contour does not reach a stable position for some ***two*** channel widths downstream of the start of the groyne field. However, if the upstream groyne is reduced to 75% of the length of the remaining groynes, then the 20% contour stabilises after only ***one*** channel width.

Another way of indicating the rate at which the flow stabilises in the groyne field is to consider the near tip velocity at the first and second groynes as a fraction of the average of the velocities near the tips of the fourth and fifth groynes. These ratios are shown in Figure 9. It can be seen that the ratios were close to unity, when the length of the first groyne was 75% of the lengths of the remaining groynes. This arrangement was used in all subsequent tests.

A1.5.3 Main channel velocity

The strongest influence on main channel velocity is the obstruction area of the groyne. The normalised main channel velocity was plotted against the two forms of normalised groyne area (A_r and A^*). It was found that a simpler, linear relation was obtained using the groyne area ratio ($A^* = sA_g/(A - sA_g)$). The relation between main channel velocity and groyne area ratio is shown in Figure 13. If the normalised main channel velocity were assumed to be simply equal to the ratio of the main flow area between the groynes and the flow area upstream of the groynes, then U_{ch} would be given by $1+A^*$. It can be seen that the main channel velocity is greater than this. The best-fit formula is $C_a = 1.34A^* + 1$.
Subtracting the best-fit value (C_a) from the monitored velocities (U_{ch}), it is possible to consider the effect of the other geometric parameters of normalised groyne spacing (S^*) and normalised groyne taper (t^*). The value of ($U_{ch}-C_a$) is shown plotted against these values in Figures A5 and A6. It can be seen that main channel velocity (U_{ch}) falls slightly with increasing values of spacing (S^*) and taper (t^*). However the effect is not large and for engineering purposes ignoring the effect provides an additional safety margin. Thus, a simple formulation for predicting U_{ch} was obtained. The overall accuracy of the predictive equation is compared with the SSIIM results in Figure A7 and Table A6. This shows that, for the tests conducted, the predictive equations represent the SSIIM results to an average accuracy of about 7%.

A1.5.4 Tip velocity

When considering the stability of stone protection, the near-bed velocity(v) is commonly quoted as the determining factor (e.g. Escarameia and May,1992 and; Izbash, 1970) but depth-averaged velocity(u) is a more familiar value to engineers. In fully developed flow, it is possible to calculate near-bed velocity from the depth averaged velocity and the Chezy number. However, near the groyne tip the flow is not fully developed and the velocity profile cannot be determined analytically. The results from the numerical tests were used to compare the two values of velocity and thus to determine whether the more familiar depth averaged velocity could be used to predict the near-bed velocity. The two values are considered below.

Near-bed tip velocity (V_{tip})

The value (V_{tip}) is defined as the normalised near-bed velocity close to the groyne tip. The position 'close to' the groyne tip was chosen by inspecting the velocity contours near the groyne tip and choosing a position which was close to the maximum velocity. It was found that the exact position for monitoring the velocity was not very important. Figure A8 shows the ratio between the near-bed velocities measured along lines parallel to the bank at 3 m and 6 m into the channel from the groyne tip. It can be seen that the two values are well correlated, with a scatter of about 10%. For the results presented, the 'tip velocity' is the near-bed velocity at 6 m from the groyne tip. The distance from the groyne tip may be expressed in dimensionless form as a distance of 5% of the channel width. However, the appropriate length scale for normalisation is not clear from the present study. The water depth, the groyne length and the bank width may also be significant in determining the position of maximum velocity in the vicinity of the groyne tip.

The most significant influence on near-bed tip velocity was found to be the area ratio as can be seen in Figure 14. When this was accounted for, the spacing ratio was found to have the next strongest influence (see Figure 18). Finally, it was found that for the same blockage area, tapered groynes resulted in reduced tip velocities, see Figure 20.The overall accuracy of the predictive equations for tip velocity is shown in Figure A9 and Table A7. This shows that the predictive equations are accurate in representing the SSIIM results to an accuracy of about 7%. The influence of bed roughness on tip velocity is considered in section A1.5.5

Depth-averaged tip velocity (U_{tip})

The depth-averaged velocity was determined at 6 m from the groyne tip and analysed using the method described above for the near-bed velocity(V_{tip}). The results from the numerical tests are shown in Figures A10, A11 and A12. It can be seen that there is a major difference in the behaviour of U_{tip} and V_{tip} when considering the influence of groyne taper. The effect of groyne taper under conditions of constant groyne area is to increase the depth-averaged velocity (U_{tip}) but to reduce the velocity near the bed(V_{tip}). This disparity shows that U_{tip} cannot be relied upon to provide a good indication of the near-bed flow conditions that may cause scour the tip of the groyne.

A1.5.5 Bank velocity

The near-bed velocity was monitored at 6 m and 12 m from the river bank. Unlike the case of the tip velocity, the velocities close to the bank were very dependent on the monitoring position. Figure A13 shows the ratio of the values at the two positions, and it can be seen that the velocities at 6 m from the bank were consistently lower than the velocities monitored at 12 m from the bank. The chosen position was 12 m from the bank because this is at the toe of the bank and scour in this position can lead to bank collapse. The velocity at the toe of the bank is commonly used in formulae for determining the stability of natural river banks or revetments.

The major influence on bank velocity (V_{bank}) is groyne area. As with the other monitored velocities, increasing the groyne area increased the bank velocity. This relationship is shown in Figure 15, together with a line proportional to the calculated mid-channel velocity (U_{ch}). This indicates that the main influence on the velocities near the bank is the obstruction effect of the groynes. However, the bank velocity falls more steeply than the main channel velocity indicating the protection provided by the groynes. The value V_{bank}-B_a is plotted against the groyne spacing ratio in Figure 19. Although there is considerable scatter, it can be seen that bank velocity reduces with increased groyne spacing up to a relative groyne spacing (S^*) of about four. The bank velocity increases markedly at $S^*=6$. This indicates that there is an optimum groyne spacing of about four groyne lengths although this value may be dependent on the geometry of the river.

Further analysis was conducted to improve the fit of the data by including a more complicated equation for the area of a single groyne. The chosen form of the equation was $V_{bank} = C_a (B_A' + B_s' + B_t')$ where $C_a = 1 + 1.3 A^*$ and B_A', B_s', B_t' are linear equations in A_r, S^* and t^* respectively. The function $(V_{bank}/C_a - B_s' - B_t')$ is plotted against the relative groyne area (A_r) in Figure A14 and a linear equation is fitted. However, it is not clear that an additional equation for groyne area can be justified with the limited data used available and the large degree of scatter between the data and the fitted equation. Clearly the dependency of bank velocity on groyne area needs further investigation, including consideration of the influence of the relative bank width.

Thus, it was decided to use a simpler equation for predicting bank velocity with the same form as used for predicting the tip velocity, $V_{bank} = B_a + B_s + B_t$.

The influence of groyne taper on bank velocity can be seen in Figure 21 and the overall accuracy of the predictive equations is shown in Figure A15 and Table A8. This shows that the predictive equations represent the SSIIM results to an accuracy of about 17%. The influence of bed roughness on bank velocity is considered in the next section.

A1.5.6 Bed roughness and Bed ratios

In Appendix 2, we consider the influence of bed roughness on the vertical velocity profile. For fully developed flow, the vertical velocity profile follows a logarithmic relationship, which may be expressed as a function of the Chezy number (C_z). A single parameter (the bed ratio) is derived to represent the shape of the velocity profile. The bed ratio (V_r) is defined as the near-bed velocity measured at 10% of the local depth (v) divided by the local depth-averaged velocity (u). For conditions in which the velocity is constant throughout the water column, the bed ratio is unity, but in fully developed flow the value is typically in the range 45% to 85%. The relationship between Chezy number and theoretical bed ratio is shown in Figure A16. It can be seen that for deep, smooth rivers, where the Chezy number is high (e.g. $C_z \approx 100$), the bed ratio is also high and changes slowly. For fully developed flow, the near bed velocity determined in the conditions of the numerical experiments (H = 5.3, n = 0.05) can be corrected to any other conditions by the using of a theoretically derived roughness correction term F_n. The bed ratio for the numerical tests was 0.478 thus (as is shown in Appendix 2).

$$F_n = \frac{V_r}{0.478} \tag{21}$$

However, the flow at the groyne tip and on the banks is not fully developed and thus the effect of roughness on tip velocity and bank velocity was studied further.

<u>Tip velocity</u>

Figure A17 shows a comparison between the theoretical value of bed ratio and the values given by the numerical model near the groyne tip. The figure shows that, for tapered groynes, the bed ratios at the groyne tips are very close to the theoretical values. We infer that near the tip of a tapered groyne the vertical velocity profile is largely governed by the bed roughness and hence a roughness correction factor based on the logarithmic velocity profile can be applied. The influence of upstream velocity profile on the velocity near the tips of rectangular groynes is less clear and thus additional tests were conducted as follows.

A field of six rectangular groynes was modelled on each side of the river (see Table A9). The groynes had a length of 20% of the river width and a spacing of 1.66 times the groyne length. The Manning's coefficients used in these tests were 0.02, 0.033, 0.05. These correspond to Chezy coefficients of 119, 72 and 48. The corresponding theoretical values of bed ratio were 84%, 75% and 48%. The bed ratios in the numerical model upstream of the groynes were found to be very similar to these theoretical values. However, near the tips of the groynes, the corresponding bed ratios were 95%, 85% and 60%. This shows that the influence of rectangular groynes is to make the flow more uniform in the vertical. The resultant increase in near-bed velocity increases the likelihood of scour at the groyne tip.

It was found that the influence of bed roughness on tip velocity could be accounted for by the use of a roughness correction term (T_n), where

$$T_n = {}^1/_3 \; (2F_n + 1)$$

The use of this term is shown in Table 9.

Bank velocity

Figure A18 shows the variation between the theoretical value of bed ratio and the ratio V_{bank}/U_{bank}. This variation indicates the need to use the need to use values of V_{bank} when predicting the potential erosion at the river bank.

Figure A19 shows the vertical velocity profiles near the toe of the bank for the rectangular groynes tested. For each case, the depth averaged velocity pattern is shown to the right of the vertical velocity profiles. The upstream velocity profile (shown as a thick line and at a reduced scale) may be compared with the profiles at the toe of the bank (y=12m) and half way up the bank (y=6m). From the diagrams the following conclusions can be draw.

1) The maximum depth-averaged velocities on the bank are not greatly influenced by bed roughness.

2) The vertical velocity profile near the bank does not follow the upstream logarithmic profile.

3) The near-bed velocities cannot be accurately estimated from the depth-averaged velocities; the bed ratio in the bank region sometimes exceeds unity.

4) The near-bed velocity at the toe of the bank is well correlated with the upstream near-bed velocity in the centre of the channel (which is close to the theoretical near bed velocity).

This latter value, which is proportional to u_{mean} $F_{n,}$ can thus be used to predict the bank velocity (v_{bank}) in the lee of rectangular groynes. The factor is used in the predictive equations, as can be seen by combining equations 4,16 and 19

$$v_{bank} = u_{mean} \, F_n \, (B_a + B_s + B_t) \qquad (22)$$

Hence for the rectangular groynes Bn = Fn. The situation for tapered groynes is different to that described above. For tapered groynes, changes to the Chezy number were found to have very little effect on the velocities at the bank. This is believed to be due to the fact that the vertical velocity distribution behind tapered groynes is mostly determined by the shape of the groyne. Thus, we do not apply the roughness correction term to the near bank velocities between tapered groynes.

Hence for tapered groynes, where $t^* > 0.5$, $B_n = 1$. The application of the roughness correction coefficient (B_n) to the bank velocities for rectangular and tapered groynes is shown in Figure A20.

Summary

These findings indicate that there is a complex interaction between the bed roughness and the geometry of the groynes. As the flow interacts with the groyne, the vertical velocity profile is altered and this influences the strength and distribution of the recirculating currents behind the groyne. The way in which the velocity profile is altered is greatly dependent on the shape of the groyne and thus the roughness correction factor is applied differently for rectangular and tapered groynes. Further work, under a variety of roughness conditions and groyne geometries would be required to fully determine the interacting effects of roughness and groyne geometry on the flow patterns at the tip and the bank

Tables for Appendix 1

Table A1 Conditions of single groyne tests

Run code	Horizontal scale	Vertical scale	Channel width (m)	Channel depth (m)	Groyne length (m)	Channel area (m^2)	Channel length (m)	bank slope	Relative bank width	Relative groyne length L/S	Upstream discharge (m^3/s)	Upstream velocity (m/s)	Manning's coefficient	Chezy coefficient $1.81H^{1/6}/n$	Theoretical bed ratio
			W	H	L	A	X	S_b	b*	L*	Q	u	n	C_z	V_r
TA-20	1	1	2	0.18	0.64	0.28	9.5	0.39	0.23	0.32	0.09	0.3	0.020	68.0	84.1%
HA-21	33	33	66	5.94	21.12	307.	313.5	0.39	0.23	0.32	576.7	1.8	0.036	68.2	71.9%
OA-21	50	50	100	9.0	32.0	705.	475.0	0.39	0.23	0.32	1629.7	2.3	0.040	65.3	70.2%
NA-22	75	75	150	13.5	48.0	1586.	715.5	0.39	0.23	0.32	4490.9	2.8	0.040	69.9	72.7%
FA-21	75	50	150	9.0	48.0	1058.	715.5	0.27	0.23	0.32	2994.	2.8	0.036	73.1	74.2%
MA-21	75	33	150	5.94	48.0	698.	715.5	0.18	0.23	0.32	1976.	2.8	0.050	48.7	50.2%
GA-21	75	25	150	4.5	48.0	529.	715.5	0.13	0.23	0.32	1497.	2.8	0.050	46.5	44.2%

Table A2 Results from single groyne tests

	Downstream Depth	Bank slope	Strickler Number	Manning's coefficient	Chezy number	Theoretical Bed ratio	Normalised Recirculation Length	Maximum normalised velocities in the recirculation zone			Maximum normalised velocities	
								Depth averaged	Near surface	Near bed	Main Channel	Near Tip
SSIIM run	H	S_b	M	n	C_Z	V_r	S_L/L	U_{max}	V_{max_surf}	V_{max}	U_{ch}	V_{tip}
TA-20	0.18	0.39	50	0.02	68.04	0.77	9.5		0.56	0.36		
HA-21	5.94	0.39	28	0.036	68.24	0.77	9.5		0.55	0.35		
OA-21	9.	0.39	25	0.04	65.30	0.76	9.3		0.55	0.35		
NA-22	13.5	0.39	25	0.04	69.86	0.77	10.0	0.51	0.58	0.36	1.88	1.5
NA-23	13.5	0.39	20	0.05	55.89	0.71	7.0	0.35	0.43	0.22	1.87	1.5
NA-25	13.5	0.39	28	0.036	78.25	0.80	10.9	0.56	0.61	0.44	1.85	2.55
FA-22	9.	0.26	28	0.036	73.13	0.78	8.6	0.48	0.54	0.33	1.87	1.55
FA-23	9.	0.26	20	0.05	52.24	0.68	5.1	0.25	0.33	0.14	1.87	1.48
FA-24	9.	0.26	26.5	0.038	69.22	0.77	8.1		0.53	0.3		
MA-21	5.94	0.17	20	0.05	48.74	0.64	3.4	0.15	0.22	0.07	1.87	1.45
MA-22	5.94	0.17	28	0.036	68.24	0.77	7.2	0.34	0.42	0.21	1.9	1.52
GA-21	4.5	0.13	20	0.05	46.54	0.61	2.9	0.14	0.19	0.06	1.9	1.35

Table A3 Run coding for groyne field tests

First letter	**Groyne positioning**	
	V--	Groynes on one side of the river
	W--	Groynes on both sides of the river
Second letter	**Groyne size and type**	
	-O-	Rectangular groynes (groyne length = 15 % width)
	-J-	Rectangular groynes (groyne length = 20 % width)
	-Q-	Rectangular groynes (groyne length = 26 % width)
	-F-	Rectangular groynes (groyne length = 30 % width)
	-L-	Angled groynes (groyne length = 30 % width)
	-M-	Angled groynes (groyne length = 20 % width)
	-N-	Tapered groynes (groyne length = 30 % width)
Third Letter	**Groyne spacing ratio**	
	--b	1.66 x groyne length
	--d	2.5 x groyne length
	--e	2.66 x groyne length
	--g	4 x groyne length
	--i	5 x groyne length
	--k	6 x groyne length
First digit	**Groyne taper, angle etc**	
Second digit	**Roughness and other parameters**	

Table A4 Conditions of groyne field tests

Run code	Horizontal scale	Vertical scale	Channel width (m)	Channel depth (m)	Bank slope	Relative bank width	Relative groyne length (L/S)	Channel area (m^2)	Channel length (m)	Upstream discharge (m^3/s)	Upstream velocity (m/s)	Groyne length (m)	Manning's coefficient	Chezy coefficient ($H^{1/6}/n$)	Theoretical bed ratio
			W	H	S_b	b*	L*	A	X	Q	u	L	n	C_z	V_r
TA	1	1	2	0.2	0.4	0.2	0.32	0.3	9.5	0.1	0.3	01	0.020	68.0	84.1%
HA-21	33	33	66	5.9	0.4	0.2	0.32	307.0	313.5	576.7	1.8	21	0.036	68.2	71.9%
OA-21	50	50	100	9.0	0.4	0.2	0.32	705.0	475.0	1629.7	2.3	32	0.040	65.3	70.2%
NA-22	75	75	150	13.5	0.4	0.2	0.32	1586.0	715.5	4490.9	2.8	48	0.040	69.9	72.7%
FA-21	75	50	150	9.0	0.3	0.2	0.32	1058.0	715.5	2994.0	2.8	48	0.036	73.1	74.2%
MA-21	75	33	150	5.9	0.2	0.2	0.32	698.0	715.5	1976.0	2.8	48	0.050	48.7	50.2%
GA-21	75	25	150	4.5	0.1	0.2	0.32	529.0	715.5	1497.0	2.8	48	0.050	46.5	44.2%
VO	rectangular groynes		120	5.3	0.4	0.1	0.13	578.4	470.0	675.0	1.2	15	0.050	47.8	47.9%
VJ & WJ	rectangular groynes		120	5.3	0.4	0.1	0.20	578.4	60-144	675.0	1.2	24	0.050	47.8	47.9%
VQ & WQ	rectangular groynes		120	5.3	0.4	0.1	0.26	578.4	470.0	675.0	1.2	31.2	0.050	47.8	47.9%
VF & WF	rectangular groynes		120	5.3	0.4	0.1	0.30	578.4	60-96	675.0	1.2	36	0.050	47.8	47.9%
VJ & WJ	rectangular groynes		120	5.3	0.4	0.1	0.20	578.4	60-144	675.0	1.2	24	0.050	47.8	47.9%
VM & VL & WL	angled groynes		120	5.3	0.4	0.1	0.20	578.4	96.0	675.0	1.2	24	0.050	47.8	47.9%
VN	tapered groynes		120	5.3	0.4	0.1	0.30	578.4	96.0	675.0	1.2	36	0.050	47.8	47.9%

Table A5 Results from groyne field tests

Run code (V : s=1) (W: s=2)	Relative groyne length (L/W)	Relative groyne area (A_g/A)	Area ratio (s A_r / 1- s A_r)	Groyne spacing / River width	Groyne spacing ratio S / L	Taper ratio t* = (t / L)	Angle of groyne to upstream bank	Normalised depth-averaged velocity in main channel	Normalised depth-averaged velocity 5%W from the groyne tip	Normalised near-bed velocity 5%W from the groyne tip	Normalised near-bed velocity 2.5%W from the groyne tip	Normalised depth-averaged velocity at toe of bank	Normalised near-bed velocity at toe of bank	Normalised near-bed velocity half way up bank
	L^*	A_r	A^*	S/W	S^*	t^*	θ	U_{ch}	U_{tip}	V_{tip}	V_{tip3}	U_{bank}	V_{bank}	V_{bank6}
Groynes on one side of the river														
VOb-31	0.15	0.115	0.13	0.25	1.667	0.	90	1.18	1.	0.55	0.53	0.14	0.11	0.75
VJb-31	0.2	0.17	0.205	0.333	1.667	0.	90	1.25	1.1	0.6	0.55	0.16	0.13	0.07
VJd-21	0.2	0.17	0.205	0.5	2.5	0.	90	1.25	1.2	0.7	0.6	0.15	0.12	0.075
VJg-31	0.2	0.17	0.205	0.8	4.0	0.	90	1.25	1.24	0.8	0.75	0.1	0.09	0.06
VJi-31	0.2	0.17	0.205	1.0	5.0	0.	90	1.25	1.28	0.85	0.88	0.1	0.07	0.06
VJk-21	0.2	0.17	0.205	1.2	6.0	0.	90	1.25	1.27	0.9	0.95	0.2	0.12	0.06
VQb-31	0.26	0.225	0.29	0.433	1.667	0.	90	1.35	1.23	0.63	0.63	0.15	0.112	0.07
VFb-31	0.3	0.28	0.389	0.5	1.667	0.	90	1.48	1.3	0.75	0.75	0.17	0.12	0.065
VFg-31	0.3	0.28	0.389	1.2	4.0	0.	90	1.5	1.55	1.	1.1	0.14	0.09	0.06
Groynes on both sides of the river														
WOb-31	0.15	0.115	0.3	0.25	1.667	0.	90	1.43	1.26	0.65	0.6	0.17	0.14	0.09
WJb-31	0.2	0.17	0.52	0.333	1.667	0.	90	1.7	1.55	0.85	0.8	0.23	0.19	0.11
WJd-31	0.2	0.17	0.52	0.5	2.5	0.	90	1.7	1.6	0.95	0.9	0.22	0.18	0.12
WJg-31	0.2	0.17	0.52	0.8	4.0	0.	90	1.65	1.68	1.1	1.12	0.14	0.13	0.09
WFb-22	0.3	0.28	1.27	0.5	1.667	0.	90	2.7	2.6	1.53	1.48	0.33	0.26	0.18
Angled groynes														
VMg-71	0.2	0.17	0.205	0.8	4.0	0.	60	1.28	1.24	0.78	0.78	0.13	0.1	0.065
VMg-61	0.2	0.17	0.205	0.8	4.0	0.	75	1.28	1.23	0.78	0.8	0.11	0.09	0.06
VMg-51	0.2	0.17	0.205	0.8	4.0	0.	105	1.25	1.25	0.8	0.8	0.12	0.09	0.065
VMg-91	0.2	0.17	0.205	0.8	4.0	0.	115	1.25	1.25	0.78	0.8	0.1	0.09	0.06
VLb-21	0.3	0.28	0.389	0.5	1.667	0.	105	1.5	1.4	0.8	0.75	0.18	0.12	0.06
WLb-31	0.3	0.28	1.27	0.5	1.667	0.	105	2.7	2.6	1.45	1.45	0.35	0.25	0.17

Table A5 Results from groyne field tests (continued)

Run code (V : s=1) (W: s=2)	Relative groyne length (L/W)	Relative groyne area (A_g/A)	Area ratio (s A_r / 1- s A_r)	Groyne spacing / River width	Groyne spacing ratio S / L	Taper ratio t* = (t/L)	Groyne slope	Normalised depth-averaged velocity in main channel	Normalised depth-averaged velocity 5%W from the groyne tip	Normalised near-bed velocity 5%W from the groyne tip	Normalised near-bed velocity 2.5%W from the groyne tip	Normalised depth-averaged velocity at toe of bank	Normalised near-bed velocity at toe of bank	Normalised near-bed velocity half way up bank
	L*	A_r	A*	S/W	S*	t*	S_g	U_{ch}	U_{tip}	V_{tip}	V_{tip3}	U_{bank}	V_{bank}	V_{bank6}
Tapered groynes														
VFe-31	0.3	0.28	0.39	0.8	2.667	0.	0	1.48	1.45	0.9	0.93	0.18	0.14	0.08
VNe-81	0.3	0.195	0.241	0.8	2.667	0.5	0.283	1.31	1.31	0.68	0.72	0.11	0.075	0.045
VNe-42	0.3	0.166	0.199	0.8	2.667	0.67	0.211	1.25	1.3	0.65	0.7	0.22	0.16	0.06
VNe-61	0.3	0.158	0.187	0.8	2.667	0.83	0.171	1.21	1.25	0.63	0.65	0.65	0.33	0.13
VNe-71	0.3	0.109	0.122	0.8	2.667	1.	0.142	1.17	1.21	0.58	0.6	0.77	0.28	0.2

Table A6 Comparison on numerical model results and formula for Main channel velocity

Test name	Results (SSIIM)	Predicted value	Error	% error
VOb-31	1.18	1.17	0.01	1%
VJb-31	1.25	1.27	-0.02	2%
VJd-21	1.25	1.27	-0.02	2%
VJg-31	1.25	1.27	-0.02	2%
VJi-31	1.25	1.27	-0.02	2%
VJk-21	1.25	1.27	-0.02	2%
VQb-31	1.35	1.41	-0.06	5%
VFb-31	1.48	1.52	-0.04	3%
VFg-31	1.5	1.52	-0.02	1%
Wob-31	1.43	1.4	0.03	2%
WJb-31	1.7	1.69	0.01	1%
WJd-31	1.7	1.69	0.01	1%
WJg-31	1.65	1.69	-0.04	2%
WFb-22	2.7	2.71	-0.01	0%
VMg-71	1.28	1.27	0.01	0%
VMg-61	1.28	1.27	0.01	0%
VMg-51	1.25	1.27	-0.02	2%
VMg-91	1.25	1.27	-0.02	2%
VLb-21	1.5	1.52	-0.02	1%
WLb-31	2.7	2.71	-0.01	0%
VFe-31	1.48	1.52	-0.04	3%
Vne-81	1.17	1.32	-0.15	12%
Vne-42	1.21	1.27	-0.06	4%
Vne-61	1.25	1.25	-0.0	0%
Vne-71	1.31	1.16	0.15	13%
		Standard error		**3%**
		Average		**2%**

Table A7 Comparison of numerical model results and formula for Tip velocity

Test name	Results (SSIIM)	Predicted value	Error	% error
VOb-31	0.55	0.54	-0.01	-1%
VJb-31	0.6	0.61	0.01	1%
VJd-21	0.7	0.67	-0.03	-4%
VJg-31	0.8	0.79	-0.01	-1%
VJi-31	0.85	0.87	0.02	2%
VJk-21	0.9	0.94	0.04	4%
VQb-31	0.63	0.7	0.07	10%
VFb-31	0.75	0.77	0.02	2%
VFg-31	1.0	0.95	-0.05	-5%
Wob-31	0.65	0.69	0.04	6%
WJb-31	0.85	0.88	0.03	3%
WJd-31	0.95	0.94	-0.01	-1%
WJg-31	1.1	1.06	-0.04	-4%
WFb-22	1.53	1.54	0.01	0%
VMg-71	0.78	0.79	0.01	1%
VMg-61	0.78	0.79	0.01	1%
VMg-51	0.8	0.79	-0.01	-1%
VMg-91	0.78	0.79	0.01	1%
VLb-21	0.8	0.77	-0.03	-4%
WLb-31	1.45	1.54	0.09	6%
VFe-31	0.9	0.85	-0.05	-6%
Vne-81	0.68	0.7	0.02	2%
Vne-42	0.65	0.65	0.0	1%
Vne-61	0.63	0.64	0.01	1%
Vne-71	0.58	0.57	-0.01	-1%
		Standard error		**4%**
		Average		**3%**

Table A8 Comparison on numerical model results and formula for Bank velocity

Test name	Results (SSIIM)	Predicted value	Error	% error
VOb-31	0.11	0.11	-0.0	-3%
VJb-31	0.13	0.12	0.01	5%
VJd-21	0.12	0.11	0.01	11%
VJg-31	0.09	0.08	0.01	15%
VJi-31	0.07	0.06	0.01	19%
VJk-21	0.12	(1)	(1)	
VQb-31	0.12	0.14	-0.02	-14%
VFb-31	0.12	0.15	-0.03	-23%
VFg-31	0.09	0.1	-0.01	-12%
WOb-31	0.14	0.14	0.0	3%
WJb-31	0.19	0.16	0.03	14%
WJd-31	0.18	0.15	0.03	18%
WJg-31	0.13	0.12	0.01	10%
		0.13	-0.13	
WFb-22	0.26	0.26	-0.0	-1%
VMg-71	0.1	0.08	0.02	23%
VMg-61	0.09	0.08	0.01	15%
VMg-51	0.09	0.08	0.01	15%
VMg-91	0.09	0.08	0.01	15%
VLb-21	0.12	0.15	-0.03	-23%
WLb-31	0.25	0.26	-0.01	-5%
VFe-31	0.14	0.13	0.01	9%
Vne-81	0.08	0.11	-0.03	-44%
Vne-42	0.16	0.16	0.0	3%
Vne-61	0.33	0.29	0.04	13%
Vne-71	0.28	0.41	-0.13	-47%
		Standard error		**19%**
		Average		**15%**

(1) Note that test VJk is outside the range of applicability of the predictive equations

Table A9 Tests to investigate the influence of roughness

Run code	Manning's roughness coefficient	No. of layers in numerical model	Downstream depth	Chezy coefficient	Theoretical Bed ratio	Roughness correction coefficient	Near bed velocity at toe of bank	Corrected V_{bank}	Near bed velocity close to groyne tip	Tip velocity correction term $^1/_3(2.F_n+1)$	Corrected V_{tip}
	n		H	C_z	V_r	F_n	V_{bank}	V_{bank}/F_n	V_{tip}	T_n	V_{tip}/T_n
WJb-31	0.05	4	5.3	47.8	0.477	1.00	0.19	0.19	0.850	1.000	0.850
WJb-32	0.0333	4	5.3	71.8	0.736	1.54	0.29	0.19	1.140	1.362	0.837
WJb-33	0.0333	10	5.3	71.8	0.736	1.54	0.29	0.19	1.140	1.362	0.837
WJb-34	0.02	4	5.3	119.6	0.837	1.75	0.33	0.19	1.300	1.503	0.865

Figures for Appendix 1

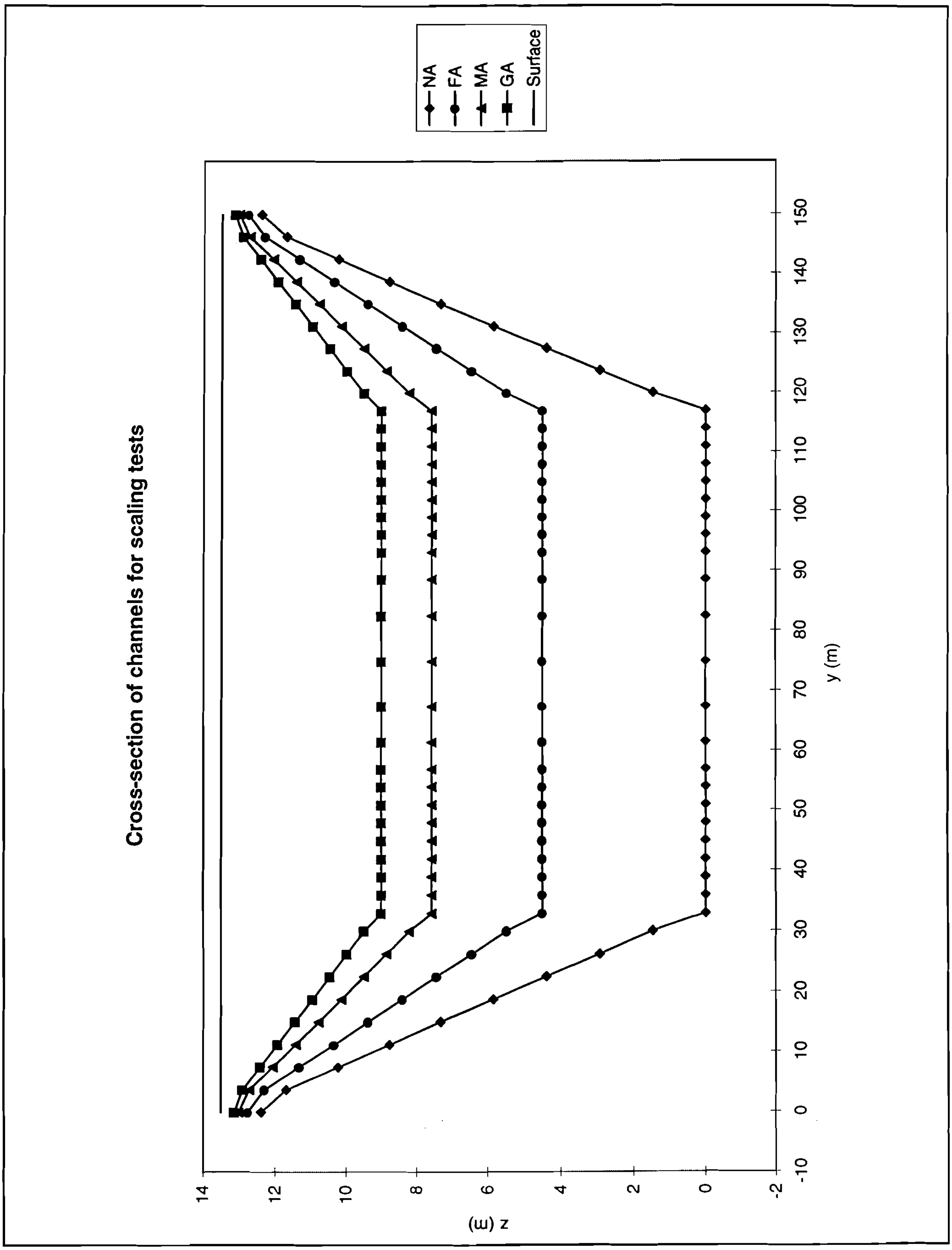

Figure A1 Cross-sections of channels for scaling tests

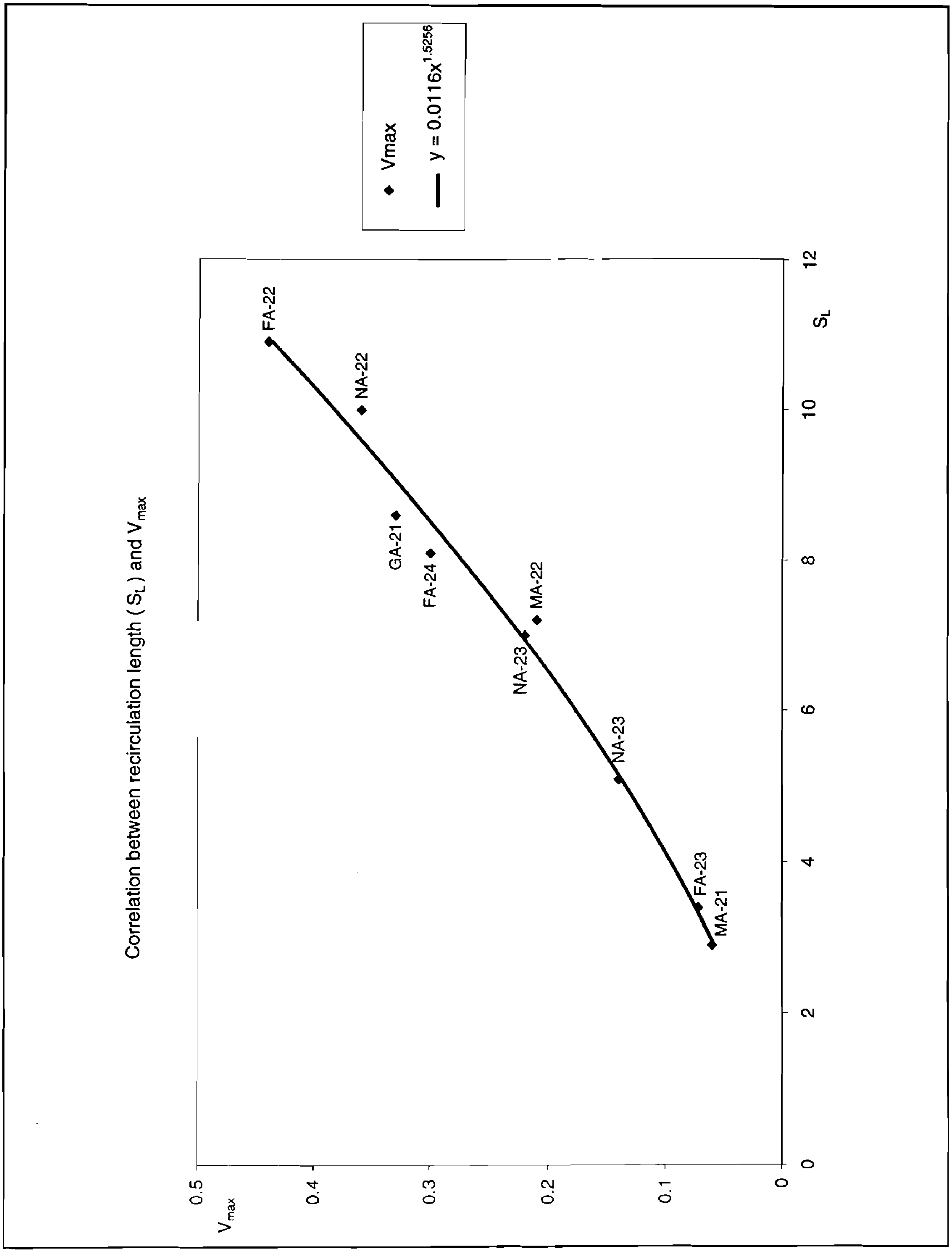

Figure A2 **Correlation between recirculation length and maximum velocity in the recirculation zone**

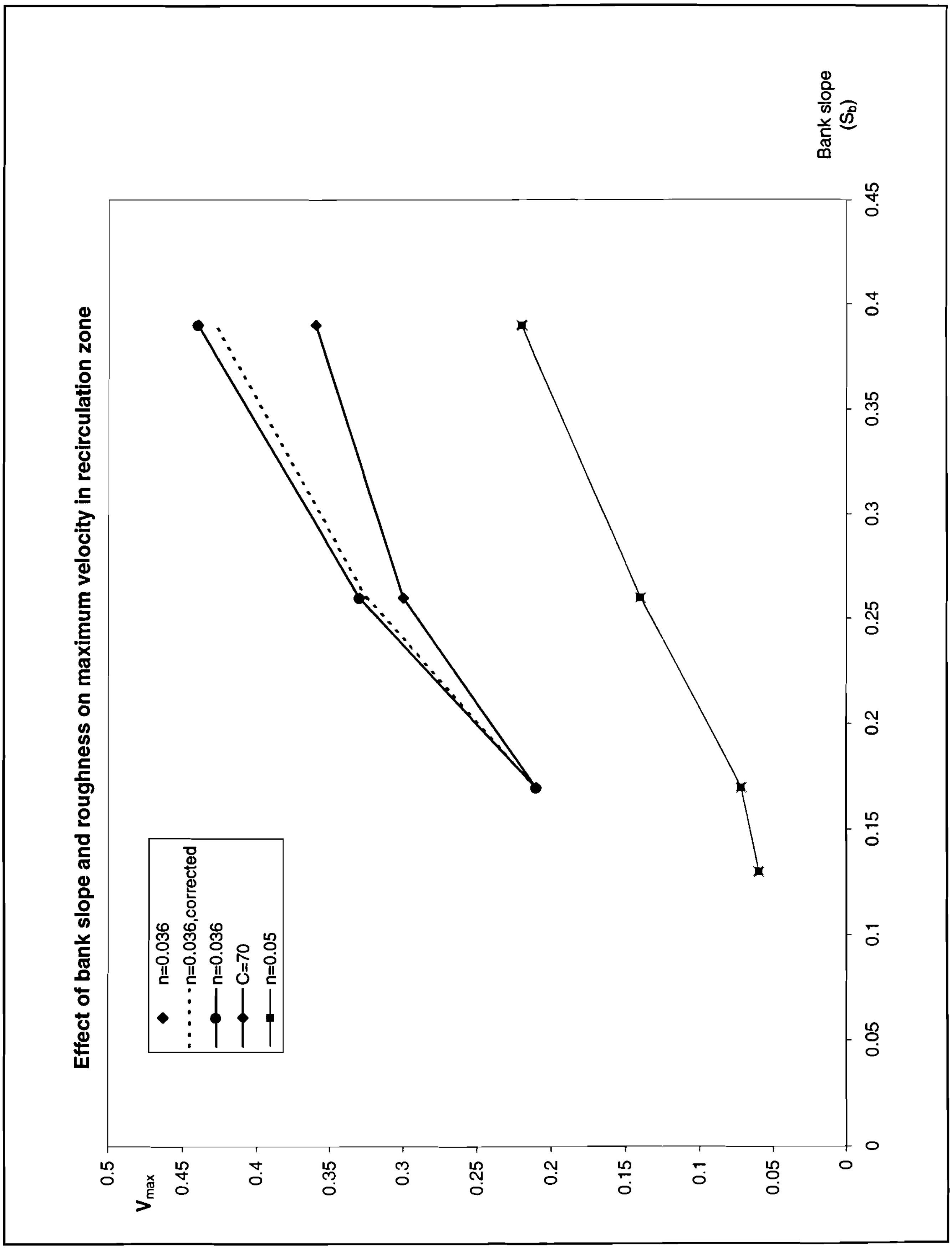

Figure A3 **Effect of bank slope and roughness on the maximum velocity in the recirculation zone for a single groyne**

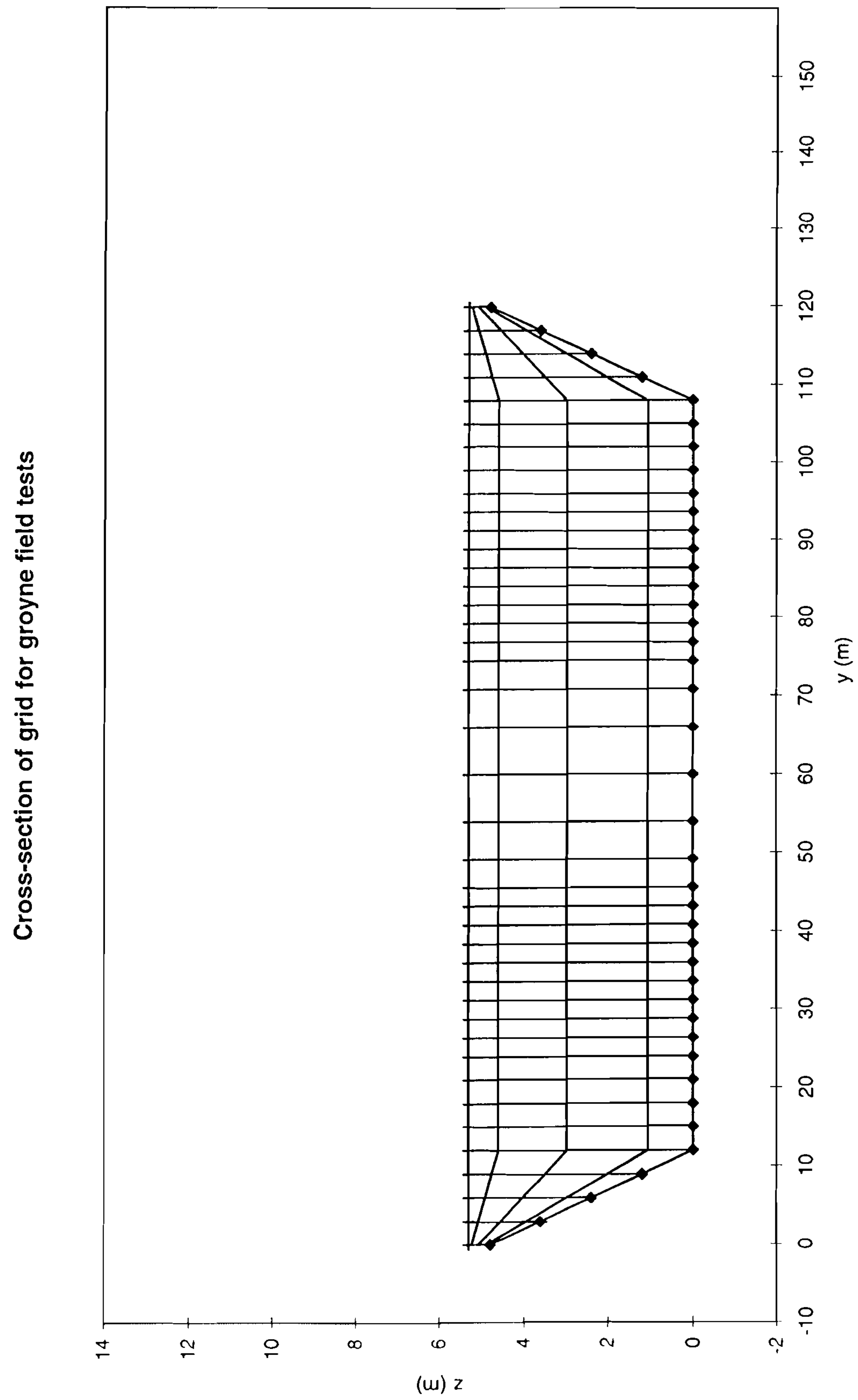

Figure A4 Cross-section of grid for the groyne field tests

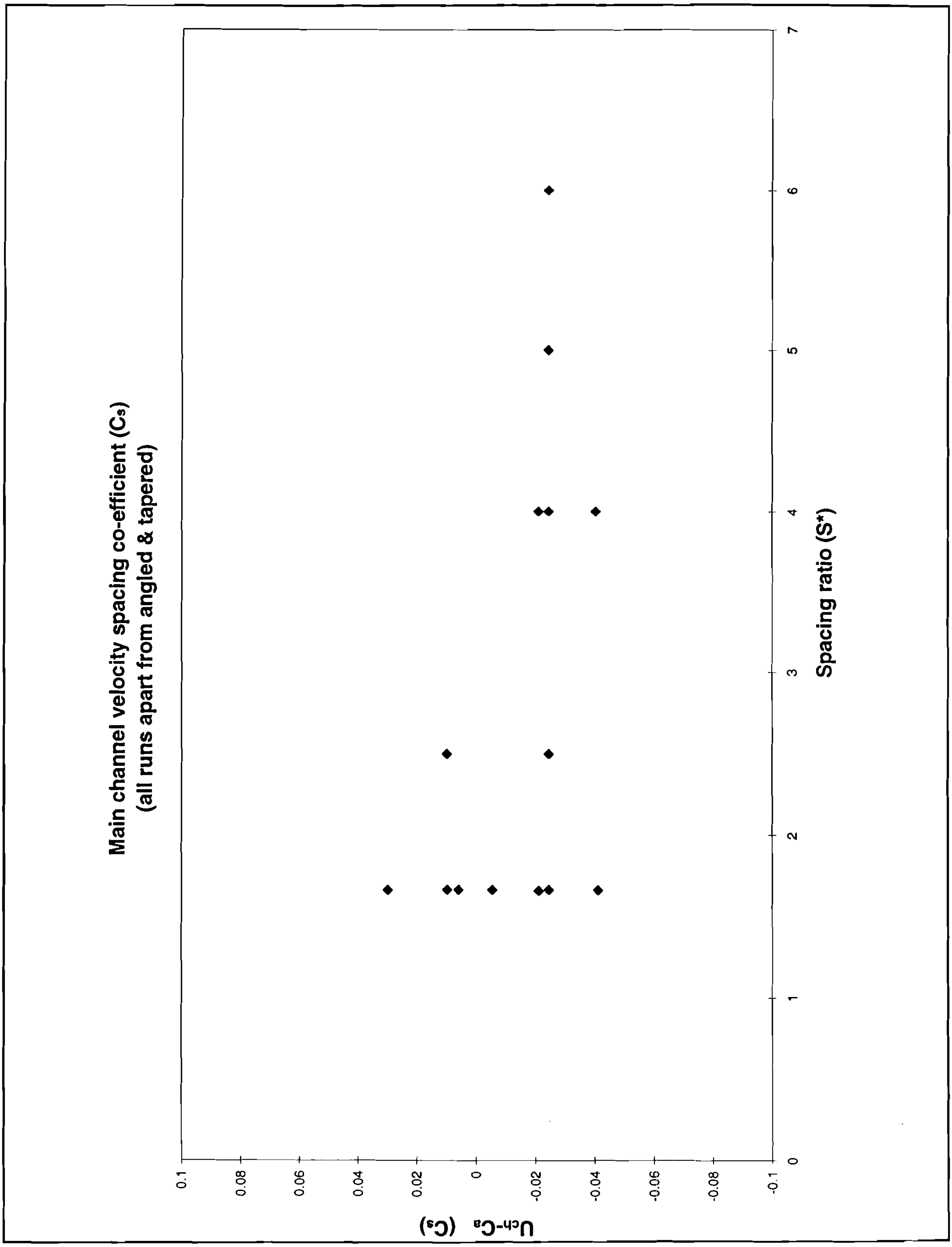

Figure A5 Effect of groyne spacing on main channel velocity

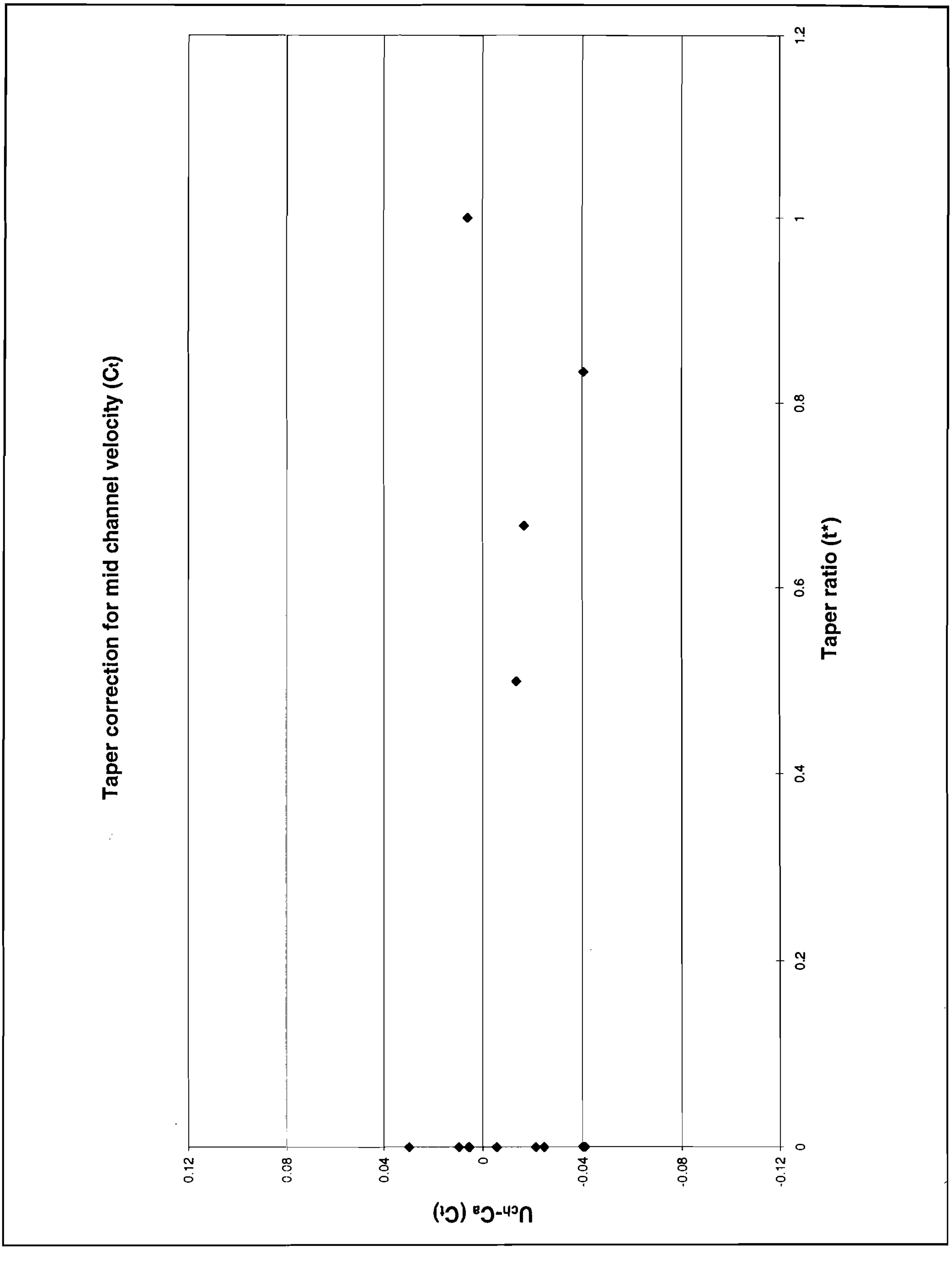

Figure A6 Effect of groyne taper on main channel velocity

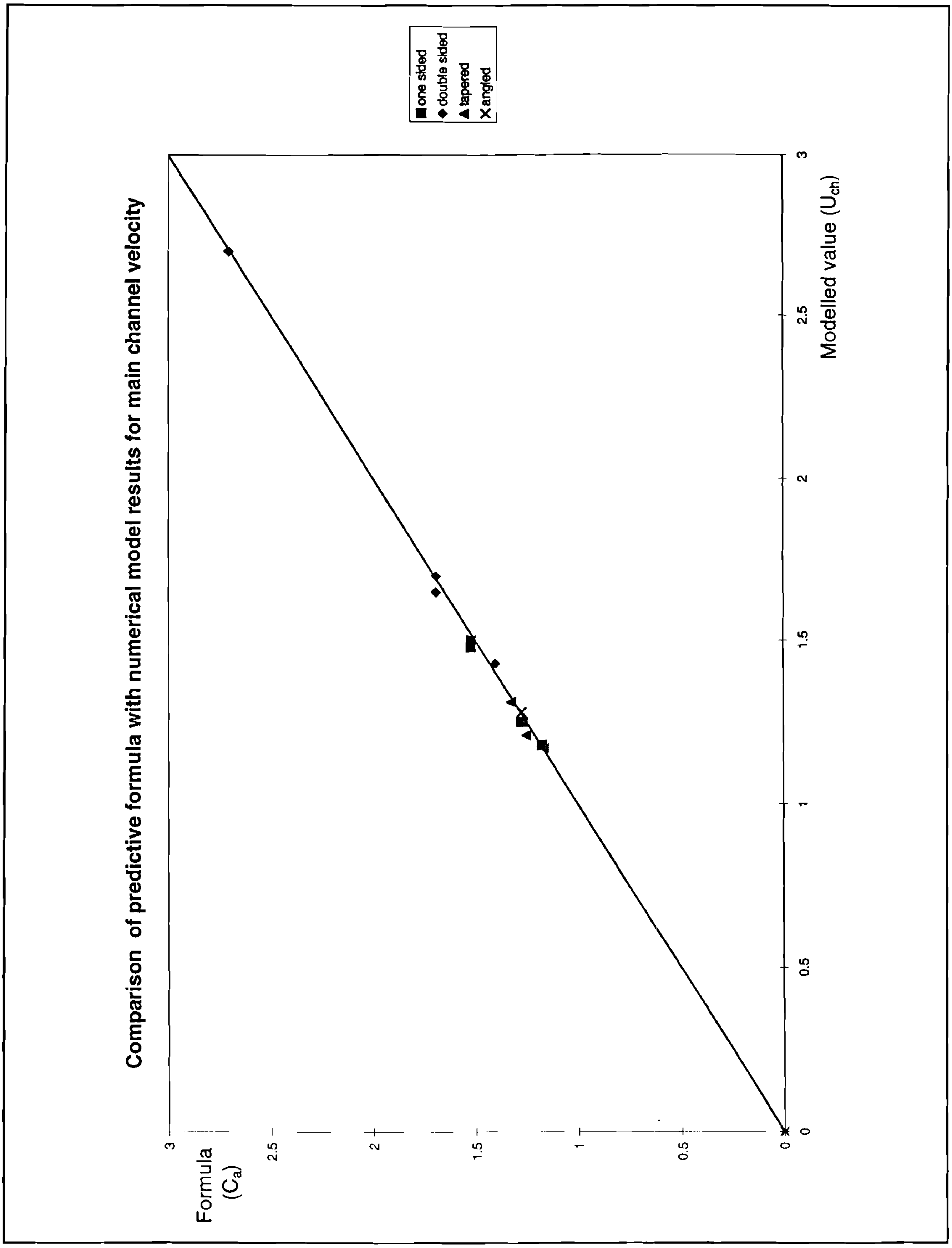

Figure A7 Comparison of predictive formula with numerical model results for main channel velocity (U_{ch})

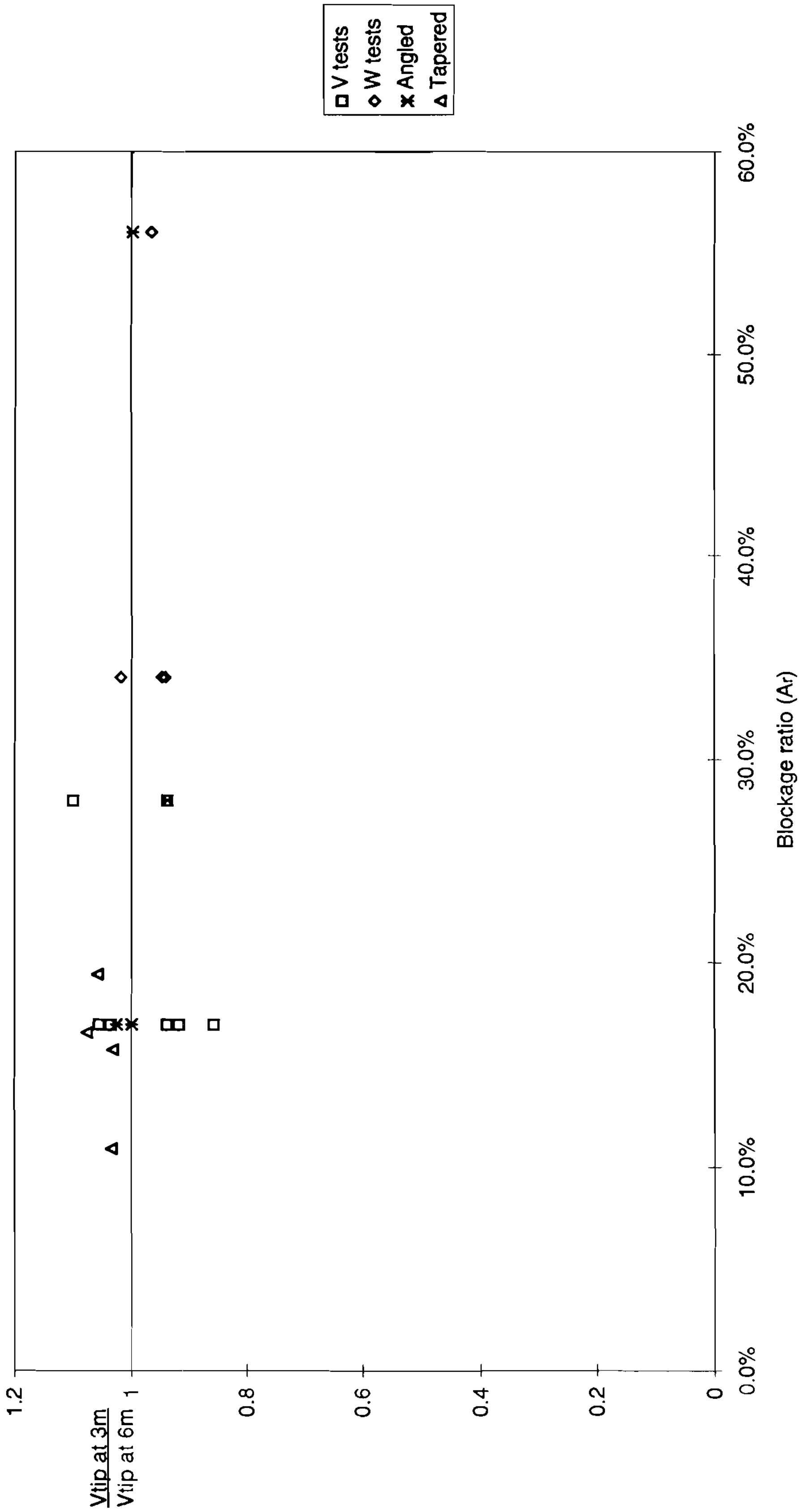

Figure A8 Ratio of near tip velocities at 6m and 3m from the groyne tip

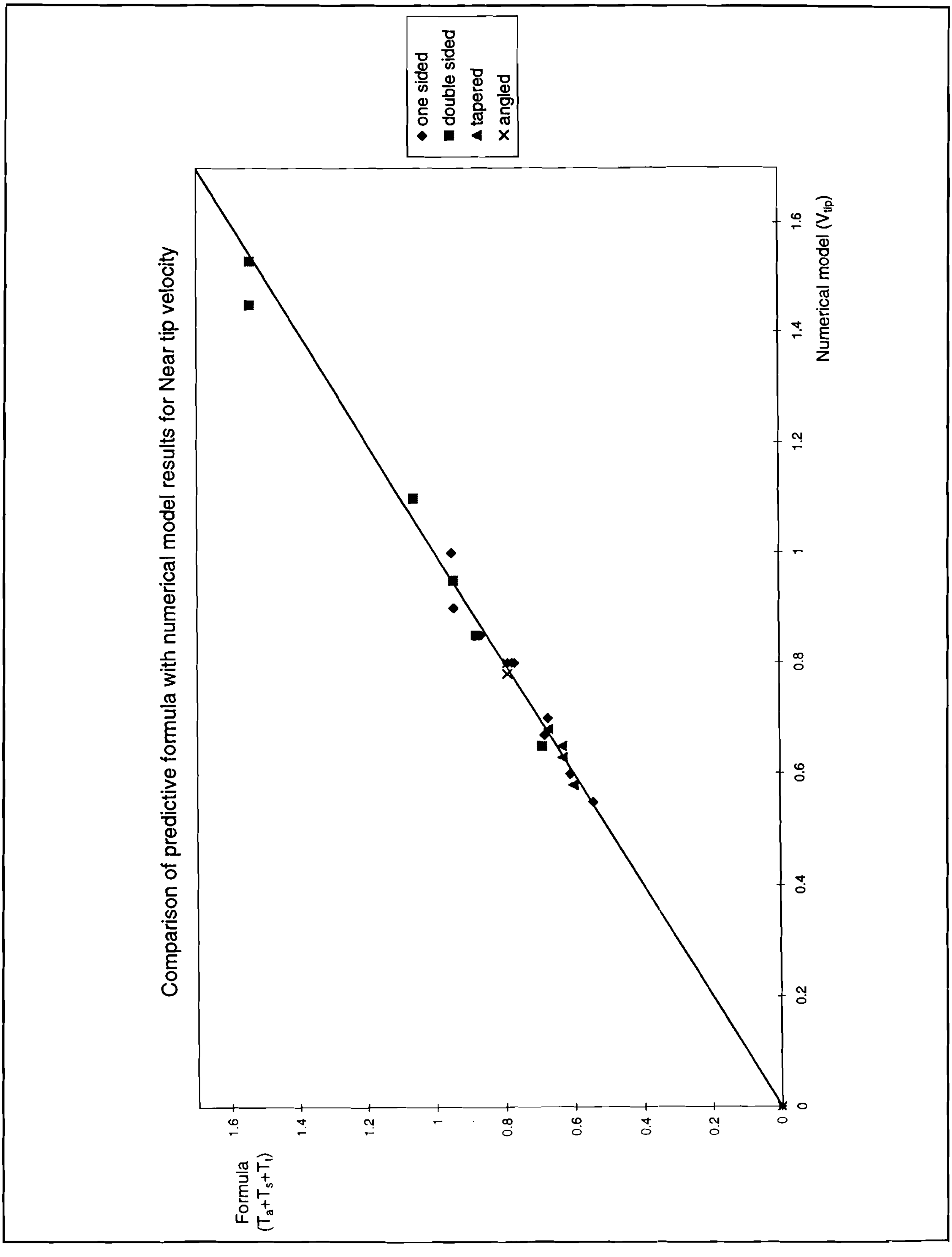

Figure A9 Comparison of predictive formula with numerical model results for tip velocity (V_{tip})

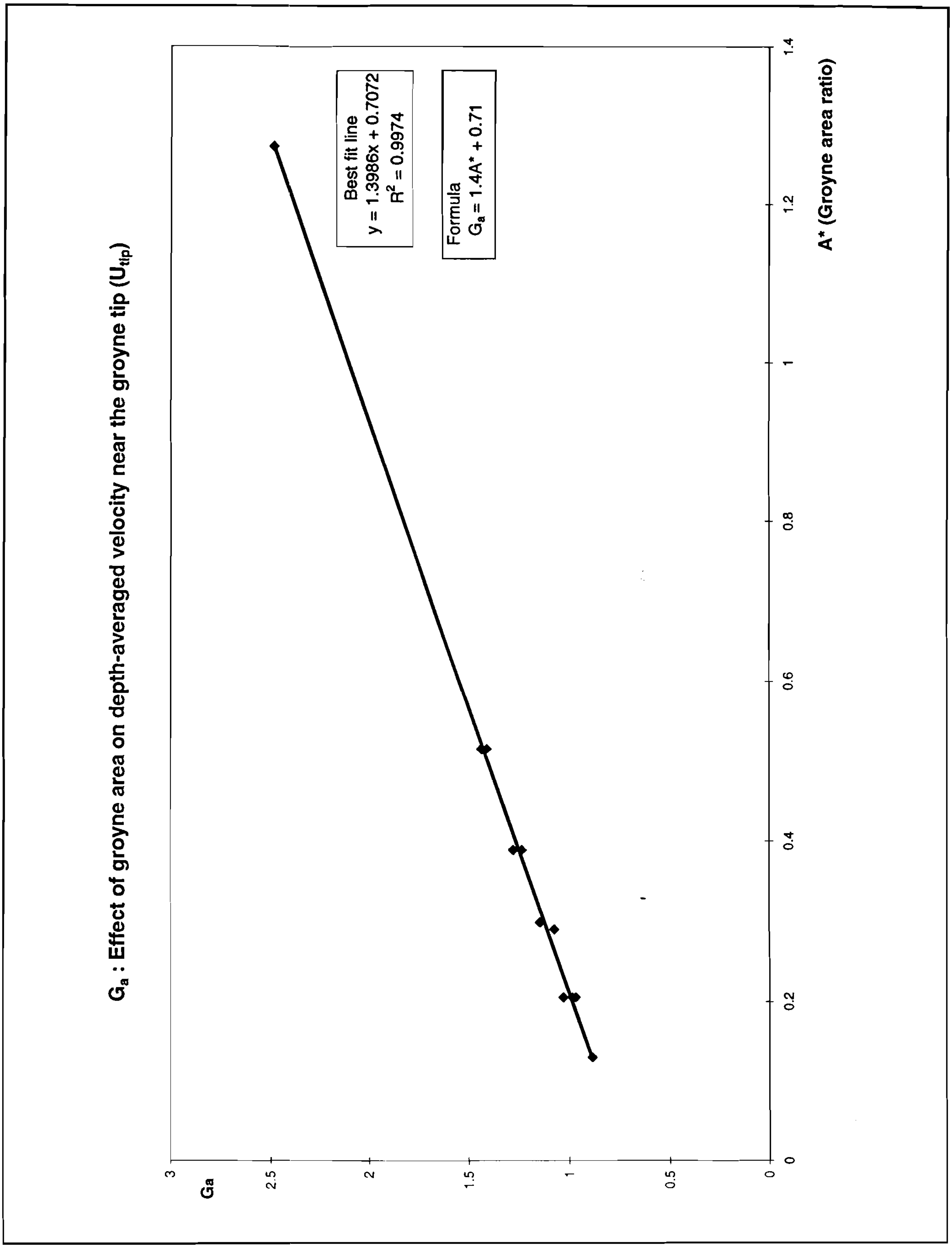

Figure A10 G_a : Effect of groyne area on depth-averaged tip velocity

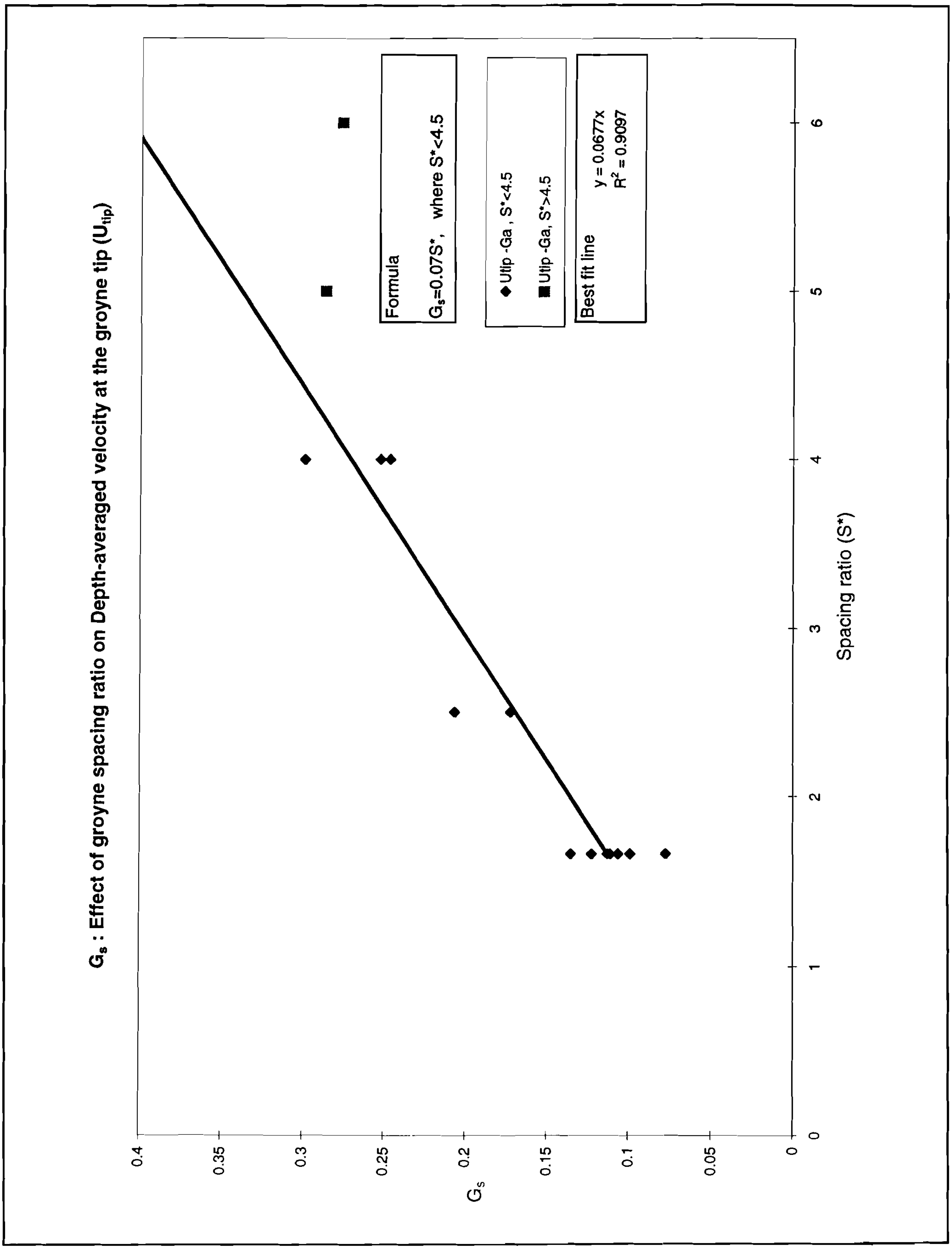

Figure A11 G_s : Effect of groyne spacing on depth-averaged tip velocity

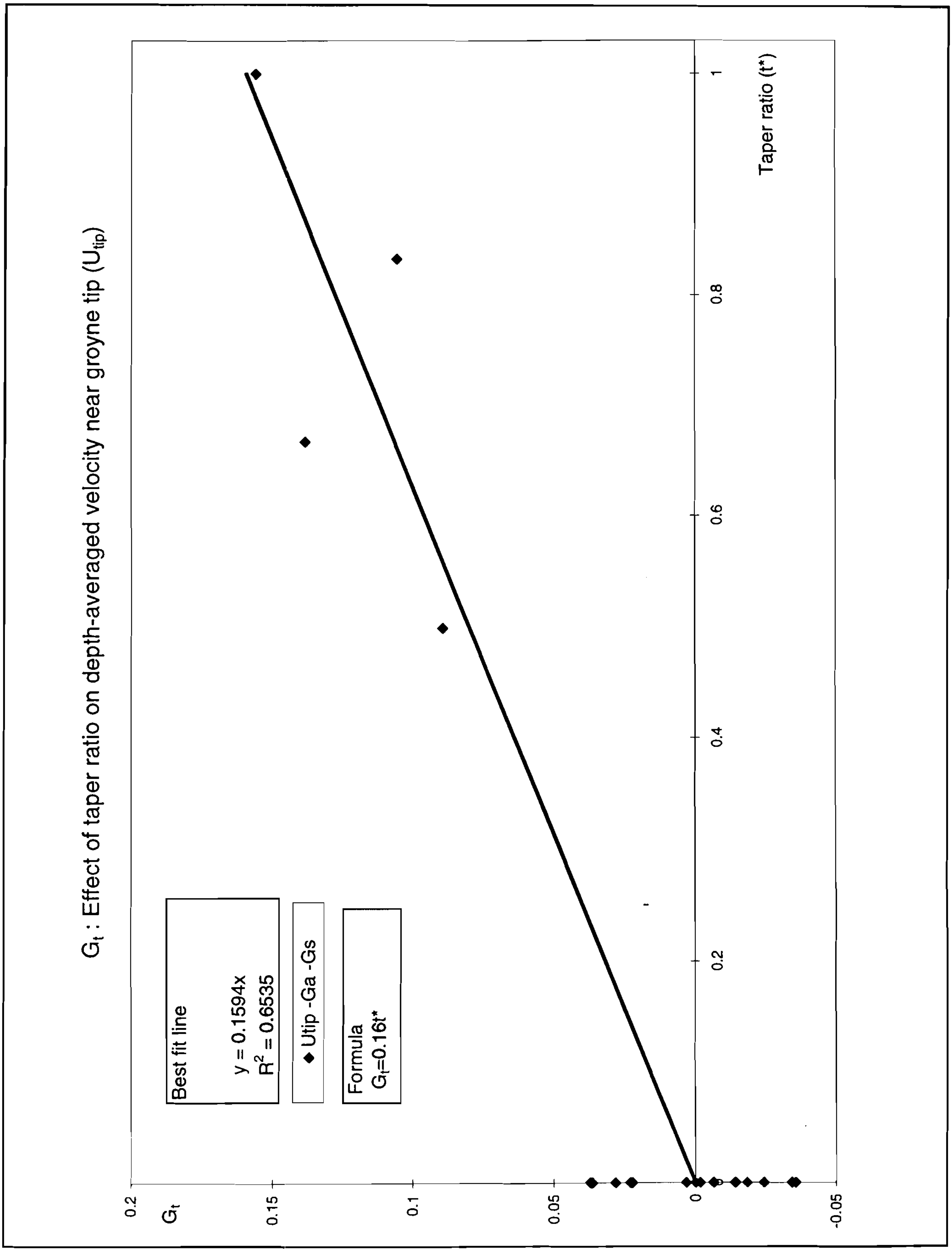

Figure A12 G_t : Effect of groyne taper on depth-averaged tip velocity

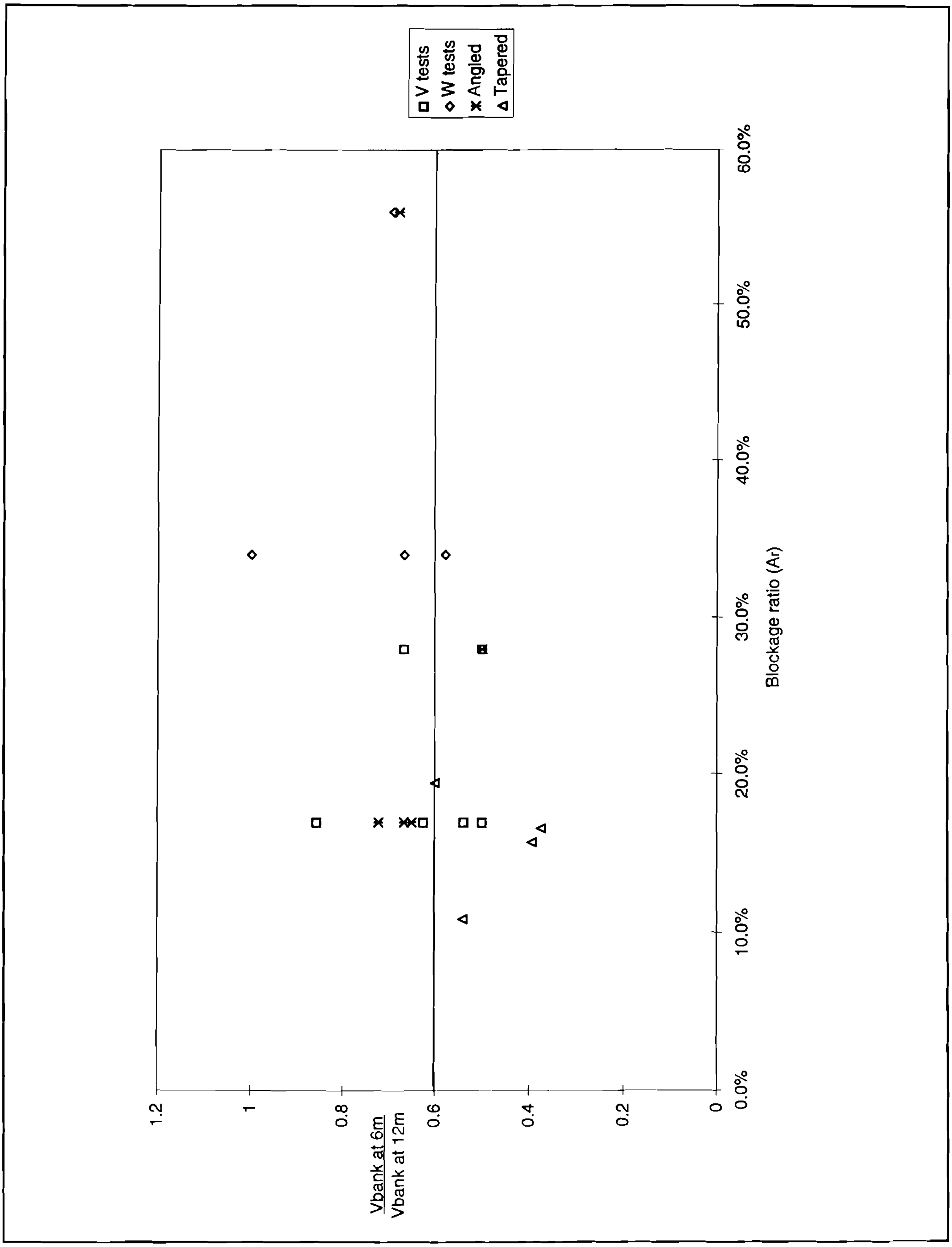

Figure A13 Ratio of near tip velocities at 6m and 12m from the bank line

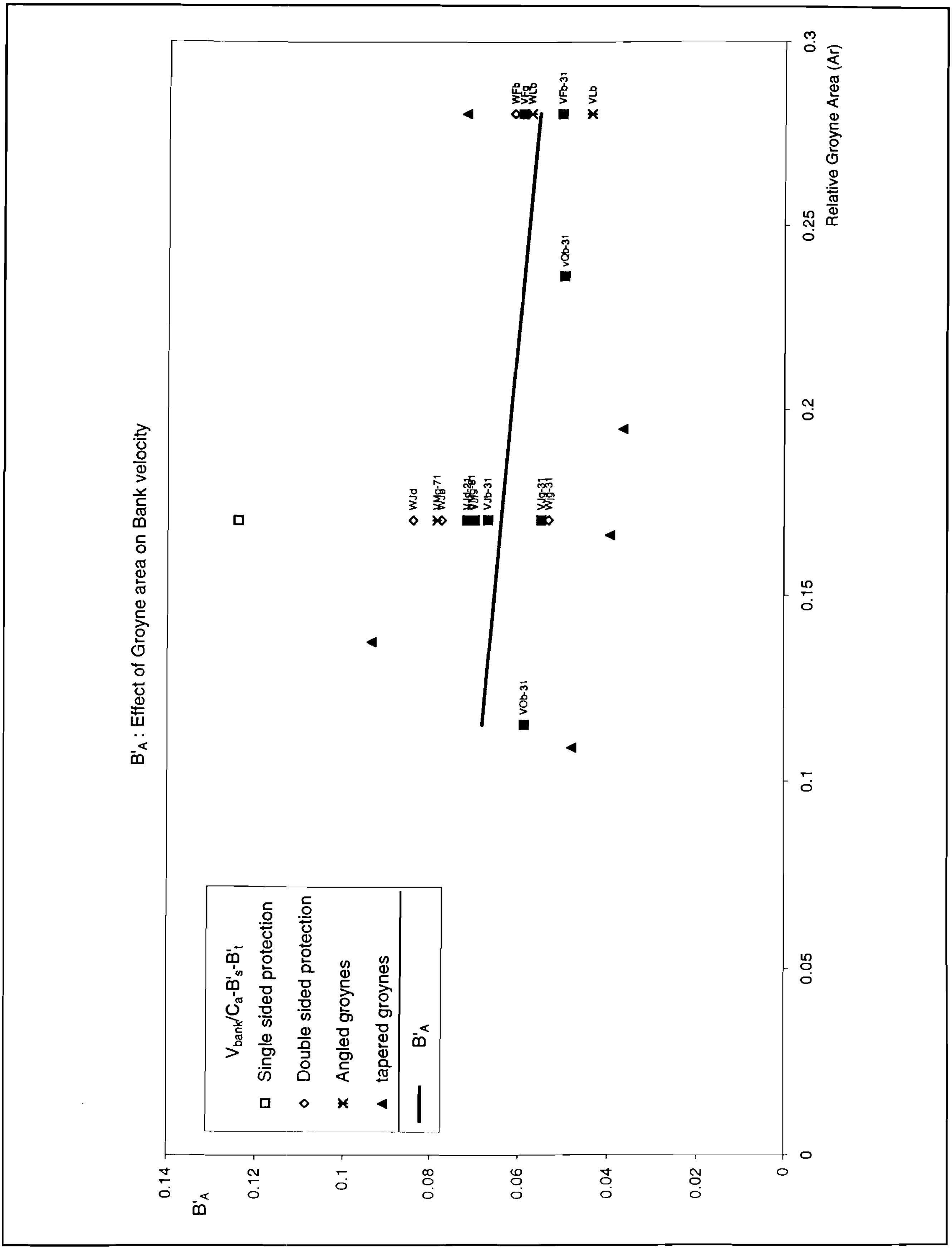

Figure A14 Groyne protection effect on Bank velocity

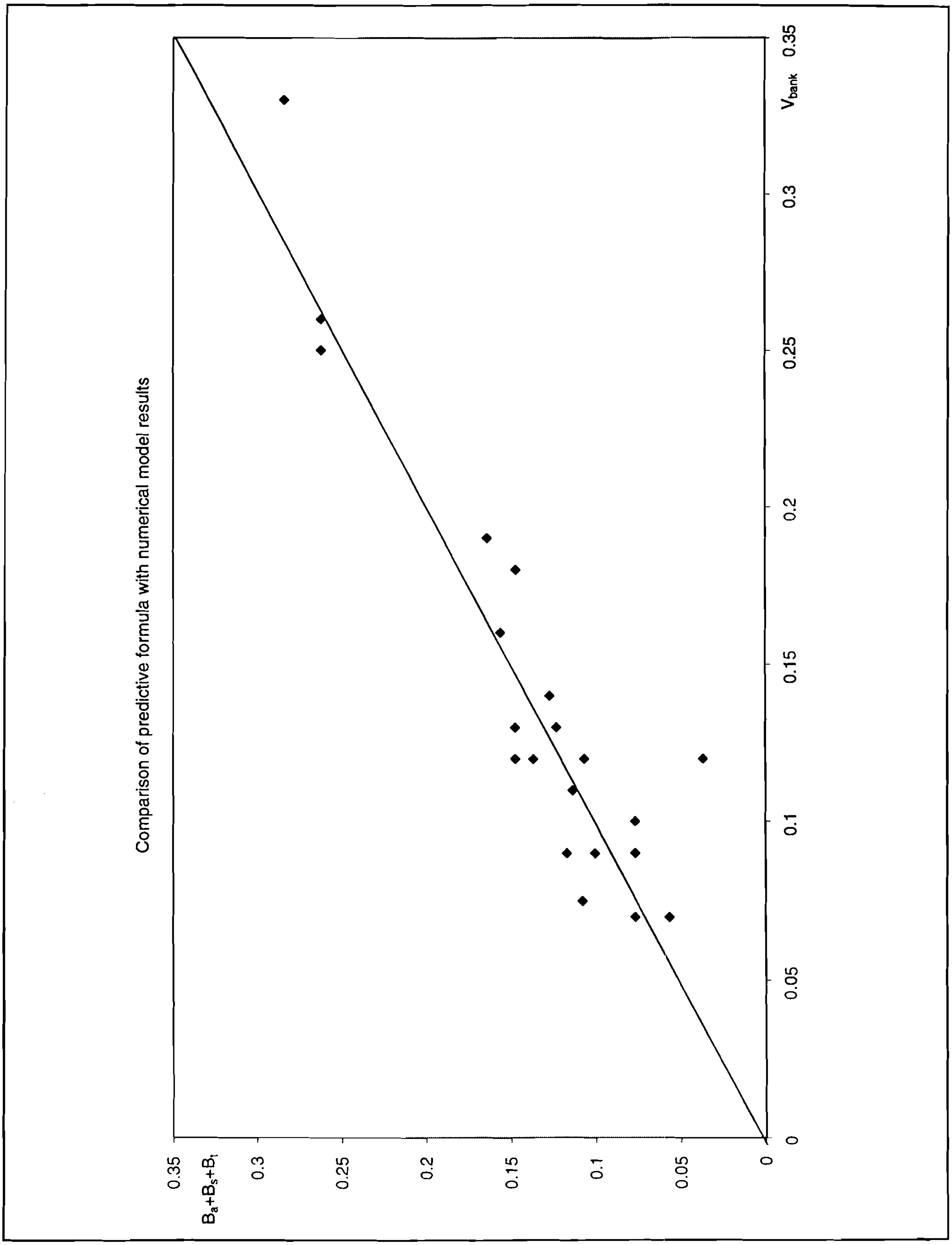

Figure A15 Comparison of predictive formula with numerical model results for bank velocity (V_{bank})

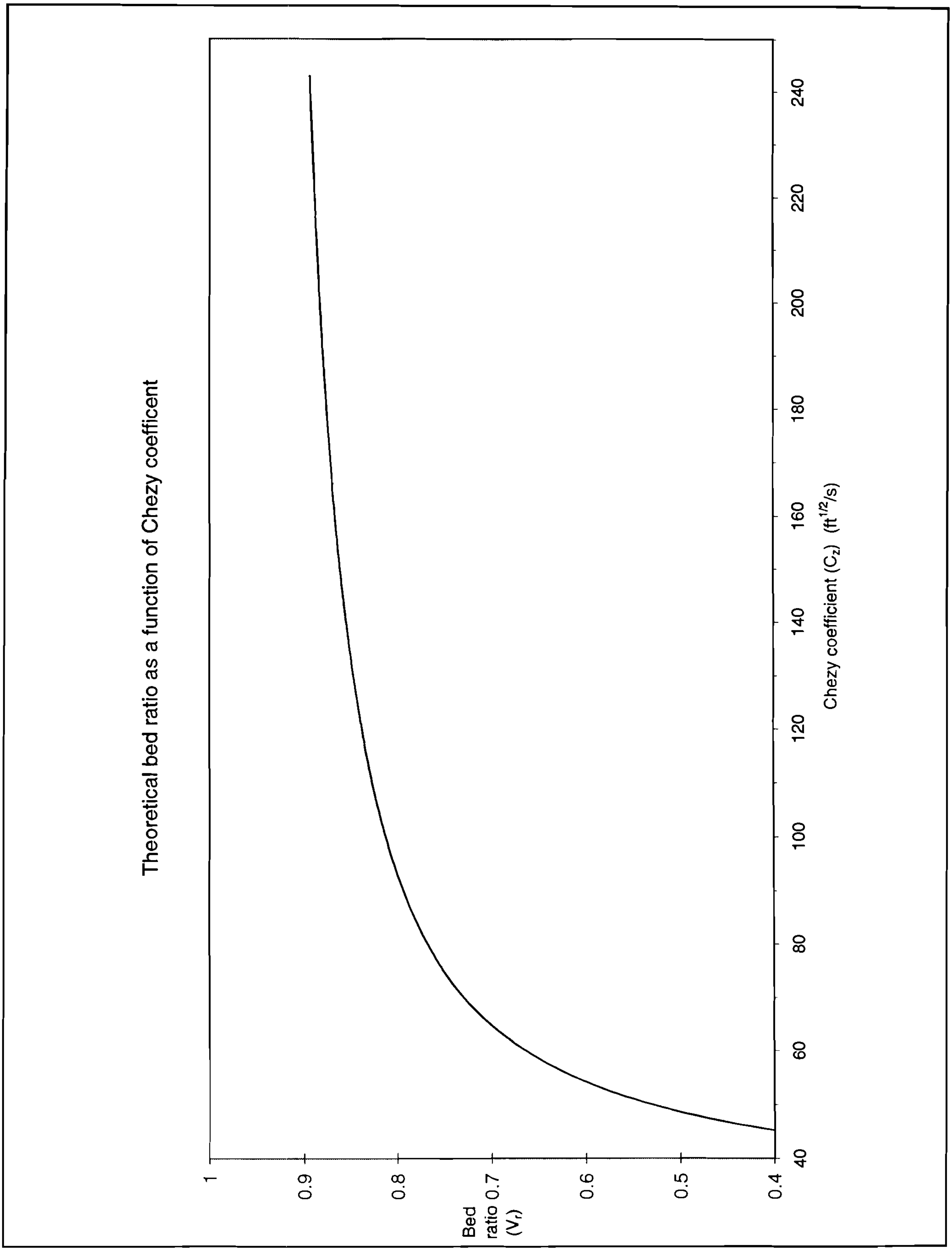

Figure A16 Theoretical bed ratio as a function of Chezy coefficient

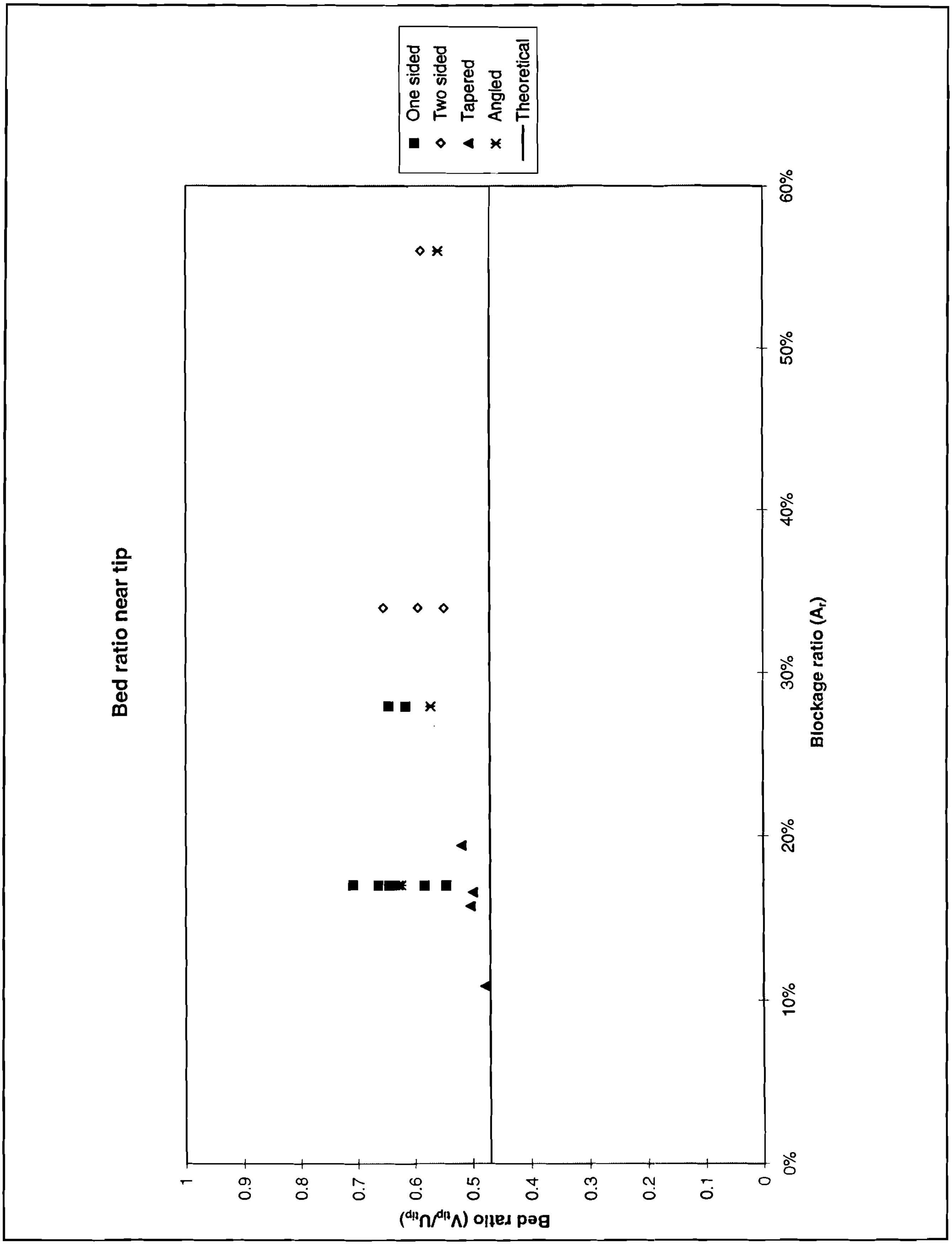

Figure A17 Ratios of maximum near-bed and depth-averaged velocities near the groyne tips (V_{tip}/U_{tip})

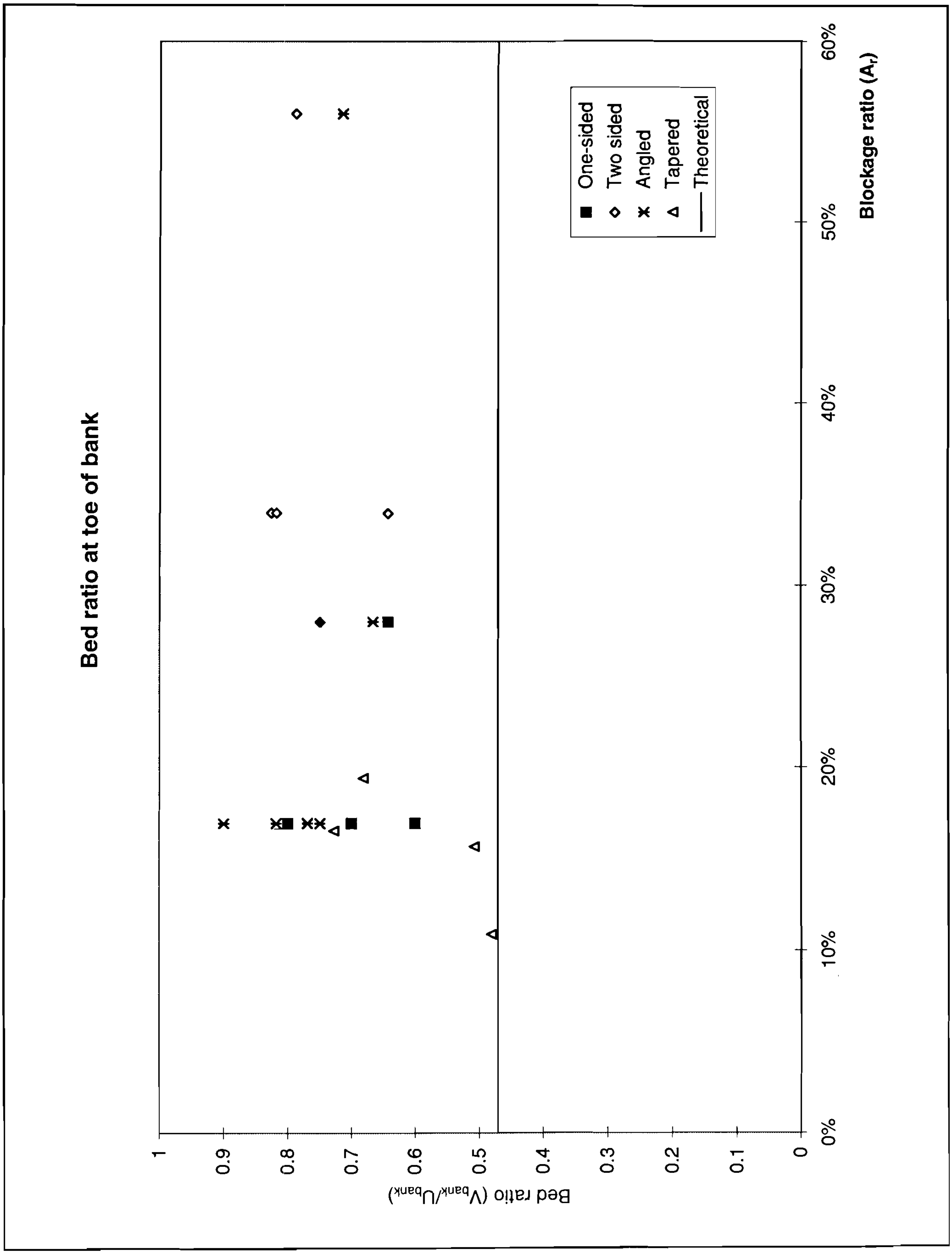

Figure A18 Ratios of maximum near-bed and depth-averaged velocities at the toe of the bank (V_{bank}/U_{bank})

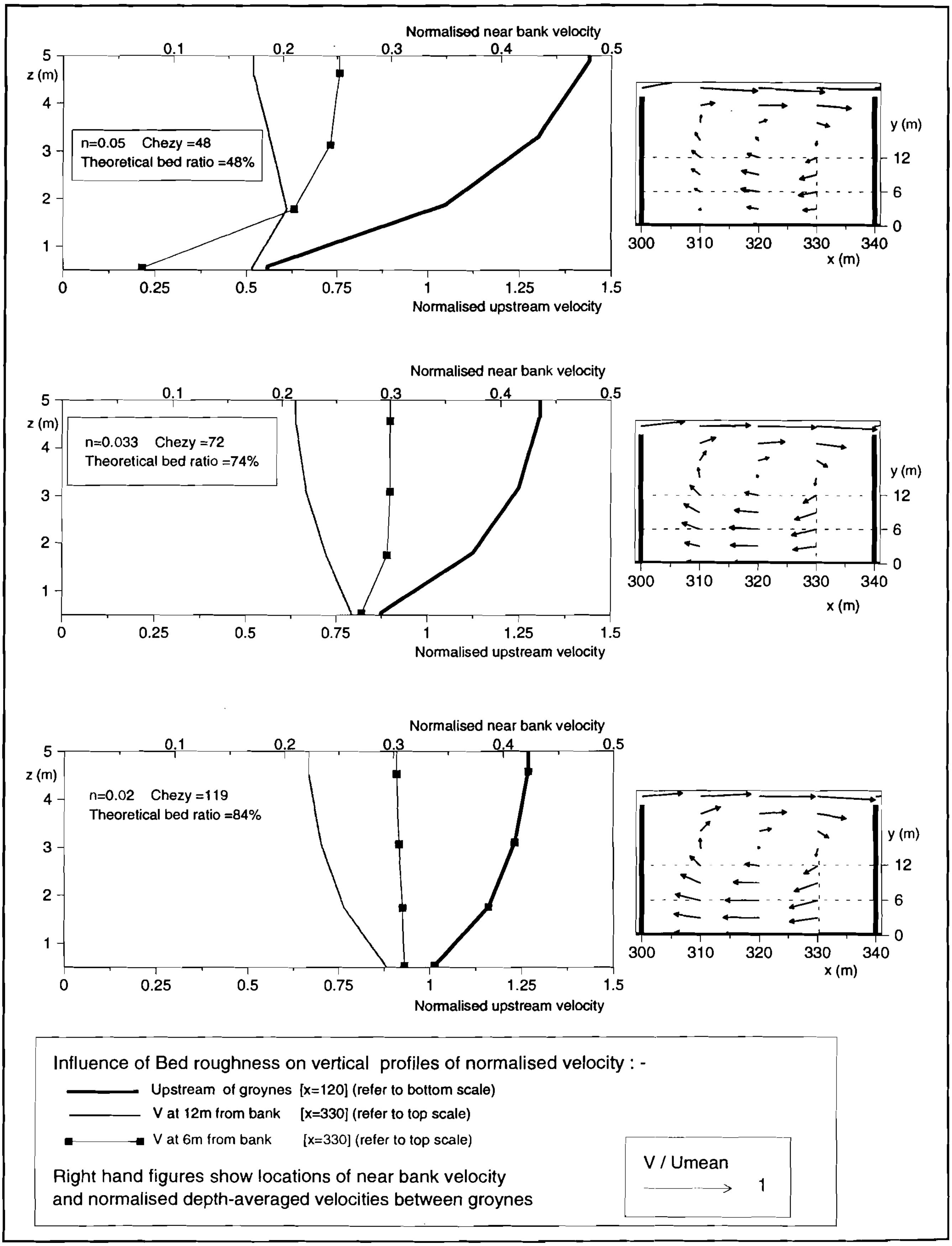

Figure A19 Influence of bed roughness on vertical velocity profiles

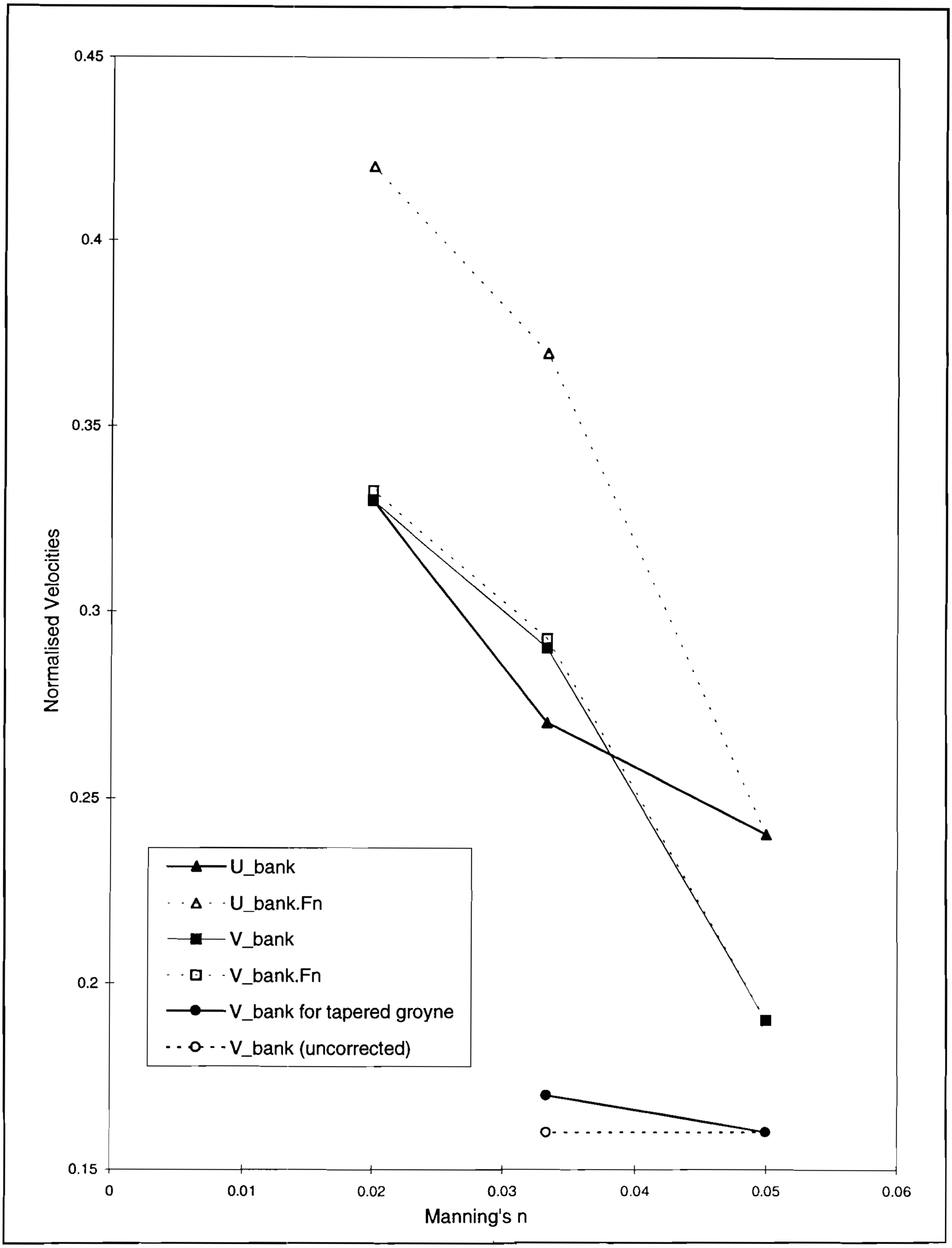

Figure A20 Application of roughness correction coefficient (B_n) to Bank velocity

Appendix 2

Derivation of theoretical values for bed ratio and roughness correction coefficient

Appendix 2 Derivation of theoretical values for bed ratio and roughness correction coefficient

For fully rough turbulent flow, the velocity profile in the boundary layer is described by a logarithmic function

$$\frac{v(z)}{v^*} = A \ln\left(\frac{B z}{k_s}\right) \qquad \text{(A2.1)}$$

Where k_s is the roughness scale,
v^* is the shear velocity,
$v(z)$ is the fluid velocity at height z above the bed and
h is the local water depth.

Following commonly used values
A = 2 and
B = 30

The depth-averaged velocity (u) is given by

$$u = \frac{1}{h}\int_{\delta}^{h} v(z)\ dz \qquad \text{(A2.2)}$$

Substituting equation A2.1

$$u = \frac{2v^*}{h}\int_{\delta}^{h} \ln\left(\frac{B z}{k_s}\right) dz \qquad \text{(A2.3)}$$

Integrating

$$u = 2\frac{v^*}{h}\left[z \ln\left(\frac{B h}{k_s}\right) - z\right]_{\delta}^{h} \qquad \text{(A2.4)}$$

The value δ used as the lower limit of z is required to be greater than zero because for very small values of z the flow is laminar and the log law is not applicable. Following common practice the above integral is approximated to:

$$u = 2\frac{v^*}{h}\left[h \ln\left(\frac{B h}{k_s}\right) - h\right] \qquad \text{(A2.5)}$$

Thus

$$u = 2v^*\left[\ln\left(\frac{B h}{k_s}\right) - \ln(e)\right] \qquad \text{(A2.6)}$$

Giving

$$u = 2v^* \ln\left(\frac{B}{e}\frac{h}{k_s}\right) \qquad \text{(A2.7)}$$

Therefore, dividing A2.1 by A2.7, we obtain:

$$\frac{v}{u} = \frac{\ln\left(\frac{B z}{k_s}\right)}{\ln\left(\frac{B}{e}\frac{h}{k_s}\right)} \qquad \text{(A2.8)}$$

From this equation it can be seen that the local velocity v is equal to the depth averaged velocity (u) at z = h/e = 0.386h

The ratio of the velocity at z = 0.1h, to the depth averaged velocity, is termed the bed ratio (V_r)

$$V_r = \frac{V(z=0.1)}{U} = \frac{\ln(0.1Bh/k_s)}{\ln(Bh/(ek_s))} = 1 + \frac{1-\ln(10)}{\ln(Bh/k_s)-1} \qquad \text{(A2.9)}$$

Thus

$$V_r = 1 - \frac{1.303}{\ln(E)-1} \qquad \text{(A2.10)}$$

where

$$E = \left(\frac{30\,h}{k_s}\right) \qquad \text{(A2.11)}$$

An equation for V_r may be obtained by substituting $k_s = (26n)^6$ which is the value used in applying the solid boundary condition in the numerical model (SSIIM) and an approximation for the Chezy number (C_z)

$$C_z = 1.811\frac{R^{1/6}}{n} \approx \frac{1.811\,h^{1/6}}{n}\left(ft^{1/2}/s\right) \qquad \text{(A2.12)}$$

using $\left(\frac{ft}{m}\right)^{1/2} = 1.811$

This equation makes the approximation that the local depth is equal to the local hydraulic radius. This is compatible with the fact that the log. law velocity profile assumes a flow with constant depth.

It follows that $E = 30.\left(\frac{C_z/1.811}{26}\right)^6$ (A2.13)

Hence $E = \left(\frac{C_z}{G}\right)^6$ where $G = \frac{26 \times 1.811}{(30)^{1/6}} = 26.72$ (A2. 14)

Substituting the above into Equation A2.11, we obtain

$$V_r = 1 - \left(\frac{1.303}{6\ln(C_z/26.72)-1}\right) \qquad \text{(A2. 15)}$$

This value of V_r is calculated for all tests making the approximation that the main channel depth H at the downstream end of the numerical model is substituted into the formula for the Chezy coefficient ($1.811H^{1/6}/n$). This is the bed ratio for uniform, fully developed, rough turbulent flow, where the depth of flow is H (metres).

The same formula is used in the calculation of the roughness correction function F_n. The value of V_r is determined for the test conditions H = 5.3, n = 0.05 and this is used to normalise the value of V_r which applies in the conditions under consideration.
i.e.

$$F_n = \frac{V_r|_{H,n}}{V_r|_{5.3,0.05}} = \frac{V_r}{0.478} = 2.09V_r \qquad \text{(A2.16)}$$

This function is shown for different values of depth and Manning's n, in Figure 23.